Application of Point-on-Wave for Controlled Switching of Capacitor Banks and Cable Circuits in the Dutch 150 kV Transmission Grid

Evaluation of the Effectiveness of Point-on-Wave and the Impact of Circuit Breaker Imperfections

Master Thesis

M. C. (Martijn) Hoogendoorn

TU Delft

Application of Point-on-Wave for Controlled Switching of Capacitor Banks and Cable Circuits in the Dutch 150 kV Transmission Grid

Evaluation of the Effectiveness of Point-on-Wave and the Impact of Circuit Breaker Imperfections

By

M. C. (Martijn) Hoogendoorn

In partial fulfilment of the requirements for the degree of:

Master of Science
in Electrical Engineering

at the Delft University of Technology,
to be defended publicly on Friday August 22nd, 2025 at 10:30 AM.

Student ID:	5870496
Project duration:	December 1, 2024 – August 22, 2025
Thesis committee:	prof. dr. M. Popov
	ir. K. Velitsikakis
	dr. M. Ghaffarian Niasar
University supervisor:	prof. dr. M. Popov
Company supervisor:	ir. K. Velitsikakis

This thesis was carried out in collaboration with TenneT TSO B.V., which is headquartered in Arnhem.

TU Delft

TenneT

Acknowledgements

This thesis marks the completion of my Master of Science degree in Electrical Engineering at TU Delft. The journey through my studies has been both challenging and rewarding, and it culminates in this research project.

I had the pleasure of carrying out my thesis work at TenneT TSO B.V., where I truly appreciated the stimulating environment and the chance to apply my academic knowledge to real-world challenges. This experience has been invaluable for developing my professional skills and deepening my understanding of the field.

I would like to thank ir. Kostas Velitsikakis, my company supervisor, for giving me the opportunity to do my thesis at TenneT and for his excellent guidance and support throughout the project. I am especially grateful for the chance to gain knowledge in EMTP-ATP and to grow as an engineer, also through his help with writing conference papers. His advice and encouragement were very important to me.

I would also like to thank prof. dr. Marjan Popov, my university supervisor, for his guidance and for sharing his knowledge with me, not only during this thesis but also throughout the entire specialization phase of my Master's. His expertise has greatly contributed to my growth and learning.

Martijn Hoogendoorn
August 2025

Abstract

In recent years, the electricity grid has evolved rapidly due to the large-scale integration of renewable energy sources and the growing demand for electricity. This development has led to more customer connections and grid expansion projects, resulting in a more dynamic and flexible system. To maintain safe and stable grid operation, frequent switching of equipment, such as reactive power compensation devices (e.g., capacitor banks) and cable circuits, is often required.

However, energising capacitor banks and cable circuits can cause severe voltage transients and inrush currents. Such transients could impose challenges such as dielectrically stressing the insulation of power apparatus and violating Grid Code limits related to Power Quality. Point-on-Wave (PoW) switching is a promising technique to suppress these unwanted effects, but its practical effectiveness is not yet fully understood by TenneT, the Dutch transmission system operator.

This study investigates the effectiveness of PoW switching for energising cable circuits and capacitor banks in a Dutch 150 kV grid scenario. It also examines how switching imperfections, such as “pole scatter” and an imperfect “Rate of Decrease of Dielectric Strength”, affect the PoW switching effectiveness. The central research question is: “Is PoW switching an effective solution for meeting the TenneT NL policy requirements when switching capacitor banks and cable circuits?”

To answer this research question, a state-of-the-art analysis is first carried out to provide the technical background of PoW switching. Next, TenneT’s current policy on PoW implementation and the voltage quality requirements of the grid are reviewed to assess whether the outcomes of this study align with these standards. Based on this foundation, a detailed simulation plan is developed, and the simulation results are analysed. Finally, a discussion section offers a critical reflection on various aspects, including alternative mitigation methods, the alignment of statistical and deterministic data, and the need for mathematical compensation of external variables.

It can be concluded that Point-on-Wave (PoW) switching significantly reduces inrush currents and transient overvoltages compared to switching without PoW. Based on 200 Monte Carlo simulations per configuration, it is shown that without PoW, all simulated capacitor banks and cable circuits exhibit Rapid Voltage Changes (RVC) exceeding the 10% limit set by TenneT’s policy. However, when PoW is applied, none of the investigated capacitor banks, rated at 25 MVAr, 50 MVAr, and 75 MVAr, nor any of the simulated cables up to 49.5 km in length exceed the 5% RVC limit specified in the grid code, whereas without PoW, these configurations do show a significant amount of exceedances above this 5% limit.

Contents

List of figures

List of tables

Abbreviations

AC	Alternating current
CB	Circuit Breaker
CSD	Controlled Switching Device
CT	Current Transformer
DC	Direct Current
TSO	Transmission System Operator
EHV	Extra High Voltage
HV	High Voltage
LV	Low Voltage
L-G	Line-to-ground
L-L	Line-to-line
MV	Medium Voltage
PoW	Point-on-Wave
RDDS	Rate of Decrease in Dielectric Strength
RRDS	Rate of Rise in Dielectric Strength
SSC	Synchronous Switch Controller
VT	Voltage Transformer
PIR	Pre-Insertion Resistor

1 Introduction

In the last years, the electricity grid has been advancing significantly. Aspects that drive this advancement are the introduction of a high number of renewable projects and, on the other hand, the increase in electricity demand. As a result, the number of customer connections to the HV and EHV grids increases, which also creates the need for grid expansion projects to meet the increasing demand in transport capacities. All in all, these aspects lead to a more dynamic operation of the system.

Dynamic behaviour in the electricity grid requires frequent adaptation to changes. Those changes are primarily caused by variations in loads and green energy yields, e.g., fluctuations in the generated power. These fluctuations may require frequent switching of, for example, reactive power compensation equipment or circuit connections.

Unless properly studied or mitigated, switching operations may result in voltage transients or inrush currents, especially when the switching instant is not ideal. Such transients could impose challenges such as dielectrically stressing the insulation of the power apparatus and violating the Grid Code limits with respect to Power Quality. For example, when a capacitor bank is energised at an instant of non-zero voltage, the capacitor voltage changes rapidly, yielding a high inrush current. High capacitive inrush currents could be proven problematic for the circuit breaker, by exceeding the type-tested withstand values. Similarly, high inrush currents could lead to excessive transient overvoltages and voltage fluctuations.

Among other options, Point-on-Wave switching is a technique that can potentially mitigate these voltage transients and high currents by controlling the exact switching instants. This is done by measuring the current and voltage. Based on that information, a digital controller can determine the optimal closing or opening instant to suppress switching transients. However, the effective implementation of Point-on-Wave switching requires extensive knowledge of PoW, the circuit breaker characteristics, system behaviour, and requirements.

This document covers the performed research regarding the effectiveness of PoW with regard to the switching of 150 kV capacitor banks and underground cable circuits in the TenneT HV grid in the Netherlands. This chapter, specifically, covers a general introduction, which includes background information about the company and subject, problem definition, research questionnaire, approach, and outline.

1.1 TenneT's transmission grid in the Netherlands

This thesis project was conducted at TenneT TSO B.V. TenneT, founded in 1998, is the Dutch so-called "Transmission System Operator", also referred to as a "TSO". TenneT's main task is to develop, maintain, and operate the power grid above 110 kV in the Netherlands and a part of Germany. In total, TenneT owns and operates over 25,000 kilometres of high-voltage lines and cables, delivering electricity to 43 million domestic and business users [1]. In Figure 1.1, TenneT's grid coverage is depicted.

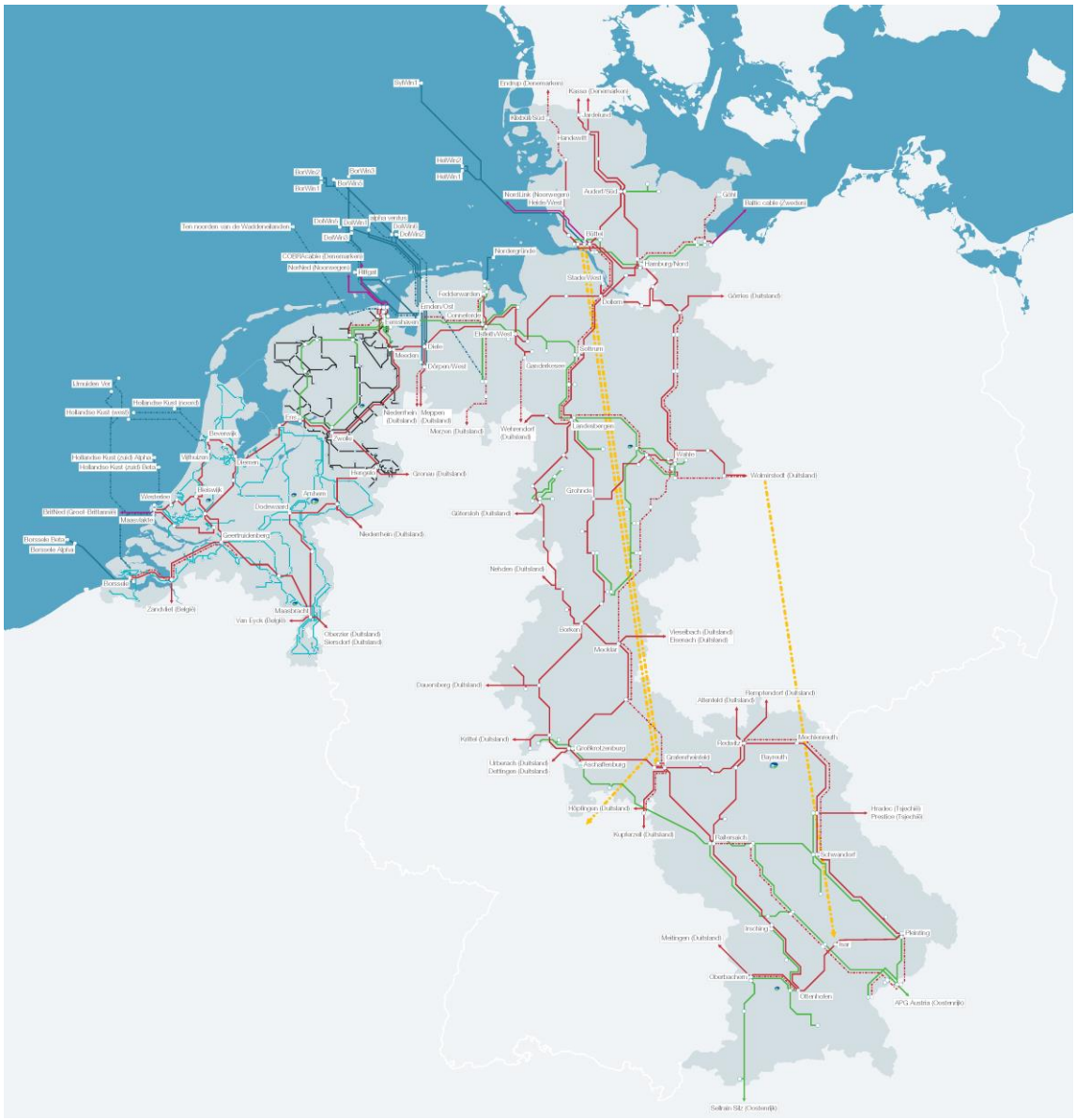

Figure 1.1: TenneT's grid [2]

1.1.1 TenneT's grid expansion

Since 2006, the number of electricity producers connected to the Dutch grid has grown significantly. This growth is driven by TenneT's energy transition goal to achieve a climate-neutral grid by 2045, ensuring a reliable power supply and energy independence. To be able to transport all the extra energy produced, TenneT is carrying out a large-scale expansion program. TenneT will build nearly 4000 km of cable circuits to reach its goals. [3] [4] [5]

This growth requires the replacement of 140 high-voltage substations with the so-called "Bay replacement program". This program focuses on replacing current substations with modular and digital ones as fast as possible, with minimal workload for the scarce technical personnel [6].

TenneT also works on load pocket formatting, which means splitting the grid up into more than 40 smaller sub-areas [7] . In this way, the loads are better distributed across the grid, as every load pocket has its connection to the 220 kV and 380 kV grid. Without this load pocket formatting, the limited connections between the 110/150kV and 220/380kV grid forms congestion problems. This load pocket formatting requires the fortification of existing and the realisation of new 110/150 kV connections and stations.

1.2 Problem definition

As described in Section 1.1.1, TenneT works on expanding the grid, which requires the implementation of cable circuits and capacitor banks. However, the energisation of these cable circuits and capacitor banks may induce transients and inrush currents, which can be mitigated with Point-on-Wave (PoW) switching.

TenneT NL has defined a policy concerning the application of PoW controllers for the switching of underground cable circuits and capacitor banks. The policy is partly based on system operational data and the rules of thumb, which originate from project-specific simulation studies. However, no extended desktop studies or analyses have been performed to evaluate the PoW effectiveness when considering component-related aspects, e.g., circuit breaker pole scatter, switching times concerning operating frequency, and temperature conditions. On the other hand, the PoW switching effectiveness has not been evaluated when considering system configurations and system conditions, e.g., system strength and system damping. Optimising these policies can potentially result in cost-effective solutions or the selection of other mitigation solutions.

1.3 Research questionnaire and scope

As a foundation to solve the problem, the following central research question was defined: “Is PoW switching an effective solution to meet the TenneT NL policy requirements when switching capacitor banks and cable circuits?”

To solve this main question, sub-questions were defined. Furthermore, for each sub-question, questions are listed as a stepping stone for giving answers to the main questions.

The sub-questions:

- What is the existing PoW policy within TenneT NL?
    - What are the requirements concerning power quality in the Dutch TenneT transmission grid?
- How is the PoW implemented at TenneT NL?
    - Wherefore is PoW implemented?
    - When is PoW implemented?
    - What is a typical engineering design per application?
    - What types of different controllers are used, and what are their specifications?
- What is the experience of other TSOs regarding PoW switching for capacitor banks and cable circuits?
    - What are the criteria/policies for PoW switching implementation?
- Are there factors that may influence the effectiveness of PoW?
    - Are there switching imperfections that may have an effect?
    - Are there environmental factors that may have an effect?
    - Are there ways to consider these factors when programming the settings of the PoW controller?

1.4 Scientific Approach

To gain reliable answers to the research questions, a proper scientific approach was defined. The basis of this approach involves performing an EMTP-ATP analysis. EMTP-ATP is an electromagnetic transient program that can be used to model and simulate electrical networks [8]. This analysis, however, required dividing all the work into multiple sub-tasks.

These sub-tasks included:
- State-of-the-art research to gain general knowledge on the PoW.
- Study of the current implementation and policy of the PoW within TenneT.
- Developing EMTP-ATP simulation models and performing simulation analyses.
- Draw conclusions based on the simulation outcome.

The following tools were used:
- Relevant TenneT documentation and international publications on Point-on-Wave switching.
- The EMTP-ATP software to model and simulate an electrical network.

1.5 Thesis outline

The thesis report is outlined as follows:

Chapter 2 describes the state-of-the-art regarding the PoW switching. In this chapter, the switching behaviour of a CB, applications of PoW, and the PoW controller are described. This knowledge provides a theoretical foundation.

Chapter 3 summarises the current implementation policy of PoW at TenneT NL and the power quality requirements of the Dutch Grid Code.

Chapter 4 describes the simulation plan, which contains the strategy for executing all the simulations.

Chapter 5 presents the simulation results regarding the effectiveness of PoW for energising capacitor banks.

Chapter 6 presents the simulation results regarding the effectiveness of PoW for energising cable circuits.

Chapter 7 presents the discussion part, which provides an in-depth critical view on aspects such as the obtained results, other potential mitigation options, and experiences from other TSOs.

Chapter 8 provides the conclusions, and recommendations for future work.

2 State-of-the-art of Point-on-Wave (PoW) switching

2.1 Switching behaviour of a circuit breaker

In the sections below, a description of the main circuit breaker parameters is provided, which are relevant to the effectiveness of the PoW application.

2.1.1 Rate of Decrease of Dielectric Strength (RDDS)

RDDS refers to the circuit breaker's closing characteristics. When the breaker closes, the dielectric strength of the moving gap between the poles cannot instantaneously change. This is an important aspect to take into account, as it can cause pre-strikes. A pre-strike occurs during the closing operation of the circuit breaker when the voltage across the approaching contacts exceeds the dielectric strength of the gap in the breaker. This causes dielectric breakdown, leading to an arc forming before the contacts physically touch. Figure 2.1 illustrates the acceptable RDDS for an ideal zero-voltage breaker closing operation. One can observe that when the RDDS is lower than the steepness of the voltage across the breaker, pre-strike may occur.

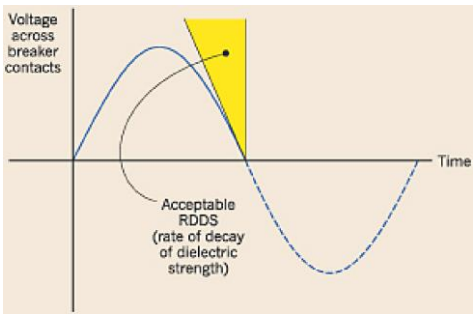

Figure 2.1: Example of acceptable RDDS [36]

When the RDDS is lower than the maximum steepness of the voltage across the breaker and zero voltage switching is desirable, then the target instant must be shifted to prevent prestrikes.

If the target instant is at a perfect zero voltage crossing, then a pre-strike occurs if the following criterion is met:

$$RDDS \leq 2\pi f U_m \tag{2.1}$$

When the criterion described by equation 2.1 is met, the new target instant should be shifted by:

$$t_{target} > \frac{1}{2\pi f} \cdot \cos^{-1}\left(\frac{-RDDS}{2\pi f U_m}\right) + \frac{U_m \sqrt{1 - \left(\frac{RDDS}{2\pi f U_m}\right)^2}}{RDDS} \pm \frac{k}{2f} \; for \; k \epsilon Z \; if \; RDDS \leq 2\pi f U_m \tag{2.2}$$

where:

$$U_m: Peak\ value\ of\ sine\ voltage\ across\ CB\ [V], f: Frequency\ [Hz]$$
$$RDDS: Rate\ of\ Decrease\ of\ Dielectric\ Strength\ [V/s]$$

Appendix A provides a detailed description of the derivation of the above formulas.

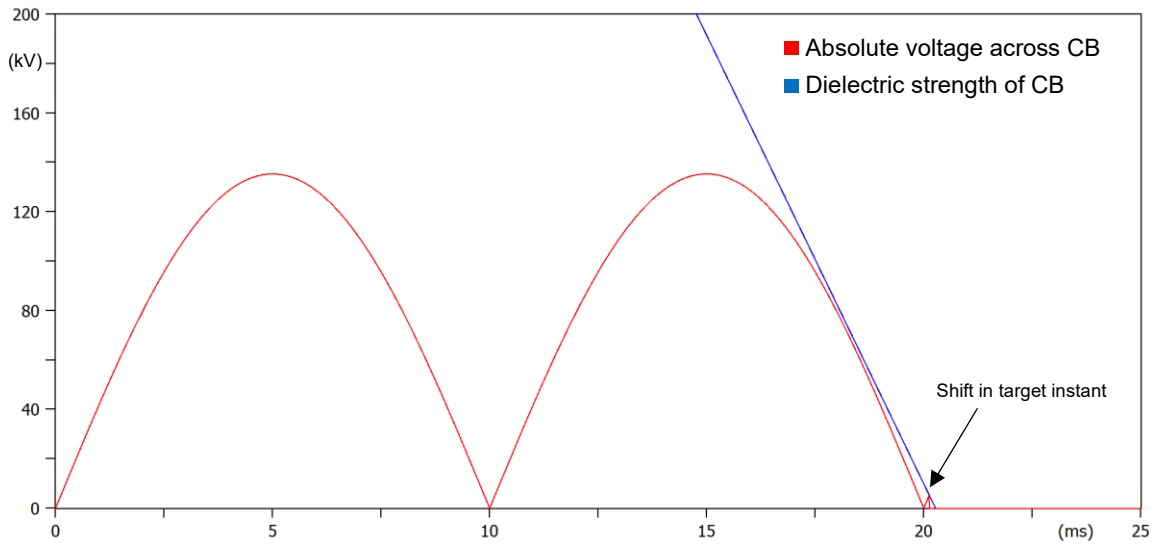

Figure 2.2: Example of shifted target switching instant to prevent a pre-strike

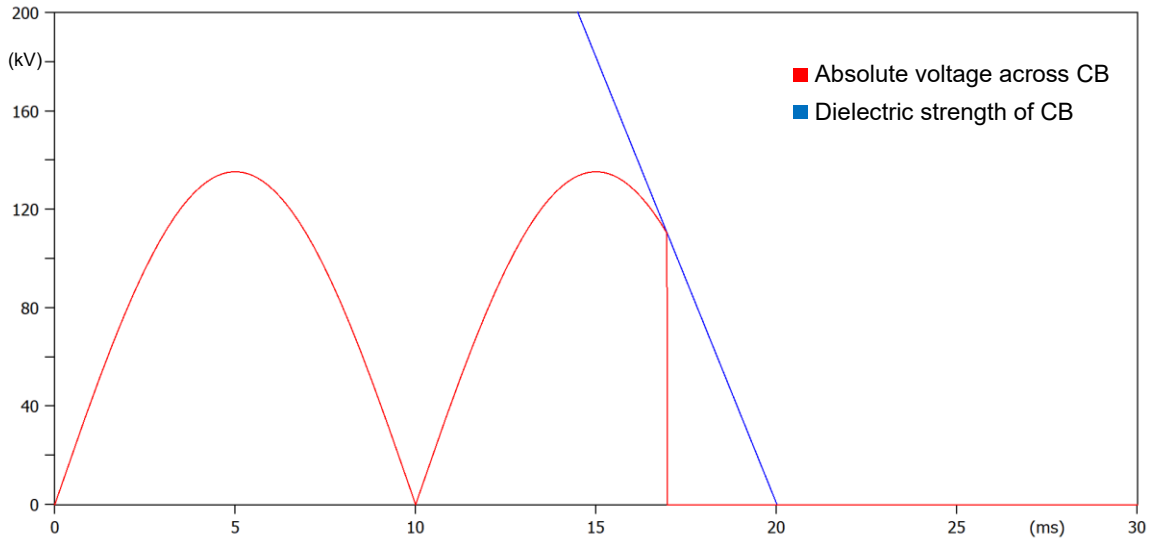

Figure 2.3: Example of a too-low RDDS without a shifted target switching instant

Figure 2.2 illustrates an example implementation of the shifted target instant. One can observe that no pre-strikes occur, but switching at a perfect zero-crossing is not possible due to the shift. In Figure 2.3, however, the RDDS is the same as in Figure 2.2, but there is no shift in the target instant. As can be observed, a severe pre-strike occurred in this case.

2.1.2 Rate of Rise of Dielectric Strength (RRDS)

Regarding the breaker opening, the RRDS becomes an important characteristic. If the Rate of Rise of Recovery Voltage (RRRV) is higher than the RRDS, a re-strike will occur. The RRRV is considered the ratio between the peak Transient Recovery Voltage (TRV) and the time required to reach that voltage after current interruption.

This study primarily focuses on inrush currents and Rapid Voltage Changes (RVCs). Re-strikes are expected to have a limited impact on inrush currents, as the capacitor bank is already energised during breaker opening. Although a re-strike can generate severe high-frequency transients, often in the tens of kilohertz, these transients damp out quickly due to system resistance and arc losses [9]. Because of this rapid damping, re-strikes are expected to have minimal effect on RVCs, since an RVC is defined as the RMS voltage measured over a half-cycle (see Chapter 3), which is significantly longer than the brief duration of a high-frequency re-strike transient. Therefore, the RRDS is not simulated in this study, as re-strikes are expected to have a negligible impact on RVCs and inrush currents compared to pre-strikes.

2.1.3 Mechanical scatter of the circuit breaker

The mechanical scatter of the circuit breaker poles impacts the closing instant, which in turn affects the resulting transients. Figure 2.4 illustrates a pole scatter by depicting the possible variation in withstand voltage, i.e., the actual switching instant can be earlier or later than desired. Furthermore, in the example depicted in Figure 2.4, the average closing instant is shifted to prevent possible pre-strikes that would occur because of the pole scatter. However, this shift in average closing time results in the breaker closing at a less optimal instant, yielding different transient behaviour.

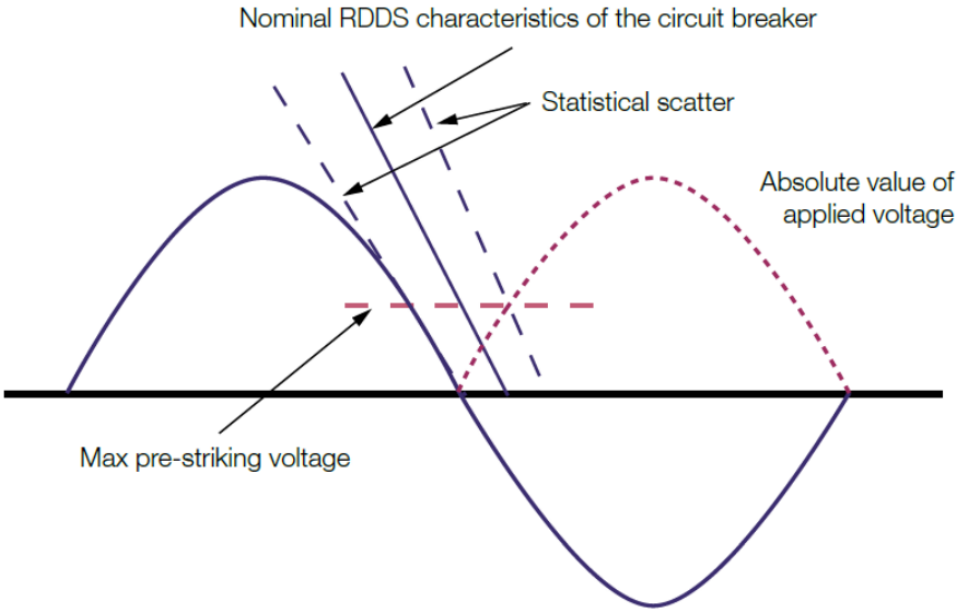

Figure 2.4: Example pole scatter of a circuit breaker [10]

2.1.4 Effect of variation in temperature on the breaker

Temperature variation causes changes in the electrical and mechanical properties of the breaker [11]. Changes in electrical properties can mean changes in resistance, inductance, or capacitance. Regarding the mechanical properties, temperature variations can cause expansion and contraction of components and changes in mechanical spring properties. For effective application of PoW switching, compensation of the temperature effects may be necessary, especially if the switching frequency is low, as the adaptive compensation has a limited effectiveness in that case (see Section 2.1.9).

2.1.5 Effect of variation in control voltage on the breaker

Circuit breakers' actuators use coils that induce a force on a switching mechanism when current is flowing through the coil [11]. Furthermore, in every circuit, a resistance is present, as every conductor has a parasitic resistance, or an extra resistance is added to limit the maximum current. Therefore, a simplified equation can be set up based on Kirchhoff's law to gain insight into the effect of a change in control voltage on the switching times.

According to Kirchhoff's law:

$$V = L\frac{dI}{dt} + RI + \epsilon \tag{2.3}$$

Where,

$$V: \textit{The control voltage applied to the actuator}, L: \textit{The inductance of the circuit}$$
$$I: \textit{The current flowing through the circuit}, R: \textit{The resistance of the circuit}$$
$$\epsilon: \textit{The induced voltage by the actuator movement}$$

Based on this equation, one can observe that an increase in voltage results in an increase in amplitude and rate of change in current. Higher electric currents mean higher mechanical force and thus higher acceleration of the CB's actuator, resulting in lower switching time.

For that reason, it may be important to compensate for variations in control voltage when applying PoW switching.

2.1.6 Effect of variation in hydraulic pressure on the breaker

For circuit breakers fitted with hydraulic drives, the amount of energy stored may differ due to the pump's start/stop pressure threshold [11]. This variation affects the opening and closing times of the breaker. Ideally, these variations are compensated for when applying PoW switching. Circuit breakers with a spring operating mechanism have a constant stored energy, and thus do not need compensation [11].

2.1.7 Effect of idle time on the breaker

The idle time can affect the opening and closing times, especially for hydraulic breakers [11]. Hydraulic breakers contain fluid that can degrade over time. Furthermore, the effect of the breaker cooling down to ambient temperature during idle time affects the viscosity of the fluid. For spring-operated breakers, the spring stiffness may be affected by the temperature. However, this affects the opening and closing time presumably less than the change in viscosity does for the hydraulic breaker. For optimal PoW switching, it may be necessary to implement idle time compensation.

2.1.8 Effect of circuit breaker ageing

Due to component wear, the mechanical times may be affected by long-term drift. Evidence of such drift is a systematic difference between computed mechanical time and measured mechanical time. For optimal PoW switching implementation, adaptive compensation may be necessary.

2.1.9 Effect of switching frequency

The effectiveness of adaptive compensation is highly dependent on how often the circuit breaker is operated. When switching occurs often, e.g., multiple times a day, adaptive compensation is more effective than when switching does not occur often, e.g., twice a year, as for regular switching, there is more data available to train the adaptive compensation model. If, e.g., the switching occurs once in the winter and once in the summer, it is hard for the adaptive compensation model to learn, as there is little data available, resulting potentially in ineffective compensation or even worsening of the PoW effectiveness. Therefore, the effectiveness of adaptive compensation in combination with a limited switching frequency must be considered.

$$\Delta T_{adapt(n)} = \Delta T_{adapt(n-1)} + k \cdot \left(T_{measured(n-1)} - T_{setpoint(n-1)}\right) \tag{2.4}$$

Where,

$$\Delta T_{adapt(n)}: Adaptive\ control\ value\ for\ upcoming\ operation$$
$$\Delta T_{adapt(n-1)}: Adaptive\ control\ value\ of\ previous\ operation$$
$$T_{measured(n-1)}: Previous\ measured\ operating\ time$$
$$T_{setpoint(n-1)}: Previous\ computed\ operating\ time$$
$$k: weighting\ factor\ for\ learning,$$

An example implementation of the adaptive compensation is described in Equation 2.4 [11]. It can be observed that this adaptive compensation works by determining the difference between the setpoint and measured value, and adjusting the next compensation value by the product of this difference and the learning factor. Therefore, if, e.g., switching takes place twice a year in different environmental conditions, the adaptive compensation can even worsen PoW effectiveness.

2.2 Applications for Point-on-Wave switching

This section elaborates on all the different applications for PoW. This gives a better understanding of the reasons for PoW implementation.

2.2.1 Point-on-Wave switching for capacitor banks

Point-on-Wave to prevent transients when energising a capacitor bank

The current through a capacitor is directly correlated to the rate of change of the voltage applied to the capacitor bank. At breaker closing, the voltage applied to the capacitor suddenly increases, thus yielding a high current. Furthermore, oscillatory behaviour can occur due to inductances in the circuit, e.g., inductance in the line between the source and the capacitor. Eventually, these oscillations are dampened by all the resistances, such as the source impedance and the line between the source and the capacitor. An example of this oscillating phenomenon is shown in Figure 2.5.

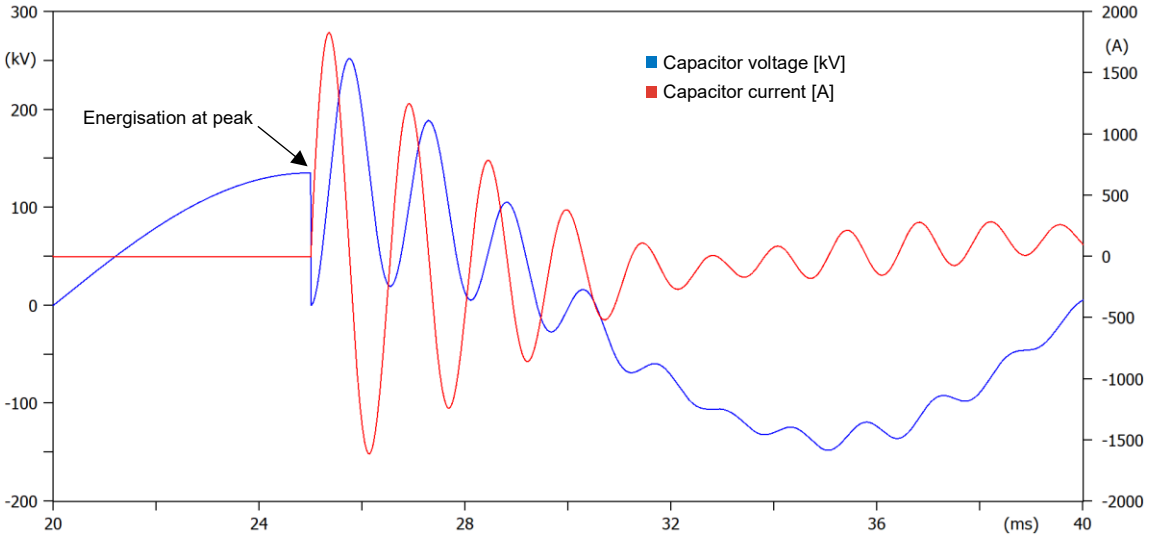

Figure 2.5: Capacitor voltage and current example during non-controlled capacitor bank switching

The exact behaviour can be modelled via differential equations. However, solving such equations is rather complicated. CIRGRE, however, has published a paper in which a time-domain solution is proposed. This time-domain solution is shown in equation 2.1 [12].

$$i(t) = I_m \frac{\beta}{\sqrt{LC}} e^{-\alpha t} \left\{ \sin(\theta_0 - \varphi) \sin(\beta t - \gamma) - \frac{1}{\omega\sqrt{LC}} \cos(\theta_0 - \varphi) \sin(\beta t) \right\} + I_m \sin(\omega t + \theta_0 - \varphi) \quad (2.1)$$

Where,

$$I_m : Amplitude\ of\ steady\ state\ current$$

$$\alpha : \frac{R}{2L}, \beta : \sqrt{\frac{1}{LC} - \left(\frac{R}{2L}\right)^2}, \gamma : \tan^{-1}\left(\frac{\alpha}{\beta}\right), \varphi : \tan^{-1}\left(\frac{\omega L - \frac{1}{\omega C}}{R}\right)$$

$$\theta_0 : Energisation\ angle, \quad \omega : Angular\ power\ frequency$$

The inrush current has a maximum value when $\theta_0 = \varphi$. When switching a capacitor bank (C >> L), this energisation angle is close to π/2. This is a logical outcome, as the voltage is approximately the highest at that point, yielding the highest voltage change when switching.

Point-on-Wave switching can potentially optimise these inrush currents in two ways:

1. By optimising the energisation angle so that the absolute maximum current of the equation is the lowest.
2. By optimising the energisation angle so that the absolute maximum of the transient current, the first part of the equation, is the lowest.

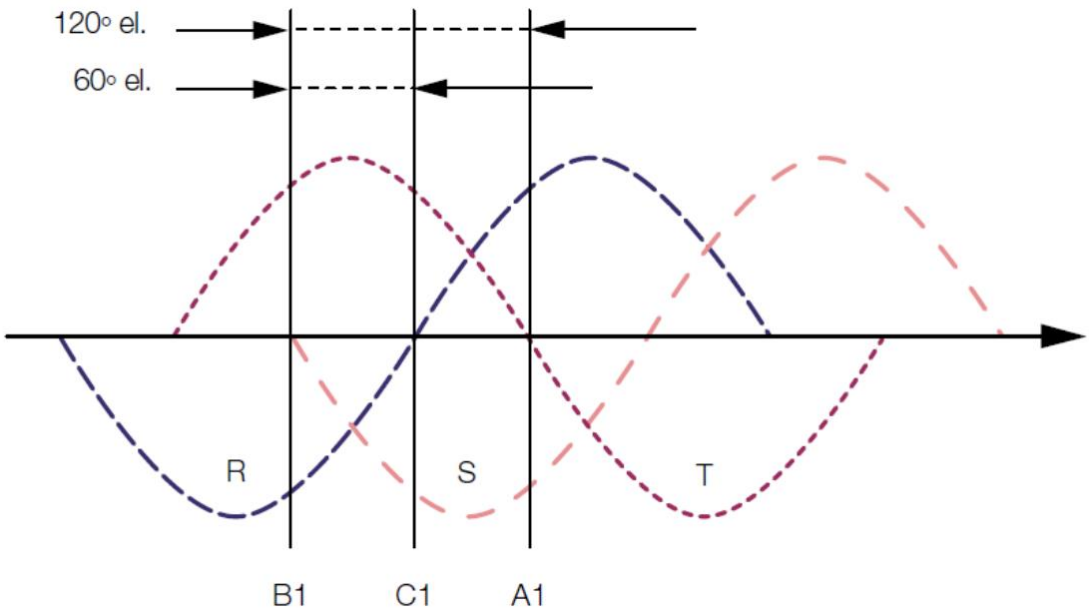

Figure 2.6: Example of ideal closing instants for a capacitor bank with grounded neutral [10]

Figure 2.6 illustrates an example of ideal closing moments when energising a grounded capacitor bank. One can observe that the perfect proposed closing instants are at each respective phase zero-crossing. If the phase voltage is at zero, then the phase voltage of the respective capacitor is also zero, as the capacitor bank has a grounded neutral.

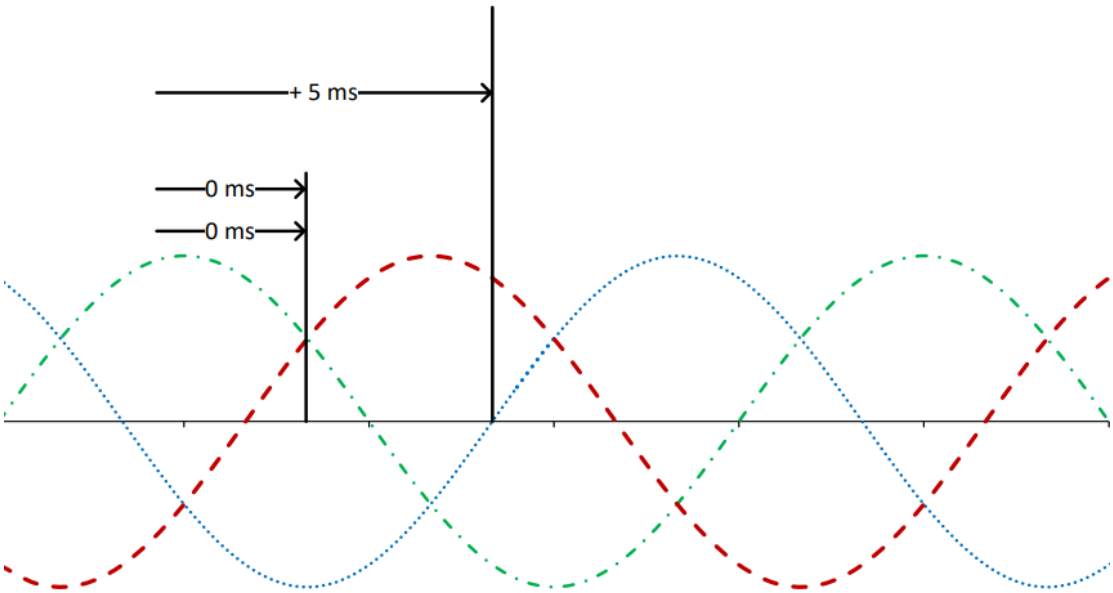

Figure 2.7: Example of ideal closing instants for a capacitor bank with isolated neutral [13]

Figure 2.7 illustrates an example of ideal closing instants for a capacitor bank with an isolated neutral. When the capacitor bank is isolated, a respective phase-to-ground zero voltage does not mean a zero voltage across the respective capacitor, as the capacitor voltages are determined by the voltage difference between the phases (phase-to-phase voltage). Therefore, the first two phases are closed when the potential difference between them is zero. The other phase is closed at its respective next zero-crossing.

Point-on-Wave for the prevention of re-ignitions during de-energisation

The dielectric strength of the breaker cannot instantaneously change. The RRDS describes how fast the dielectric strength of the breaker can rise (See section 2.1.2). If the breaker opening occurs at an instant in which the capacitor voltage is rising faster than the RRDS, a re-strike will occur. This problem can be mitigated by optimising the breaker opening instants with PoW.

2.2.2 Point-on-Wave for switching cable circuits (lines)

When a voltage is applied to a line, the voltage wave will travel through the line as a wave. When the impedance of the medium through which the wave travels suddenly increases, a part of the wave is reflected and added to the original voltage. When the line is open-ended, the new impedance can be considered infinite, thus yielding a full reflection of this voltage. As this full reflection is added to the original voltage, theoretically, a voltage peak of 2 p.u. can occur.

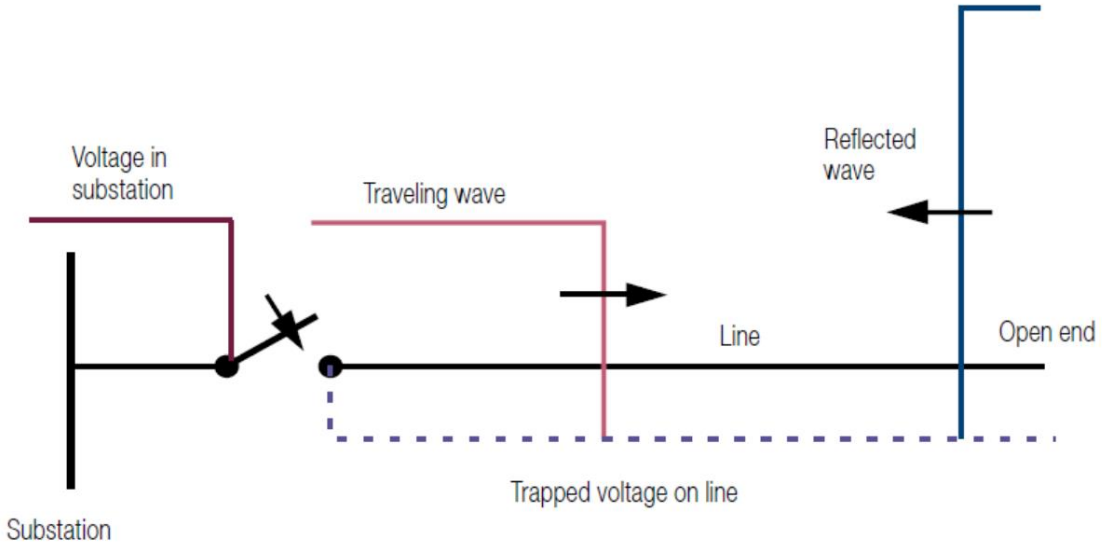

Figure 2.8: Travelling wave phenomenon [10]

When considering mitigation techniques, the transmission line arrangement must be taken into consideration [12]:

- Lines without compensation elements.
- Lines with shunt reactors.

Lines with shunt reactors (Shunt compensated line)

The application of PoW for switching shunt-compensated lines is not considered in this study. However, information about the optimal switching instant when switching shunt-compensated lines can be found in Appendix B.

Uncompensated lines

There is no shunt reactor present to compensate for the capacitive component in an uncompensated transmission line. Therefore, similar to the capacitor bank case, energising near voltage zero is optimal, as a DC offset in current will not occur. Energising near voltage zero will result in the lowest overvoltage transients. Furthermore, the de-energisation of an uncompensated line is similar to that of a capacitor bank, as an uncompensated line behaves primarily capacitive.

2.2.3 Point-on-Wave for other switching applications

Point-of-Wave switching can also be applied for other switching applications, namely:

- Point-on-Wave switching for preventing transients when de-energising shunt reactors.
- Point-on-Wave switching for energising transformers.
- Point-on-Wave switching for preventing overvoltages when de-energising power cables.

These applications, however, are not considered in this study. Nevertheless, Appendix B elaborates more on these PoW applications.

2.3 Point-on-Wave controller

For controlling the circuit breaker, a Point-on-Wave controller, also known as Synchronous Switching Controller (SSC) or Controlled Switching Device (CSD), is needed. This controller determines the optimal switching instant based on the desired switching application.

One of the biggest challenges of a CSD system is to dispatch control commands such that the CB contacts reach the desired electrical and mechanical targets at the optimal moment. It is required for the controller to know the voltage at the source for proper PoW switching. An input signal of the voltage at the load side is required for some applications, e.g., for switching applications involving residual flux [13]. A current input signal could be important for monitoring purposes or adaptive corrections [14]. The voltage signal can be realised with a voltage transformer (VT) and the current signal with a current transformer (CT). Figure 2.9 provides an example overview of the inputs and outputs of a Point-on-Wave controller.

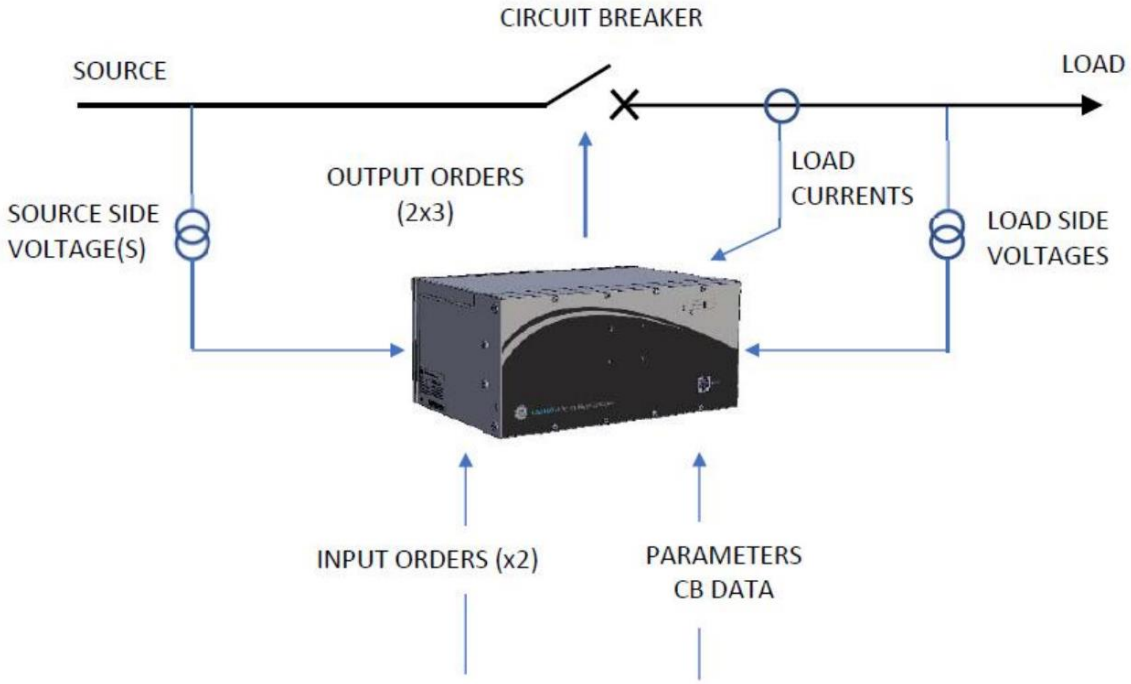

Figure 2.9: Input and output example of a Point-on-Wave controller [13]

3 Power quality and PoW policies of TenneT NL

3.1 Policy on Power Quality

In the Dutch grid code, all the requirements regarding the voltage quality are listed. NEN-EN 50160 is also included in this grid code [15]. Furthermore, NEN-EN 50160 is used by TenneT and ACM (Autoriteit Consument en Markt) as a guideline, except for a few deviations [16]. TenneT NL is obliged to comply with the Dutch "Grid code". In this section, requirements regarding the Power Quality of the grid are elaborated.

3.1.1 Rapid voltage changes (RVC)

Rapid Voltage Changes (RVCs) are considered changes in the half-cycle RMS line-to-line voltages by the Grid Code. The half-cycle RMS line-to-line voltage can be calculated with Equation 3.1.

$$U_{LL\,RMS}(t) = \sqrt{2f \int_{t-\frac{1}{2f}}^{t} U_{LL}(t)^2 dt} \tag{3.1}$$

where:

$$U_{LL}: instantaneous\ LL\ voltage, f: frequency\ of\ the\ source\ voltage$$

The limits regarding these RVCs are described by the allowed change of the steady-state RMS voltage ΔU_{ss} and the peak RMS voltage ΔU_{max} [17]. Equations 3.2 and 3.3 describe how these values can be calculated. Figure 3.1 shows the maximum and the steady-state RMS voltage change, respectively.

$$\Delta U_{ss} = \left|U_{ss_{new}} - U_{ss_{old}}\right| \rightarrow \Delta U_{ss}[\%] = \frac{\Delta U_{ss}}{U_{nom}} \cdot 100\% \tag{3.2}$$

$$\Delta U_{max} = \left|U_{peak} - U_{ss}\right| \rightarrow \Delta U_{max}[\%] = \frac{\Delta U_{max}}{U_{nom}} \cdot 100\% \tag{3.3}$$

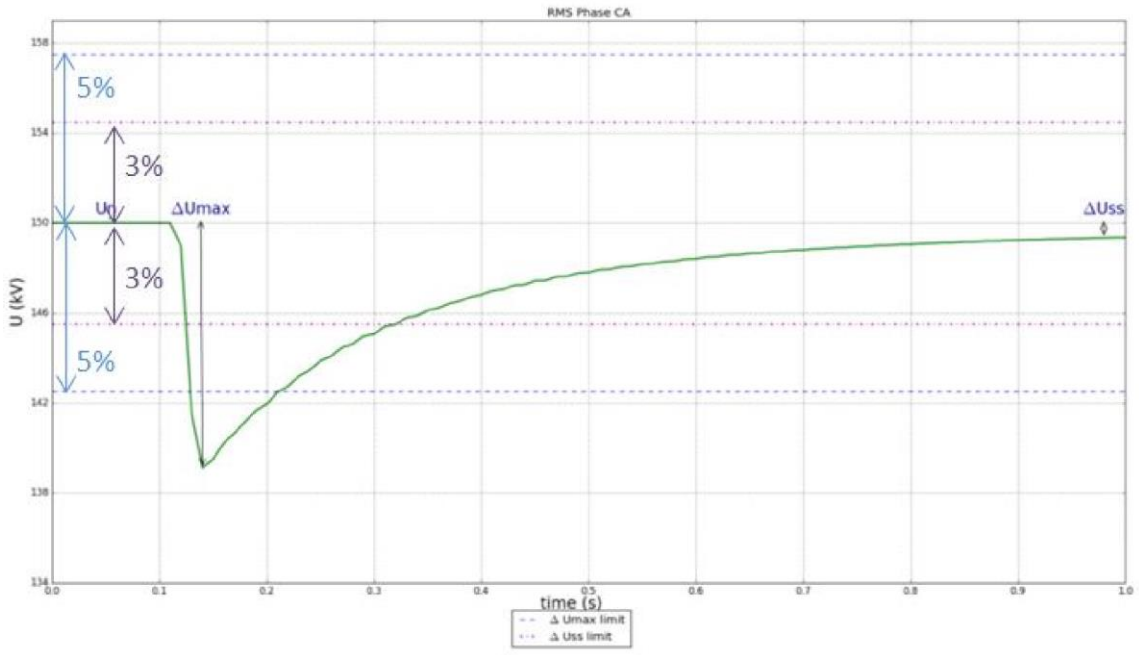

Figure 3.1: Description of the RVC definitions and the allowed limits [17]

Table 3.1: Limits regarding Rapid Voltage Changes for Uc ≥ 35kV [17]

Time	**Limit**
100%	$\Delta U_{ss} \leq 10\%\ U_n$
100%	$\Delta U_{ss} \leq 3\%\ U_n$*
100%	$\Delta U_{max} \leq 5\%$*

* In cases without failure of production, big users, or connections;

Table 3.1 describes the allowed limits regarding the Rapid Voltage Changes in more detail. One can observe that in case of exceedances of the ΔUmax limit, mitigation options should be considered to suppress the peak RMS line-to-line overvoltages below 1.05 p.u.

3.1.2 Other Power Quality-related aspects

There are more power quality-related distortions, such as harmonic distortion, flicker, and voltage asymmetry. However, these distortions are not applicable to the PoW implementation and are, therefore, not considered. Appendix C elaborates on the requirements regarding these distortions.

3.2 Policy on PoW application

Currently, TenneT NL applies a policy concerning the PoW application, as a mitigation option for meeting the power-quality requirements, as described in section 3.1. This policy applies to power transformers, underground cable and hybrid cable-line circuits, capacitor and filter banks. This section elaborates on the implementation of the associated requirements by TenneT.

3.2.1 PoW implementation for underground cable circuits

Whether PoW is implemented within TenneT for switching cable circuits depends on the length of the cable (see Table 3.2).

Table 3.2: TenneT's current implementation for switching cable circuits

Condition	Implementation of PoW
Cable length ≤ 10 km	PoW is not implemented
10 km < Cable length ≤ 20 km	An EMT study should be conducted to determine the need for PoW implementation
Cable length > 20 km	PoW is implemented

Furthermore, regarding the mitigation of the Rapid Voltage Changes (RVC), the following policy is applied by TenneT [17]:

- From the Power Quality perspective, PoW switching is regarded as an acceptable mitigation option against RVCs between 3% and 10%. For RVCs higher 10%, a different option should be applied, as a voltage dip is not acceptable.
- Inaccuracies of PoW switching shall be considered.

3.2.2 Implementation for switching capacitor banks

At the time of conducting this study, the policy for the PoW implementation for capacitor bank switching was still under development. A general requirement was that an EMT study should be conducted on a project basis to determine the need for PoW implementation, irrespective of the MVAr rating of the capacitor bank. Similar to the cable circuit switching, the following policy is applied:

- From the Power Quality perspective, PoW switching is regarded as an acceptable mitigation when the switching of a capacitor bank without PoW does not result in RVCs higher than 10%. Otherwise, a different option should be considered.
- Inaccuracies of PoW switching shall be considered.

4 Study approach and assumptions

It is essential to have a defined plan before designing the simulation models and performing the simulations.

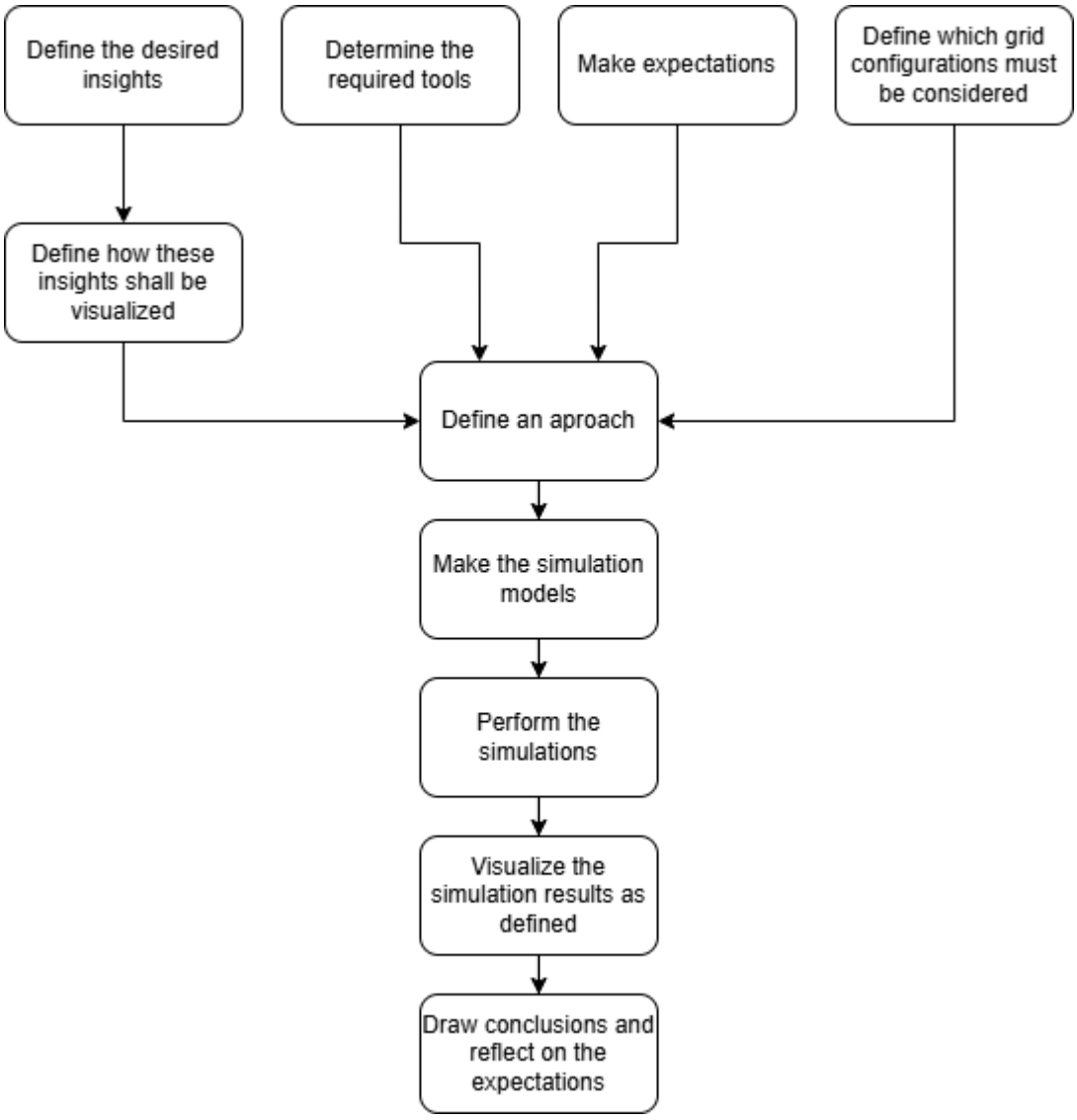

Figure 4.1: Simulation plan

This chapter further elaborates on the simulation plan by describing the aspects shown in Figure 4.1.

4.1 Desired simulation outcomes

It is essential to define all the desired outcomes before setting up a modelling plan, as they will affect the required model. Furthermore, it is important to specify how the data must be presented.

4.1.1 Desired insights

Performed simulations should provide insight into:
- The overall effectiveness of PoW for energising cable circuits and capacitor banks.
- The effect of switching imperfection, such as pole scatter and imperfect RDDS, on the effectiveness of PoW.
- The effect of imperfect compensation of external variables, such as variations in control voltage, temperature, hydraulic pressure, idle time and mechanical time drift.

The effectiveness of PoW is described by the following aspects:
- The difference between the maximum overvoltages with and without PoW.
- The difference between the maximum inrush currents with and without PoW.
- Whether the overvoltages comply with TenneT's policies and the Grid Code.

In this study, de-energisation of capacitor banks and cable circuits is not considered, as during de-energisation, the grid is less prone to RVCs and inrush currents (see Section 2.1.2).

4.1.2 Desired representation of the simulation outcomes

The overall effectiveness of PoW switching

The overall effectiveness of PoW can be determined by comparing the peak overvoltages and inrush currents with and without the implementation of PoW. This comparison must be made by depicting box plots of the statistical simulation data with and without the utilisation of PoW for the capacitor banks and cable circuits.

The effect of deviations from the optimal switching instant

As the scatter is described by a Gaussian distribution, comparisons between different standard deviation values must be made to gain insight into the effect of scatter on the effectiveness of PoW. This can be done by representing the statistical data of the peak overvoltages and inrush currents via box plots.

The effect of non-ideal RDDS

To gain insight into the effect of RDDS, a comparison must be made between a CB with an infinitely high RDDS (ideal CB) and an RDDS that is most applicable to the switching gear used by TenneT. Again, the statistical box plots of the peak overvoltages and inrush currents must be depicted to present the comparison.

4.2 Approach

In this section, the simulation approach is divided into multiple parts. Each part has its simulation model configuration. Ultimately, the simulation outcomes of each part must be compared to each other to gain answers to the research questions.

4.2.1 Determining the effectiveness of PoW

To determine the effectiveness of PoW, the switching surge with and without PoW must be considered. Otherwise, it would not be possible to make a comparison.

Without PoW

When there is no PoW utilised, the switching instant is random. However, all three switching poles are commanded to close at the same random instant, but the exact closure instant can vary a bit due to pole scatter. This pole scatter has to be taken into account. Due to the randomness of the scatter and the closing instant, multiple simulations must be performed for different capacitor and cable circuit

configurations to gain insight into the peak overvoltages and inrush currents that can occur if no PoW is utilised.

With PoW

If PoW is applied, the commanded closing instant is perfectly at the zero-crossing of every phase. However, statistical pole scatter is still playing a role. Therefore, again, multiple statistical simulations must be performed to give insight into the peak overvoltages and inrush currents that can occur if PoW is utilised.

4.2.2 Determining the effect of breaker imperfections on the effectiveness of PoW

To determine the effect of breaker imperfections on the effectiveness of PoW, multiple simulations have to be performed in which the imperfections are implemented to varying degrees. These outcomes have to be compared to the ideal PoW implementation result.

Pole scatter

Pole scatter, or breaker scatter, can be simulated by running multiple statistical simulations with different pole scatter standard deviations. The effect of pole scatter can then be visualised by depicting peak overvoltages and inrush currents for the different standard deviations.

Rate of Decrease of Dielectric Strength

To determine the effect of imperfect RDDS, all desired simulations must be performed with an ideal switch (infinitely high RDDS) and with an RDDS that is the most applicable to TenneT's switching gear. In this way, it is possible to compare the effect of RDDS on the effectiveness of PoW.

4.2.3 Determining the effect of imperfect compensation of external variables

Imperfect compensation of external variables results in deviations in the actual switching instant. However, the exact relationship between the switching deviations and imperfect compensation of the possible external variables, such as temperature or control voltage, is unknown, as it falls outside the scope of this study. Still, an impression of the effect of imperfect compensation can be made by studying the outcomes for different pole scatter values.

4.3 Implementation of PoW in EMTP-ATP

In this section, the exact implementation of PoW in the EMTP-ATP environment is described.

4.3.1 Specification of different simulation configurations

Cable configurations

Regarding the cable configuration, three types of aluminium cables are considered (see Table 4.1).

Table 4.1: Cable dimensions [18] [19] [20]

Cable type	Rout (Conductor)	Rin (Sheath)	Rout (Sheath)
1x1600 mm2 aluminium	25,2 mm	46,5 mm	47,5 mm
1x2500 mm2 aluminium	30,8 mm	51,4 mm	52,5 mm
1x3500 mm2 aluminium	36,3 mm	58,3 mm	59,5 mm

For each cable, six different lengths are considered, which are 10.5 km, 15 km, 21km, 30 km, and 49.5 km. These lengths are chosen to be divisible by 1.5, as sheath cross-bonding is applied after every 1.5 km of cable.

Capacitor bank configurations

Capacitor banks with the following power ratings are considered: 25 MVAr, 50MVAr, 75 MVAr, and 100 MVAr. As the base voltage is 150 kV and the frequency is 50 Hz, the corresponding capacitances are: 3.5 µF, 7.1 µF, 10.6 µF, and 14.1 µF. Furthermore, only capacitor banks with a grounded neutral are considered.

Variation in the deviation of the switching instant

The variation of the switching instants is simulated via a Gaussian distribution (see Figure 4.2). A standard deviation σ of 0.15 ms is chosen, as it corresponds best to the performance of the switching gear used by TenneT [21]. This means that 68,2% of the simulated deviations fall within 0.15 ms.

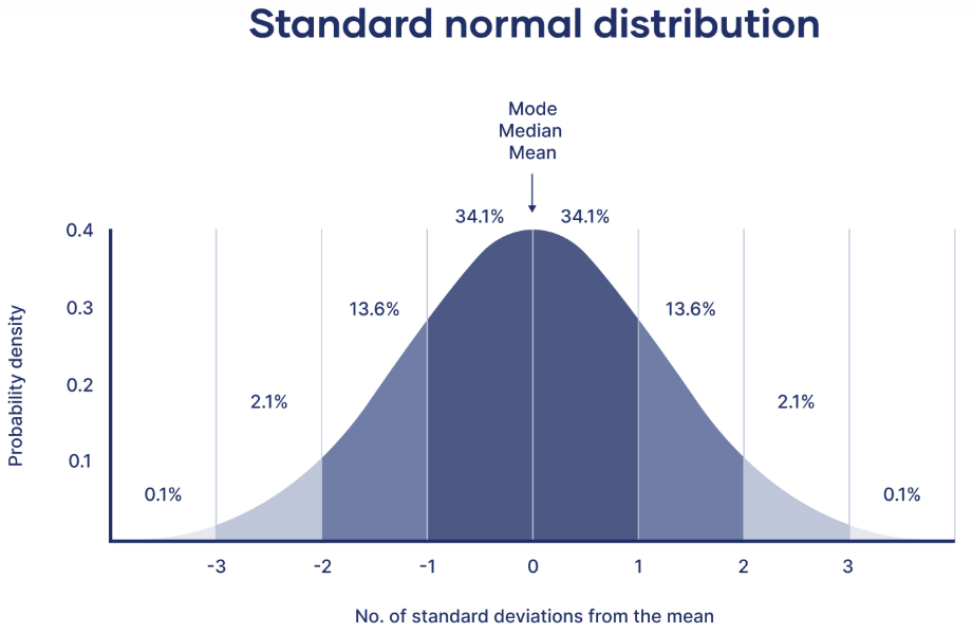

Figure 4.2: Gaussian distribution [22]

Imperfect RDDS

The movement time of the CB contacts and the maximum dielectric strength determine the “Rate of Decrease in Dielectric Strength” (RDDS).

The RDDS can be calculated with the following formula:

$$RDDS = \frac{U_{CB\ max}}{t_{CB\ movement}}$$

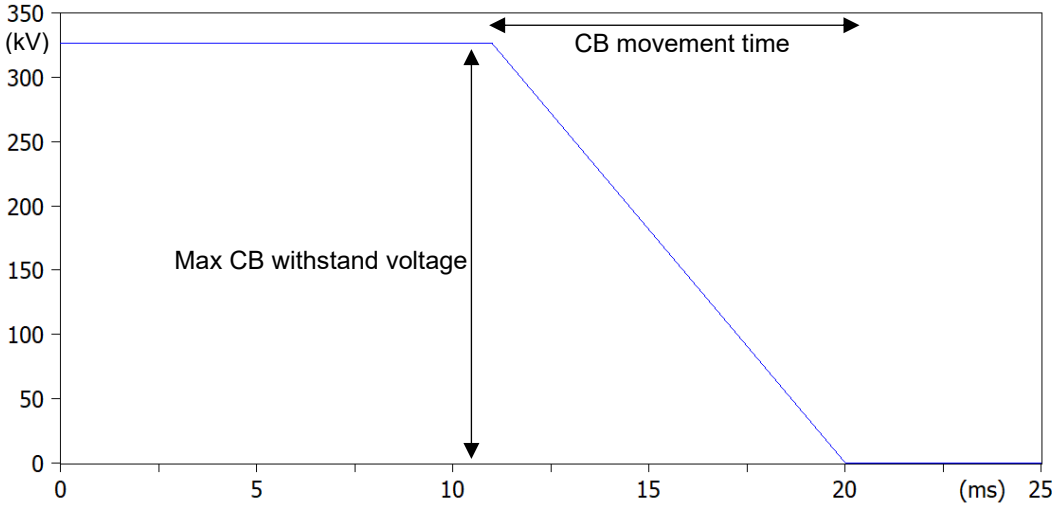

Figure 4.3: Example of CB withstand voltage during switching operation

Preferably, a realistic RDDS value is chosen to show the effect of RDDS on the effectiveness of PoW. Therefore, a performance test for a TenneT commonly implemented switchgear is applied to determine the most realistic RDDS value.

During a CB closure test of a CB commonly used by TenneT, a prestrike of 2.3 ms at 206.5 kV was measured [23]. This means that the corresponding RDDS would approximately be 90 kV/ms (206.5/2.3). Therefore, a RDDS of 90 kV/ms is used for the simulations.

Number of simulation runs

All the simulations will be run 200 times to acquire an accurate result. This value is chosen based on an accuracy comparison between 100 and 200 runs.

100 runs				200 runs		
	Standard deviation [s]	Error [s]			Standard deviation [s]	Error [s]
1	0,000134202	1,58E-05		1	0,000151798	1,80E-06
2	0,000148803	1,20E-06		2	0,000154638	4,64E-06
3	0,000158642	8,64E-06		3	0,000145775	4,23E-06
4	0,00016704	1,70E-05		4	0,000163962	1,40E-05
5	0,000138084	1,19E-05		5	0,000156744	6,74E-06
6	0,000164108	1,41E-05		6	0,000155071	5,07E-06
7	0,000153916	3,92E-06		7	0,000147325	2,68E-06
8	0,000143305	6,70E-06		8	0,000147544	2,46E-06
9	0,000140227	9,77E-06		9	0,000142461	7,54E-06
10	0,000138873	1,11E-05		10	0,000142665	7,33E-06
11	0,0001343	1,57E-05		11	0,000160871	1,09E-05
12	0,000138469	1,15E-05		12	0,000146722	3,28E-06
	Average error [s]:	1,06E-05			Average error [s]:	5,88E-06

Figure 4.4: Comparison between 100 and 200 runs

In Figure 4.4, a comparison between 100 and 200 simulations is shown by listing the standard deviation and the relative error for the 0.15 ms standard deviation of 12 sets of 100 or 200 runs, respectively. This data is obtained with the Excel Typescript code presented in Appendix D. It can be observed that 200 runs are more accurate than 100 runs, as the observed standard deviation errors are overall smaller for the 200 runs. 200 runs are chosen, as only 17% of the sets have a bigger error than 0.01 ms, compared to 50% for the 100 simulations case. Even more simulations than 200 would increase the accuracy more, but also require more computational power, and is, therefore, not chosen.

4.3.2 EMTP-ATP model

The grid model

In Figure 4.5, the simplified grid model used is depicted. The model consists of two transformers connected in parallel, an ideal voltage source, and an impedance between the transformer and source. This grid model represents a common grid scenario within TenneT.

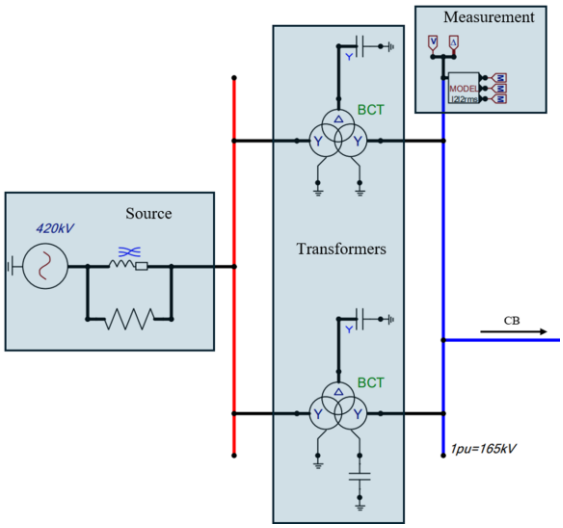

Figure 4.5: The grid model in EMTP-ATP

Ideal switch

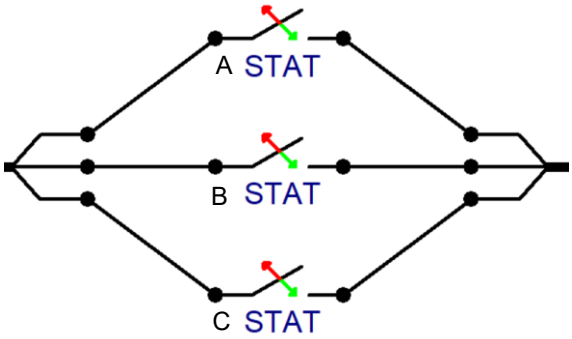

Figure 4.7: For simulating with PoW

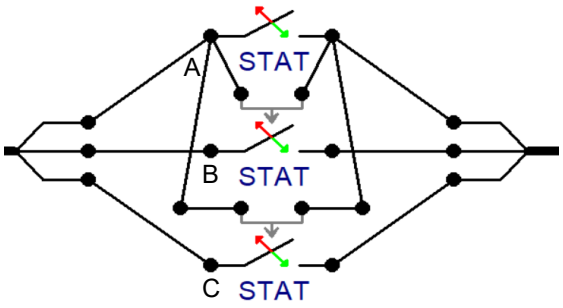

Figure 4.6: For simulating without PoW

Figure 4.7 depicts the ATP-EMTP implementation of the PoW switching behaviour. Every statistic switch closes independently to simulate the PoW switching at every pole (see Table 4.2).

Table 4.2: Description of closing instants when PoW is not simulated

Phase	Closing instant
Switch A	Master switch that closes based on a uniform distribution between two peak voltages, e.g., between 0.15-0.35 ms
Switch B	Slave switch that closes according to the Gaussian distribution with the closing instant of switch A as the mean value.
Switch C	Slave switch that closes according to the Gaussian distribution with the closing instant of switch A as the mean value.

Figure 4.6 depicts the implementation of the switching behaviour without PoW implementation. The first pole closes at a random instant based on a uniform distribution. The other poles close around that instant based on a Gaussian distribution with a standard deviation of 0.15 mm (see Table 4.3).

Table 4.3: Description of closing instants when PoW is simulated

Phase	Closing instant
Switch A	Independent switch that closes according to the Gaussian distribution with the zero voltage instant of phase A as the mean value.
Switch B	Independent switch that closes according to the Gaussian distribution with the zero voltage instant of phase B as the mean value.
Switch C	Independent switch that closes according to the Gaussian distribution with the zero voltage instant of phase C as the mean value.

Circuit breaker with RDDS

For the modelling of a CB with non-ideal RDDS, a TACS switch and a programmed MODEL are used (see Figure 4.8). The TACS switch is a switch that closes if a positive signal is applied to the TACS signal input. In the MODEL, the TACS signal is determined accordingly based on the RDDS, target switching instant and the instantaneous voltage across the CB.

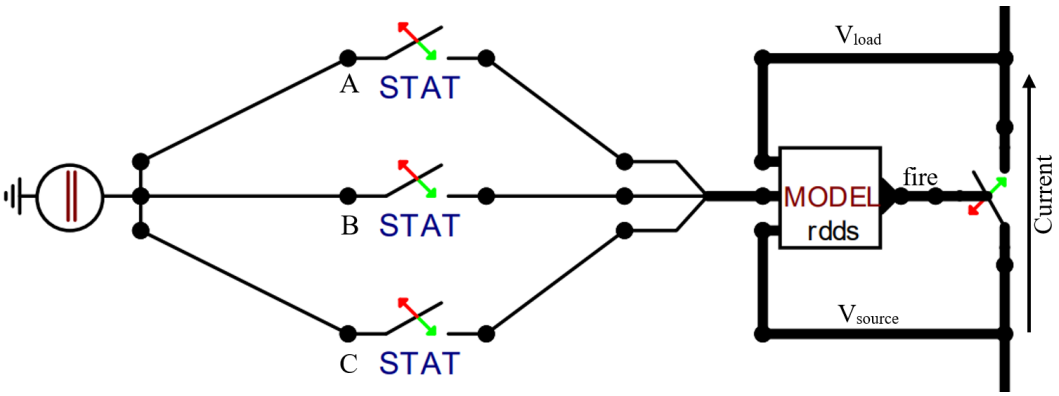

Figure 4.8: Model of CB with non-ideal RDDS

RMS scope

According to the Grid Code, for determining the RVCs in the TenneT Onshore grid, the half-cycle RMS value must be used. The half-cycle RMS value can be calculated with the following formula:

$$U_{LL\,RMS}(t) = \sqrt{2f \int_{t-\frac{1}{2f}}^{t} U_{LL}(t)^2 dt}$$

This formula is implemented in a so-called MODEL (see Figure 4.9). This MODEL calculates the continuous half-cycle phase-to-phase RMS voltages.

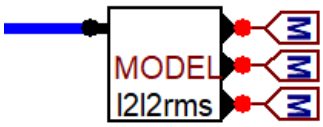

Figure 4.9: Implementation of RMS voltage scope

Extraction of the peak values and switching instants

To extract the peak values, the “EXTREMA OUTPUT FOR EXCEL” command is used in the “User specified” block. This creates an Excel file with all the extrema. An Excel Typescript code is written to extract and organise this data, which is described in Appendix D.

For testing the statistical accuracy of EMTP-ATP (see Section 4.3.1) and to plot the instantaneous graphs of specific outliers, code has been written to extract the exact switching instances of every pole (see Appendix D).

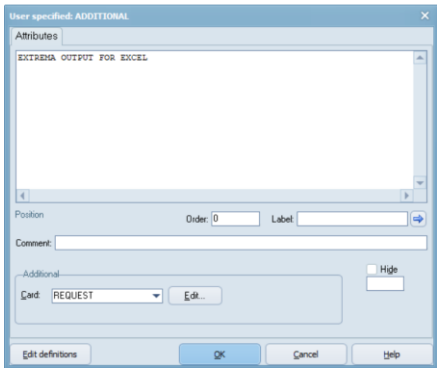

Figure 4.10: User specified -> Additional block

Cable implementation

Figure 4.11 depicts the implementation of a short cable. After every 1.5 km, cross-bonding is applied to the shielding. This cross-bonding is implemented to cancel out the induced voltages in the shielding.

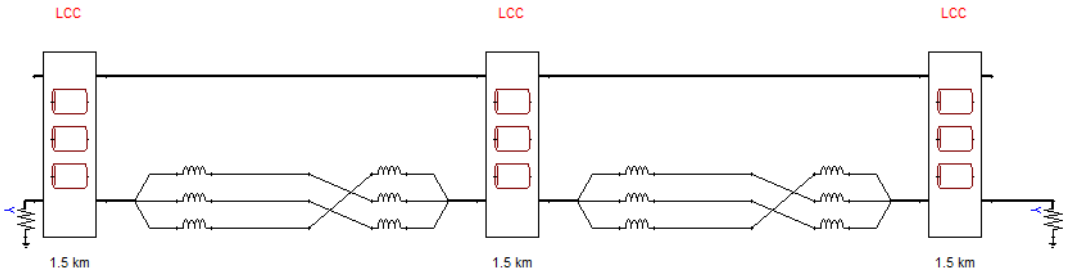

Figure 4.11: Implementation of a cable

An example configuration of a 1.5 km cable part is depicted in Figure 4.12. In this menu, parameters such as conductor sizes and conductor locations can be configured.

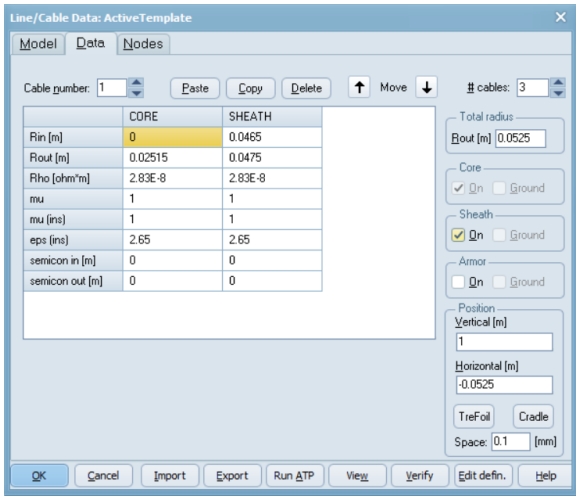

Figure 4.12: Configuration of a cable

4.4 Expectations

Setting expectations is important to minimise errors, as deviations from expectations prompt re-evaluation of potentially inaccurate results. This section elaborates on these expectations.

4.4.1 Expected effectiveness of PoW switching

It is hard to predict expectations regarding the effectiveness of PoW, as they depend on the configuration. However, within TenneT, an EMT analysis was performed on various capacitor banks [24]. In that study, a reduction in overvoltage from 8% (switched at peak voltage) to 4.5% (switched at zero voltage) was observed at a 110 kV 60MVAr capacitor bank. It is expected that the result of this study can be referred to this outcome if the differences in voltage and capacitance are considered.

4.4.2 Expected impact of deviations in switching instant on the effect of PoW switching

Deviations from the switching instant are expected to negatively impact the effectiveness of PoW. Presumably, up to 90 degrees, a higher deviation means worse PoW effectiveness. A deviation of 90 degrees is expected to result in the highest overvoltages, as this is the shift between zero and peak voltage. For the statistical study, however, the switching deviations are based on a Gaussian distribution. Therefore, one would expect to see bigger transient overvoltages and inrush currents for higher standard deviations.

4.4.3 Expected impact of RDDS on the effectiveness of PoW

For the statistical study, one would expect that an increase in RDDS results in a wider spread in transient overvoltages and inrush currents, as the limited RDDS causes pre-strikes. However, if the slope of the RDDS is lower than the highest slope of the voltage across the breaker, one would expect a severe increase in transient overvoltages and inrush currents, due to the pre-strikes. Figure 4.13 depicts an RDDS that is equal to the steepest slope of the sine wave and a target instant. One can observe that no pre-strike occurs in this case. However, a slight decrease in RDDS can result in a significant pre-strike (see Figure 4.14).

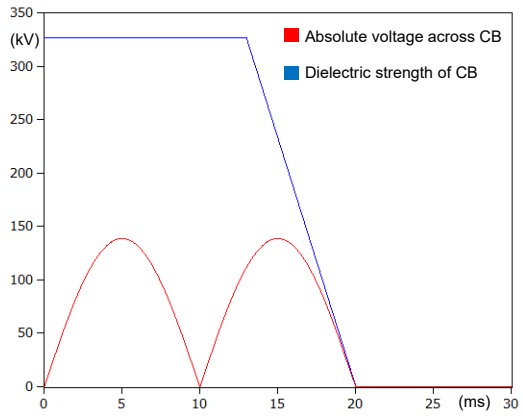

Figure 4.13: Sufficient RDDS

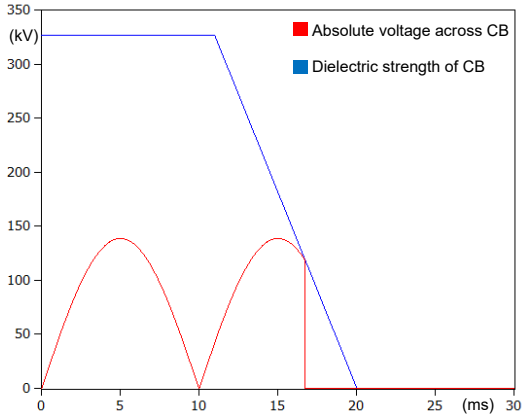

Figure 4.14: Insufficient RDDS

5 Simulation results: Capacitor bank energisations

In this chapter, the simulation results regarding capacitor bank energisation are presented. Firstly, the results on the effectiveness of PoW are summarised for the various capacitor bank sizes and RDDS values considered in the study. Then, the analysis results of the effect of pole scatter on the effectiveness of PoW are presented.

5.1 Effectiveness of PoW implementation

As described in Chapter 4, the simulation analysis considered two cases for the RDDS value, namely a) the ideal CB case (i.e., infinite RDDS) and b) the CB case with an RDDS of 90 kV/ms, as this RDDS corresponds to a typical characteristic of standard 170 kV circuit breakers used by TenneT NL (see Section 4.3.1).

5.1.1 Inrush currents

Figure 5.2 depicts the effectiveness of PoW for multiple capacitor bank sizes on the reduction of inrush currents. This effectiveness is presented by depicting the statistical data with a boxplot. As can be seen in Figure 5.1, the boxplot visualises the data by putting it in multiple categories. The average value is not described in Figure 5.1, but it is indicated with a cross in the simulation result data.

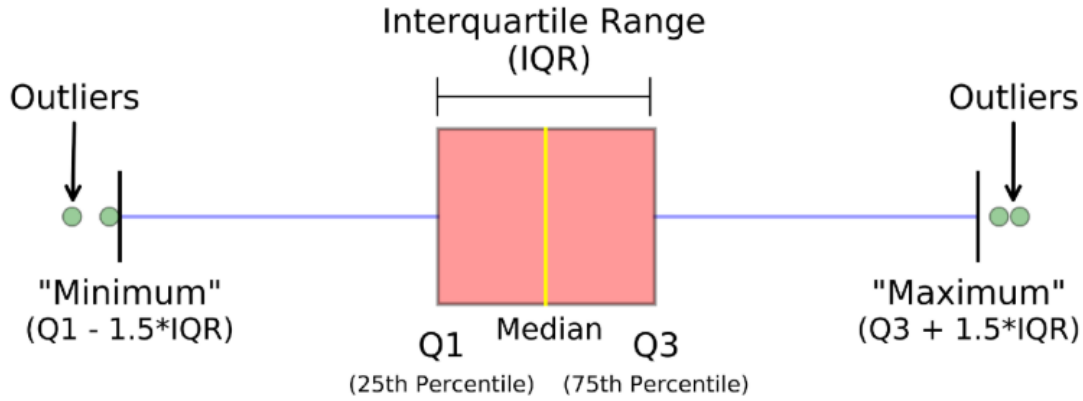

Figure 5.1: Technical description of a boxplot [25]

Remarks about a boxplot:

- 50% of all values lie within the interquartile range (IQR), between the first (Q1) and third quartile (Q3).
- The median represents the central value of the dataset.
- 25% of the values fall between Q1 and the median, and another 25% fall between the median and Q3.
- The minimum and maximum values are typically within 1.5 times the IQR from the nearest quartile (Q1 or Q3). Values beyond this range are considered outliers.

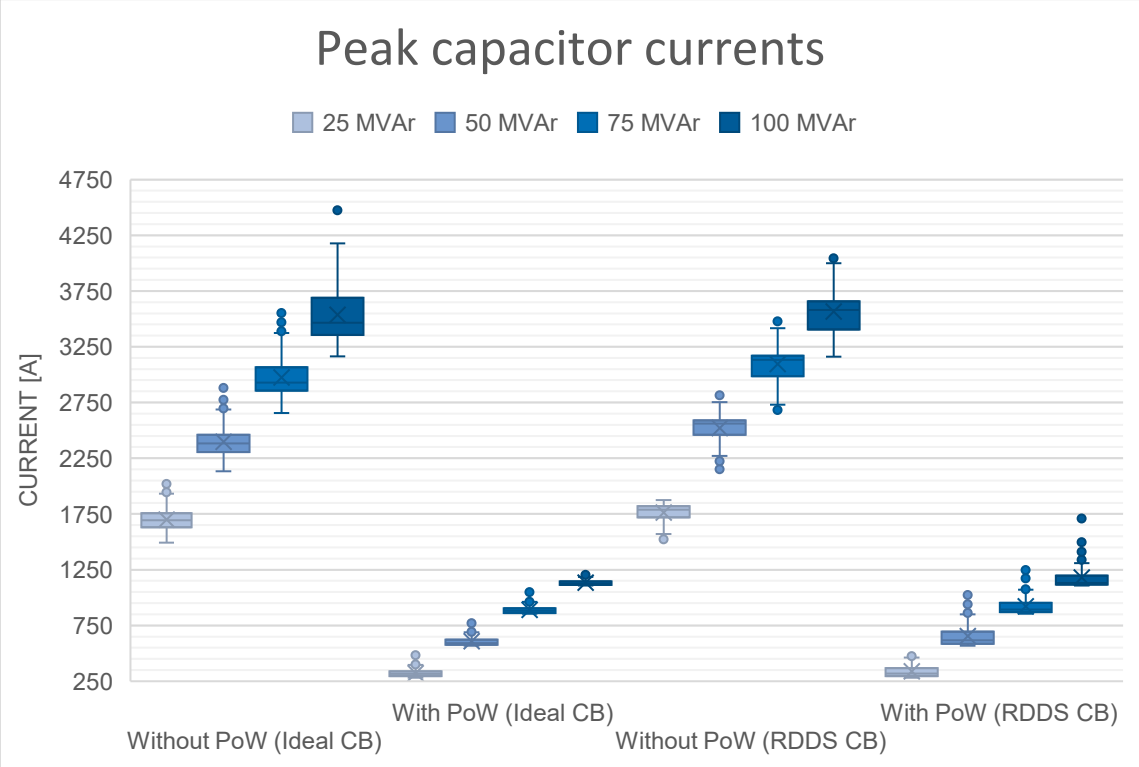

Figure 5.2: Effectiveness of PoW on the inrush currents

One can observe in Figure 5.2 that an increase in capacitor size increases current, as a capacitor's impedance is inversely proportional to its capacitance. This not only affects the inrush currents but also the nominal currents. The nominal peak current and nominal RMS current can be calculated with equations 5.1 and 5.2.

$$I_{peak} = 2\pi f C V_{peak} \quad (5.1)$$

$$I_{rms} = 2\pi f C V_{rms} \quad (5.2)$$

Where:

$$f: frequency, C: capacitance, V_{peak}: nominal\ peak\ voltage$$
$$V_{rms}: nominal\ RMS\ voltage, I_{peak}: nominal\ peak\ current,$$
$$I_{rms}: nominal\ RMS\ current$$

Table 5.1: Nominal currents per capacitor bank size

Capacitor bank size	Nominal RMS current [A]	Nominal peak current [A]
25 MVAr	105,38	149,03
50 MVAr	213,77	302,32
75 MVAr	319,15	451,35
100 MVAr	424,53	600,38

In Table 5.1, the nominal RMS currents and nominal peak currents of each capacitor bank for the nominal voltage and frequency are listed. As the nominal current also increases with the capacitor bank size, the exact effectiveness of PoW becomes unclear. However, in Figure 5.3, the scaled peak capacitor currents are depicted, offering a clearer illustration of the effectiveness of PoW in suppressing the inrush currents relative to the capacitor bank size.

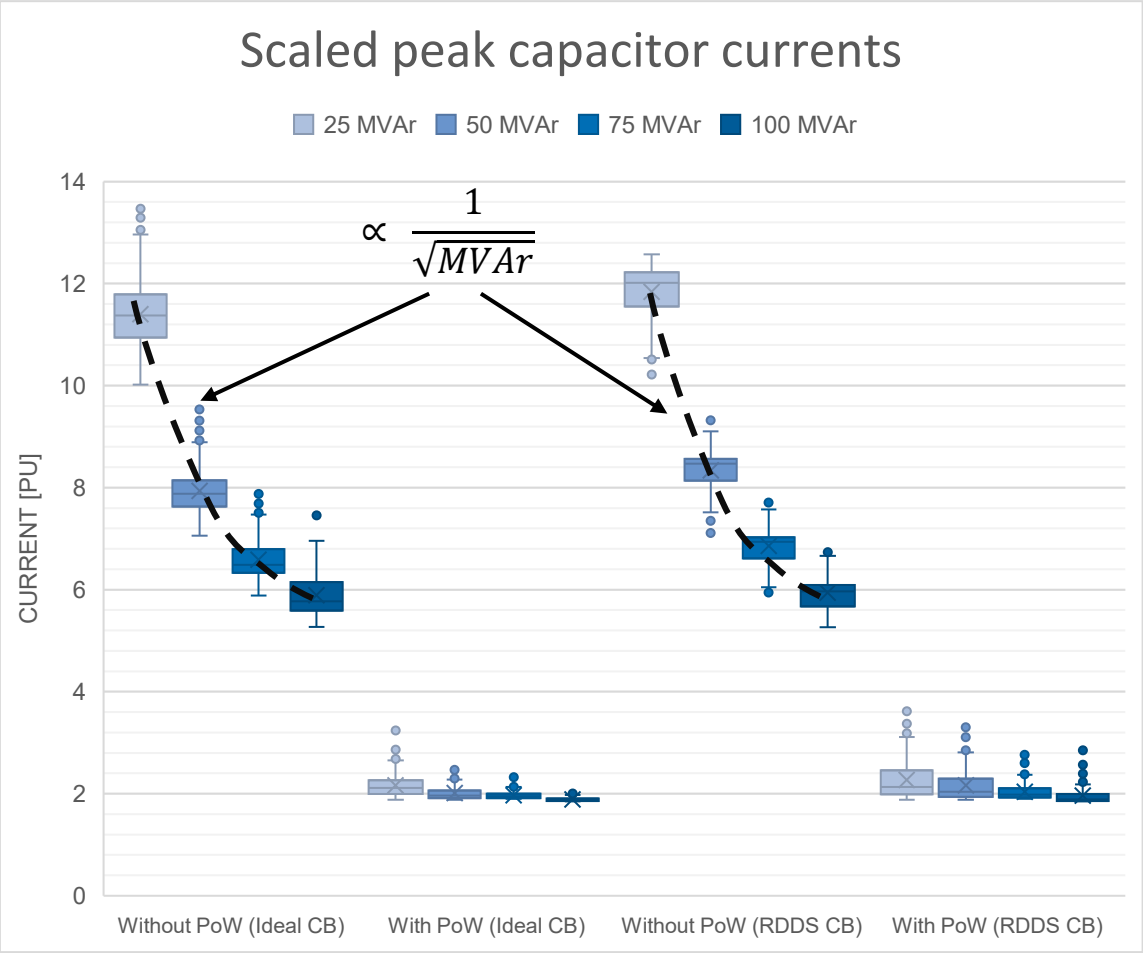

Figure 5.3: Scaled peak capacitor currents

Based on this plot, the following remarks can be made:

- Without PoW utilisation, the relative peak inrush current decreases by a factor of approximately $\sqrt{2}$ when the capacitor bank size doubles.
- With PoW utilisation, a similar trend can be observed compared to the case without PoW, but the values of every capacitor bank lie much closer compared to the case without PoW.
- For the case with PoW and RDDS, more outliers are observed compared to the case with PoW and an infinite RDDS (ideal CB). Because of the limited RDDS, the CB's making instant can be shifted (see Figure 5.4), resulting in a larger deviation in switching instant, thus resulting in bigger outliers.
- With PoW implementation, the scaled inrush currents stay rather constant around 2 p.u. As a consequence, full inrush current mitigation is impossible with only PoW switching.

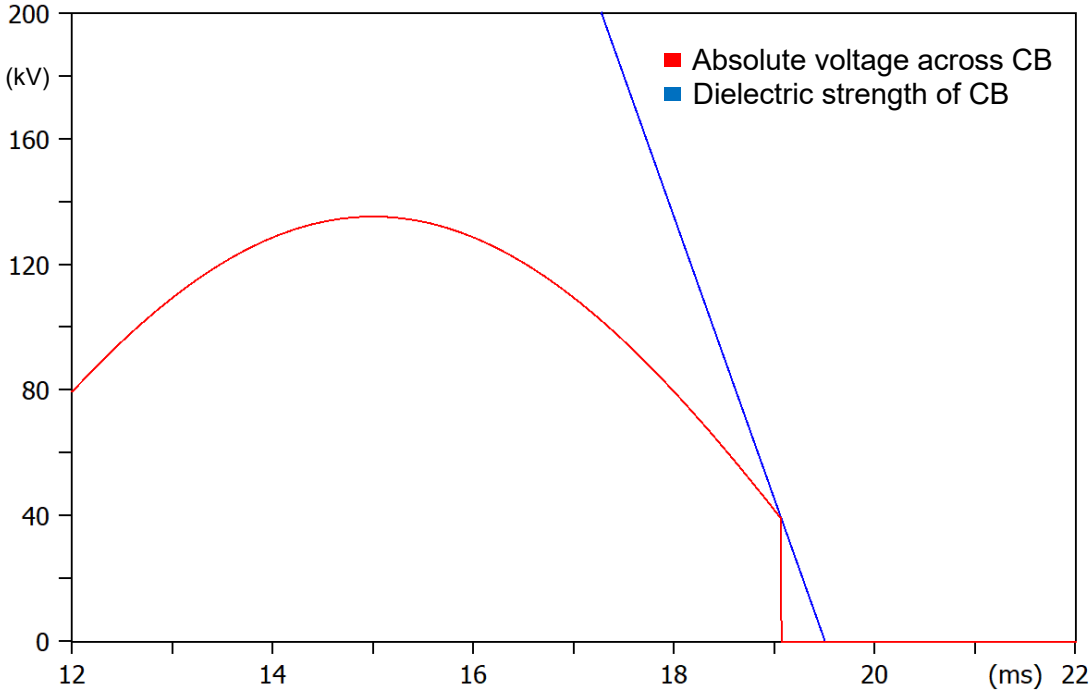

Figure 5.4: Effect of RDDS on the making instant

Explanation for the peak inrush current to be twice the peak nominal current when energised at zero voltage

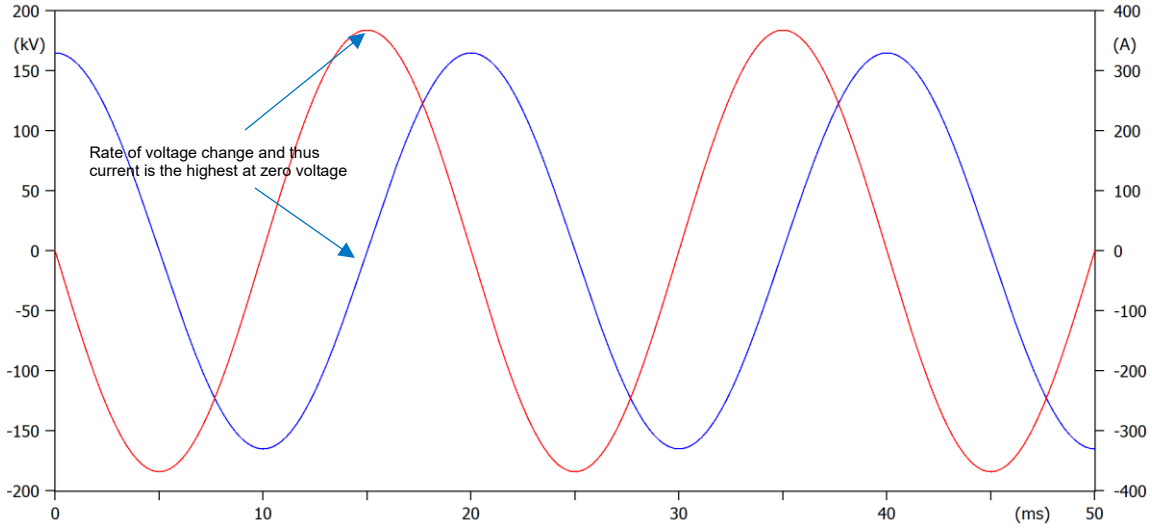

Figure 5.5: Relation between capacitor voltage and current

The current flowing through the capacitor is directly proportional to the rate of change of the voltage across it. As a result, the capacitor current reaches its maximum when the capacitor voltage is zero (see Figure 5.5). When the capacitor is energised at this zero-voltage point, the source attempts to drive the capacitor current instantly to its nominal peak value. However, this abrupt change in current is physically impossible due to the presence of the inductor in series. To satisfy the initial condition of zero inductor current at the moment of switching, a transient current is induced with an amplitude equal to the nominal current. This transient component superimposes on the forced (steady-state) current, resulting in a peak current amplitude that is twice the nominal current.

Mathematical proof that the relative peak current decreases with approximately $\sqrt{2}$ per capacitor doubling

The reason the relative peak inrush current without PoW decreases by a factor of approximately √2 per capacitor bank size doubling, while the with PoW case shows little change (see Figure 5.3), is due to the physical transient behaviour of an RLC circuit. The worst-case inrush current occurs when switching at peak voltage, as this effectively applies a voltage step to the circuit. Close to the moment of breaker operation, the inrush current therefore resembles the step response of a series RLC circuit (see Figure 5.6).

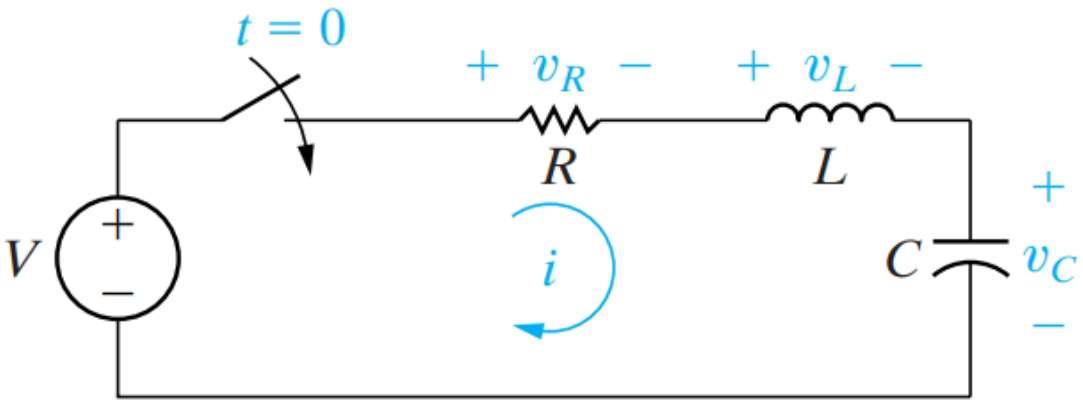

Figure 5.6: Circuit to illustrate the step response of a series RLC circuit [26]

To determine the current step response, a second-order differential equation can be formulated and solved. The solution for this equation is also presented in *Electric Circuits* by Nilsson and Riedel [26], as shown below.

$$i(t) = A_1 e^{s_1 t} + A_2 e^{s_2 t} \quad (overdamped)$$
$$i(t) = B_1 e^{-\alpha t}\cos(\omega_d t) + B_2 e^{-\alpha t}\sin(\omega_d t) \quad (underdamped)$$
$$i(t) = D_1 t e^{-\alpha t} + D_2 e^{-\alpha t} \quad (critically\ damped)$$

where:

$$\alpha = \frac{R}{2L}\ rad/s, \quad \omega_0 = \frac{1}{\sqrt{LC}} rad/s$$
$$\omega_d = \sqrt{\omega_0^2 - \alpha_0^2}$$
$$s_{1,2} = -\alpha \pm \sqrt{\alpha^2 - \omega_0^2}$$

As the peak scaled inrush currents are higher than 1 p.u. (see), the response is underdampened

Therefore:

$$i(t) = B_1 e^{-\alpha t}\cos(\omega_d t) + B_2 e^{-\alpha t}\sin(\omega_d t) \tag{5.3}$$

The initial conditions must be considered to find the values for B_1 and B_2:

$$I(0) = 0 \tag{5.4}$$
$$I'(0^+) = \frac{V_{step}}{L} \tag{5.5}$$

The initial condition given in Equation 5.5 follows from the fact that, at t=0, the entire voltage V_{step} appears across the inductor, as the voltages across the resistor and capacitor are zero due to the absence of current.

By substituting the initial condition from Equation 5.4 into the current expression in Equation 5.3, the value of B_1 can be determined:

$$B_1 e^{-\alpha * 0}\cos(\omega_d * 0) + B_2 e^{-\alpha * 0}\sin(\omega_d * 0) = 0 \rightarrow B_1 = 0$$

This simplifies Equation 5.3 to:

$$i(t) = B_2 e^{-\alpha t}\sin(\omega_d t) \tag{5.6}$$

The derivative of the current in Equation 5.6 must be calculated to determine the value of B_2:

$$i'(t) = B_2\left(\frac{d(e^{-\alpha t})}{dt}\sin(\omega_d t) + e^{-\alpha t}\frac{d\sin(\omega_d t)}{dt}\right) = B_2(\omega_d \mathrm{e}^{-\alpha t}\cos(\omega_d t) - \alpha e^{-\alpha t}\sin(\omega_d t)) \tag{5.7}$$

By substituting the initial condition from Equation 5.5 into the current expression in Equation 5.7, the value of B_2 can be determined:

$$B_2(\omega_d \mathrm{e}^{-\alpha * 0}\cos(\omega_d * 0) - \alpha e^{-\alpha * 0}\sin(\omega_d * 0)) = \frac{V_{step}}{L} \rightarrow B_2 = \frac{V_{step}}{L\omega_d}$$

The final current step response becomes:

$$i_{step}(t) = \frac{v_{step}}{L\omega_d}e^{-\alpha t}\sin(\omega_d t) = \frac{v_{step}}{L\sqrt{\frac{1}{LC} - \left(\frac{R}{2L}\right)^2}}e^{-\frac{R}{2L}t}\sin(\omega_d t) \tag{5.8}$$

Assuming that the resistance is negligible, such that $\frac{1}{LC} \gg \frac{R}{2L}$:

$$i_{step}(t) = \frac{v_{step}\sqrt{LC}}{L}e^{-\frac{R}{2L}t}\sin(\omega_d t) \tag{5.9}$$

One can observe from the step response expression shown in Equation 5.9 that when the step voltage V_{step}, which is the voltage at energisation, and the inductance L remain constant, the step response current is proportional to $i_{step} \propto \sqrt{C}$. This means that the peak scaled inrush currents are proportional to $i_{scaled} \propto \frac{1}{\sqrt{C}}$, as shown in Figure 5.3.

As the peak L-G and capacitor current voltages are strongly correlated, it can also be proved that the peak capacitor current, without PoW utilisation, increases approximately by a factor of $\sqrt{2}$ when the capacitor bank size doubles with a different approach. The L-G peak voltages, without PoW utilisation, remain rather constant, as proved in Appendix E. With this information, the change in capacitor current can be proved.

The current through the capacitor can be described with the following equation:

$$I = C\frac{dV_{cap}}{dt} \tag{5.10}$$

Furthermore,

$$\omega_0 = \frac{1}{\sqrt{LC}} \rightarrow dt \propto \sqrt{LC} \tag{5.11}$$

As the scaling of the capacitor bank dV_{cap}, and the inductance L remains constant and the time scaling increases proportional to $dt \propto \sqrt{LC}$, the total current increase is proportional to $I \propto \frac{C}{\sqrt{C}} = \sqrt{C}$. Again, this means that the peak scaled inrush currents are proportional to $i_{scaled} \propto \frac{1}{\sqrt{C}}$, as shown in Figure 5.3.

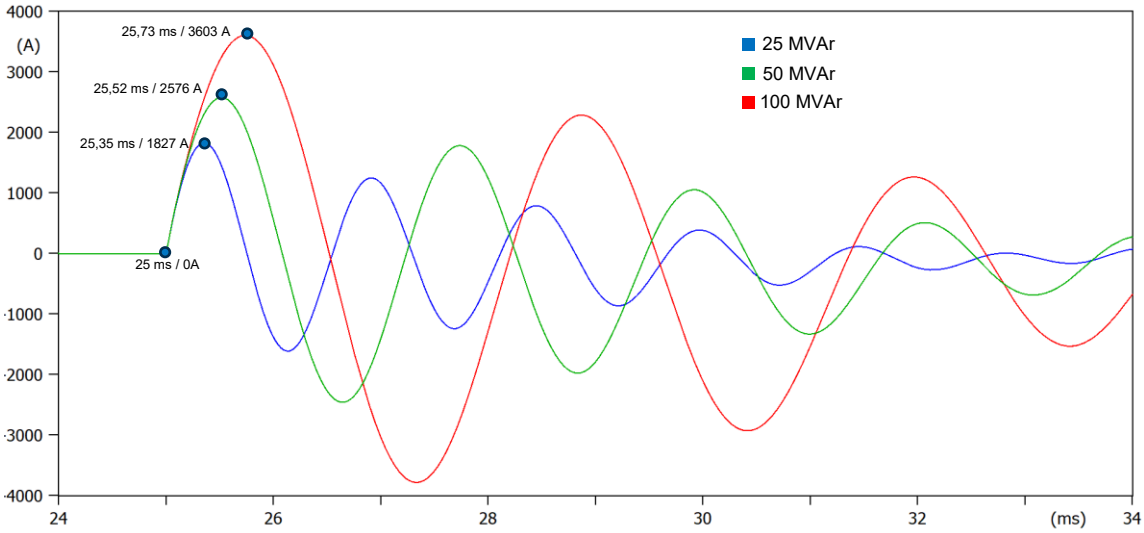

Figure 5.7: Instantaneous inrush currents

In Figure 5.7, the effect of capacitor size on the instantaneous inrush current is depicted when energised during peak voltage. It can be observed that when the capacitor bank size is doubled, the rise time and amplitude increase by a factor of approximately the square root of two. The resistance in the circuit, however, causes a small voltage drop, resulting in a bit lower amplitude increase than $\sqrt{2}$ per capacitor size doubling.

5.1.2 Line-to-ground voltages

The effectiveness of PoW for suppressing line-to-ground voltages was not the focus of this study, as there are no policies and Grid Code requirements for the line-to-ground voltage. However, more detail on the effectiveness of PoW for line-to-ground voltage suppression of capacitor banks is given in Appendix E, as this appendix contains the following:

- The simulation results are in the form of a graph with the peak line-to-ground voltages.
- A list of remarks that are made on the data.
- An explanation of why having a limited RDDS results in lower peak values when no PoW is utilised.
- Mathematical proof that the line-to-ground voltages without PoW are hardly affected by the capacitor bank size.

5.1.3 Line-to-line voltages

The effectiveness of PoW for suppressing line-to-line voltages was not the focus of this study, as there are no policies and Grid Code requirements for the line-to-line voltage. However, more detail on the effectiveness of PoW for line-to-line voltage suppression of capacitor banks is given in Appendix E, as this appendix contains the following:

- The simulation results are in the form of a graph with the peak line-to-ground voltages.
- A list of remarks that are made on the data.
- An explanation of why the 75 MVAr capacitor bank with PoW forms an exception to the trend.

5.1.4 Rapid voltage changes

The effectiveness of PoW on the peak RMS L-L voltages is depicted in Figure 5.8. One can observe that the implementation of PoW significantly reduces the peak half-cycle RMS voltage. The simulation of imperfect RDDS does not affect the maximum of the observed peak values by much compared to the ideal CB case. However, the implementation of RDDS introduces more spread in the observed peak values, especially for the cases without PoW.

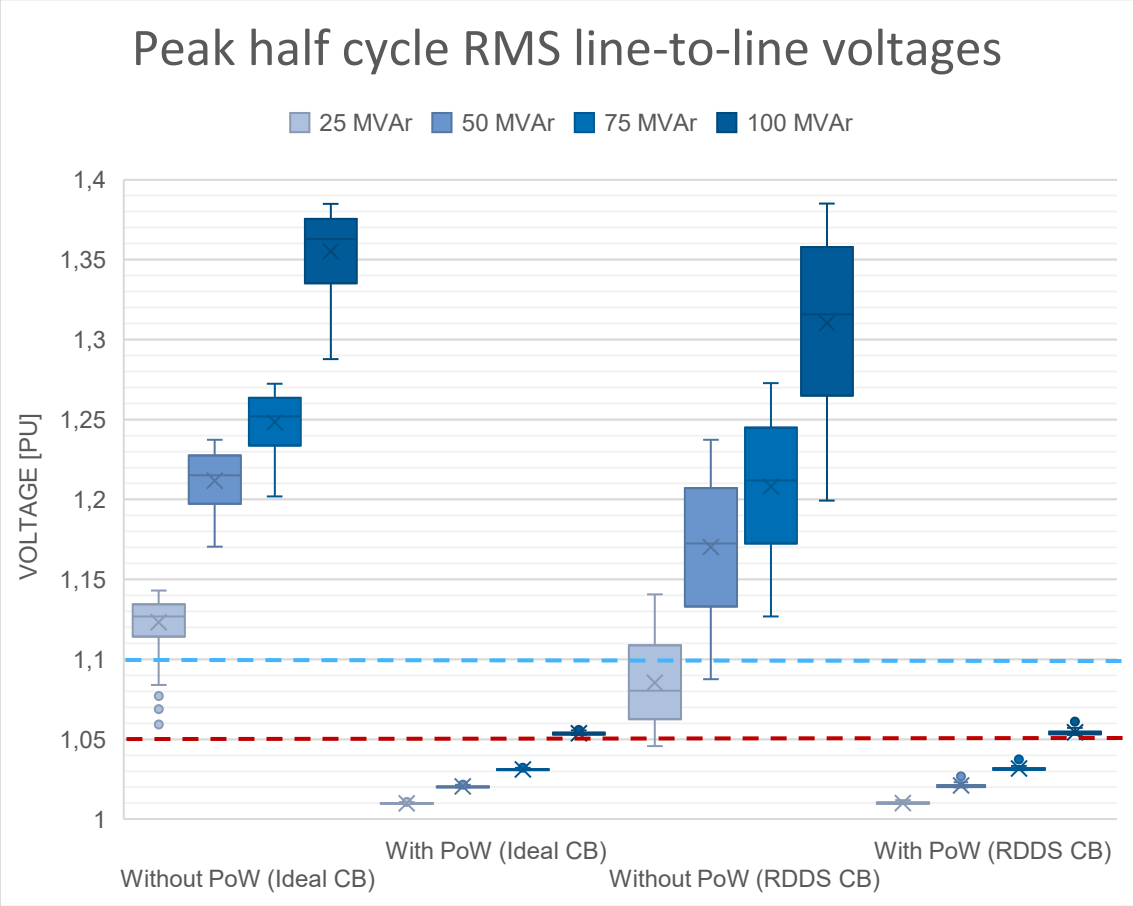

Figure 5.8: Effectiveness of PoW on half-cycle RMS voltages

Based on the simulation results, the following remarks can be made:

- As mentioned in Chapter 3 and in the Grid Code, the maximum allowed RVC is 5%, and thus the maximum allowed peak RMS L-L voltage is 1.05 p.u. As depicted in Figure 5.8, without PoW utilisation, in almost all simulations, the 5% limit is exceeded.
- As mentioned in Chapter 3, for PoW to be a feasible mitigation option, the maximum allowed RVC is 10% when PoW is not applied. As can be observed in Figure 5.8, most of the simulations without PoW exceed this 10% limit.
- As mentioned in Chapter 3 and according to the Dutch Grid Code, the allowed peak RVC is 5%, thus 1,05 p.u. As can be observed in Figure 5.8, only the 100 MVAr exceeds this 5% limit.

5.2 Effect of CB scatter on the effectiveness of PoW

The goal of this subsection is to provide insight into the effect of different CB scatter values. This is done by depicting voltage or current peak values for different switching standard deviations and capacitor bank sizes.

5.2.1 Capacitor currents

Figure 5.9 depicts the effect of scatter on peak inrush currents. It can be observed that higher standard deviations lead to a bigger spread in the peak current values. This is expected, as the larger deviation of the switching instant results in a higher sudden voltage change across the capacitor, and thus higher inrush current accordingly.

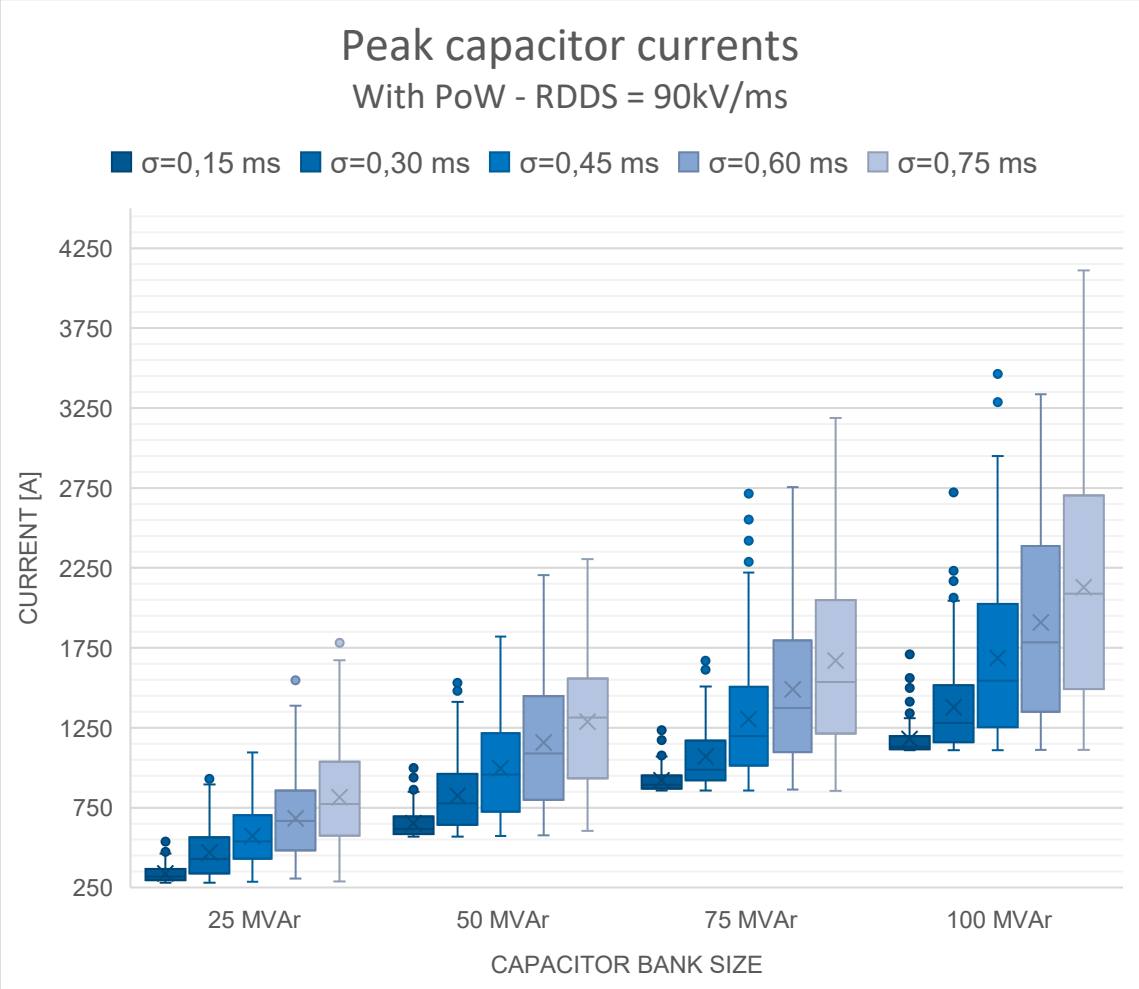

Figure 5.9: Effect of scatter on capacitor currents

The scaled peak capacitor currents are shown in Figure 5.10. Again, it can be observed that higher standard deviations lead to a broader spread in the peak current values. Furthermore, it can be observed that for higher standard deviations, the trend of the scaled inrush currents matches the case without PoW more. This is logical as the higher standard deviation makes switching near the voltage peak more common.

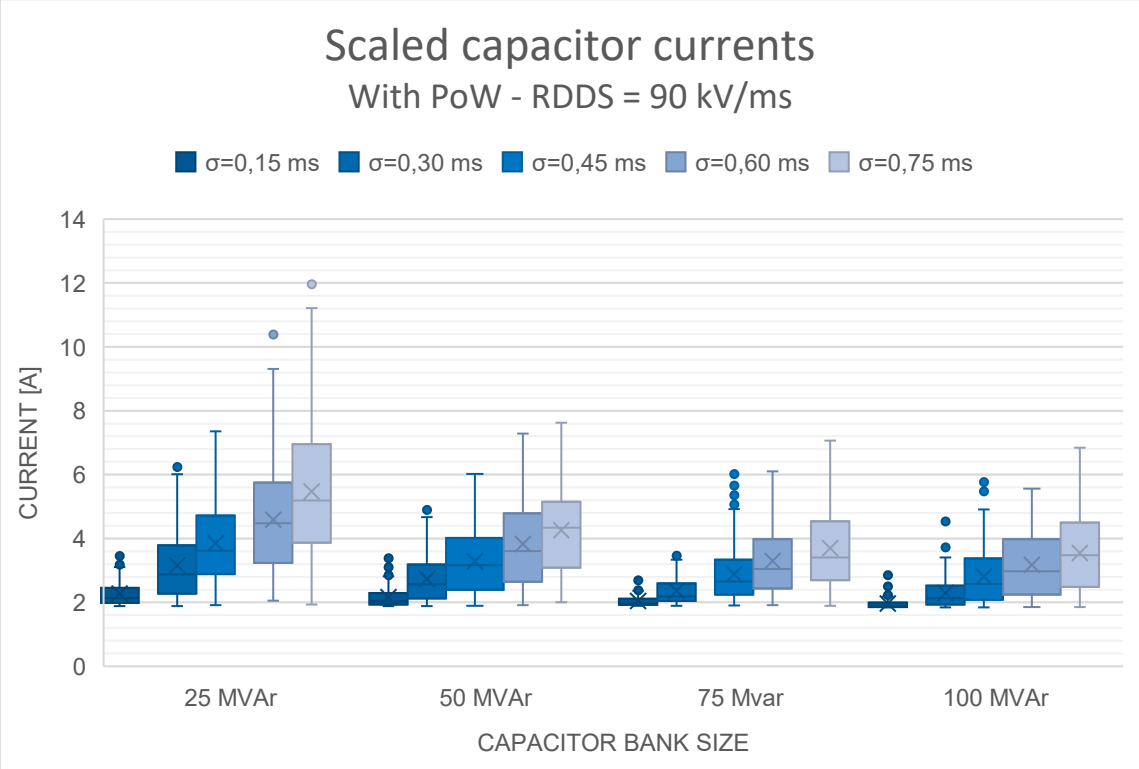

Figure 5.10: Effect of scatter on the scaled capacitor currents

5.2.2 Line-to-ground voltages

The effect of pole scatter on the effectiveness of PoW for suppressing line-to-ground voltages was not the focus of this study, as there are no policies and Grid Code requirements for the line-to-ground voltage. However, more detail on the effect of pole scatter on the effectiveness of PoW for the line-to-ground voltage suppression of cable circuits is given in Appendix E, as this appendix contains the following:

- The simulation results in the form of a graph with the peak line-to-ground voltages for different standard deviations.
- A list of remarks that are made on the data.
- An explanation of why, at a high standard deviation of 0.75 ms, the outliers are the highest for the lowest capacitor bank of 25 MVAr.

5.2.3 Line-to-line voltages

The effect of pole scatter on the effectiveness of PoW for suppressing line-to-line voltages was not the focus of this study, as there are no policies and Grid Code requirements for the line-to-line voltage. However, more detail on the effect of pole scatter on the effectiveness of PoW for the line-to-line voltage suppression of cable circuits is given in Appendix E, as this appendix contains the following:

- The simulation results in the form of a graph with the peak line-to-line voltages for different standard deviations.
- A list of remarks that are made on the data.

5.2.4 Rapid voltage changes

The effect of scatter on the half-cycle RMS L-L voltages is depicted in Figure 5.11. Based on the simulation results, the following remarks can be made:

- As expected, higher standard deviations result in a higher spread in RMS voltages.
- To comply with the Dutch “Grid code”, the peak RMS voltages are not allowed to be higher than 1,05 p.u. As can be seen in Figure 5.11, higher standard deviations reduce the chance of meeting this requirement.

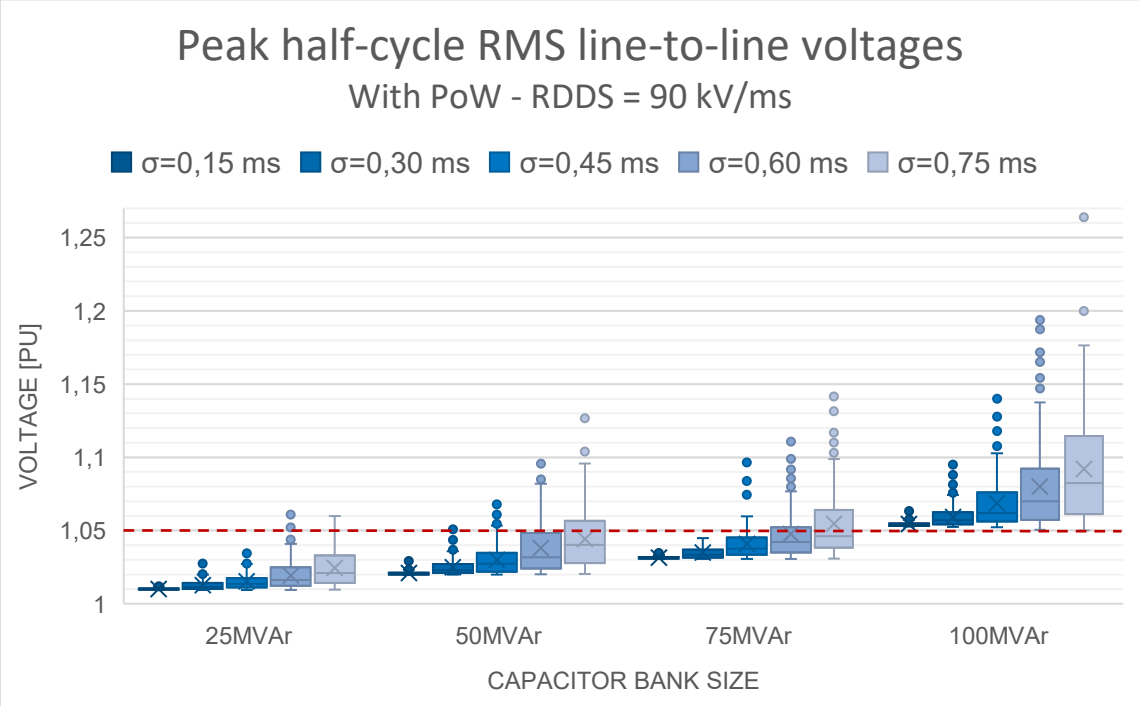

Figure 5.11: Effect of scatter on RVCs

6 Simulation results: Cable circuit energisation

In this chapter, the simulation results regarding cable circuit energisation are described. At first, the effectiveness of PoW is described for various cable sizes (1600 mm², 2500 mm², and 3500 mm²), cable lengths, and RDDS. Secondly, a comparison between cables and capacitor banks of equal capacitance is described.

6.1 Effectiveness of PoW implementation

In this section, the effectiveness of PoW for cable circuits is described by presenting several simulation results for different cable lengths and sizes. These simulation results consist of peak L-G voltages, peak L-L voltages, peak RVS's and peak inrush currents. Furthermore, in this section, a comparison between cable circuits and capacitor banks of equal capacitance is made.

6.1.1 Inrush currents

Figure 6.1 depicts the effect of the cable type (see Section 4.3.1), cable length, and RDDS without PoW application on the peak inrush currents.

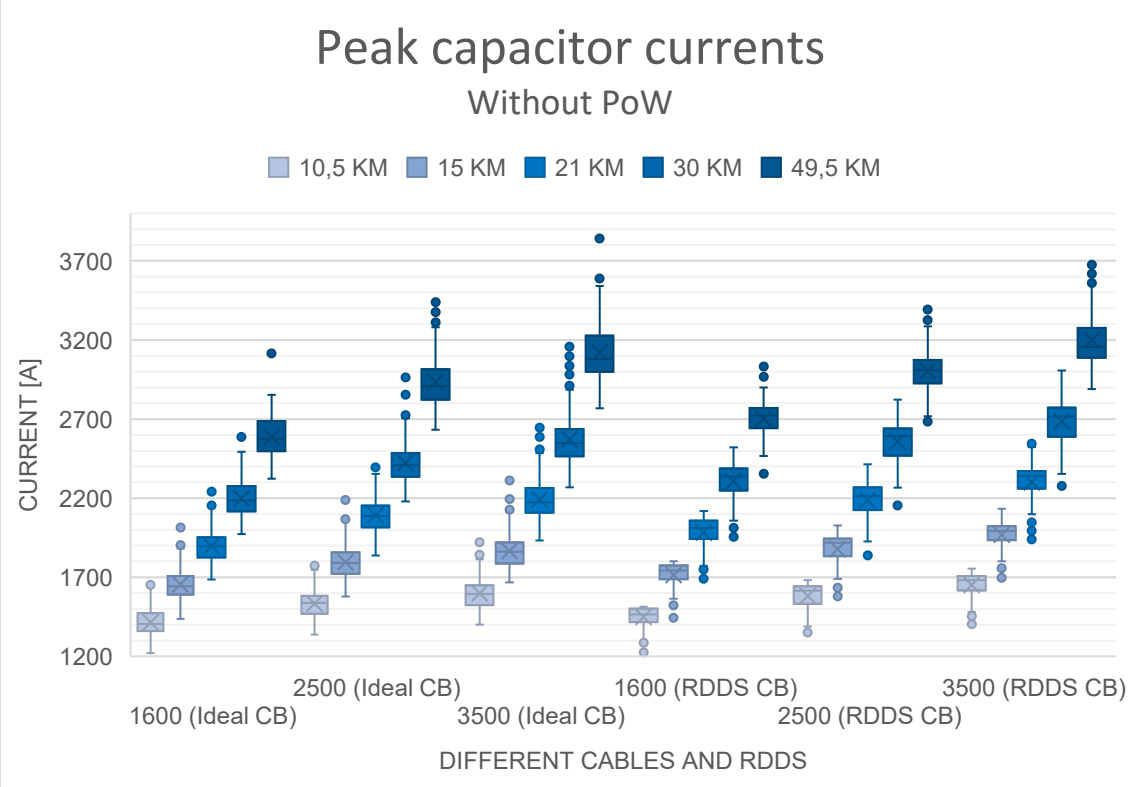

Figure 6.1: Effect of cable type, cable length, and RDDS on capacitor current without PoW utilisation

Based on the simulation results, the following remarks can be made:

- As expected, an increase in cable size or cable length results in an increase in inrush currents, as the capacitance of the cable increases as well.
- Imperfect RDDS tend to perform worse than the ideal CB case, as the peak currents are, on average, higher than the ideal CB case. The reason for this is discussed in Section 5.1.1.

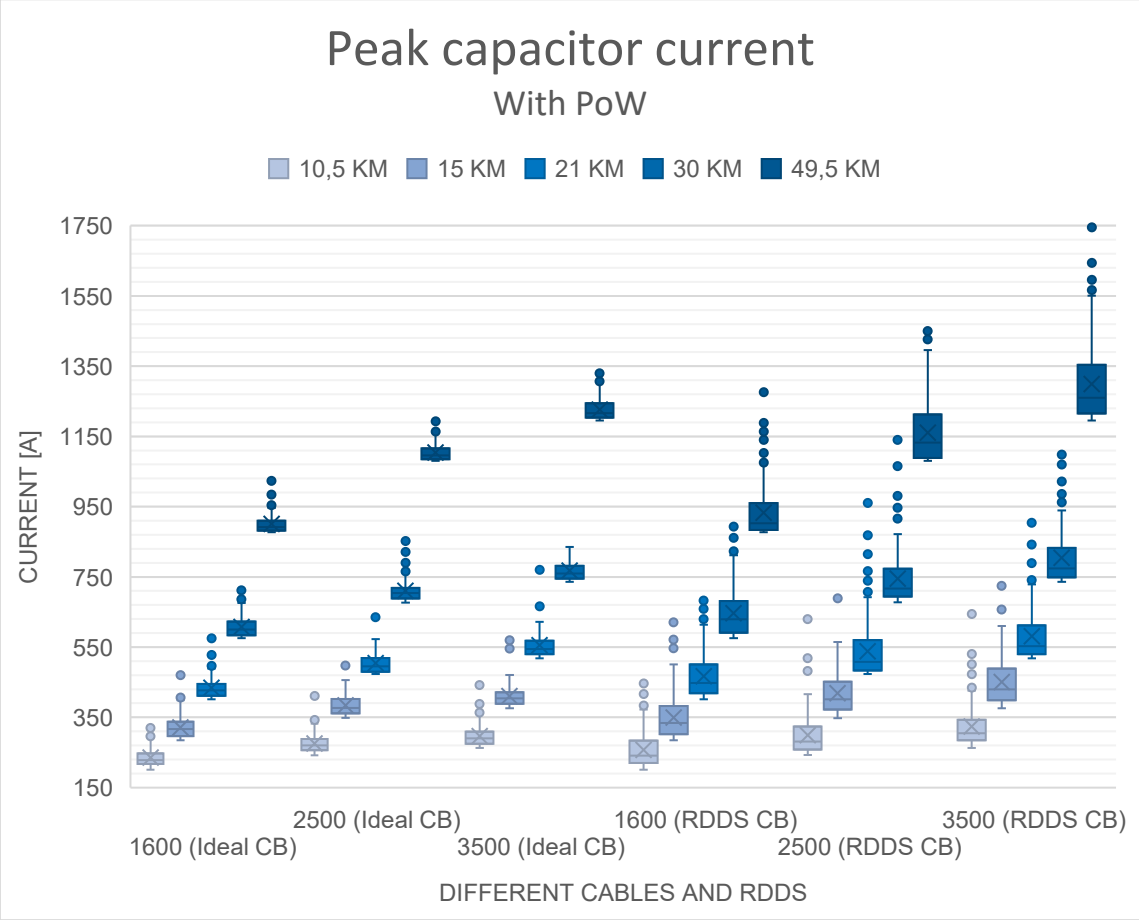

Figure 6.2: Effect of cable type, cable length, and RDDS on capacitor current with PoW utilisation

Figure 6.2 depicts the inrush currents when PoW is utilised. Based on the simulation results, the following remarks can be made:

- As expected, the trend is similar to when no PoW is applied, but the currents are overall lower.
- The CB with imperfect RDDS performs, on average, worse than the ideal CB, as the average peak currents are higher than in the ideal CB case. The reason for this is described in Section 5.1.1.

6.1.2 Line-to-ground voltages

The effectiveness of PoW for suppressing line-to-ground voltages was not the focus of this study, as there are no policies and Grid Code requirements for the line-to-ground voltage. However, more detail on the effectiveness of PoW for line-to-ground voltage suppression of cable circuits is provided in Appendix F, as this appendix contains the following:

- The simulation results in the form of graphs with the peak line-to-ground voltages with and without PoW.
- A list of remarks that are made on the data.
- An explanation of why a cable circuit of 30 km has higher peak overvoltages, when PoW is not applied, than the 49,5 km cable circuit.

6.1.3 Line-to-line voltages

The effectiveness of PoW for suppressing line-to-line voltages was not the focus of this study, as there are no policies and Grid Code requirements for the line-to-ground voltage. However, more detail on the effectiveness of PoW for line-to-line voltage suppression of cable circuits is provided in Appendix F, as this appendix contains the following:

- The simulation results in the form of graphs with the peak line-to-line voltages with and without PoW.
- A list of remarks that are made on the data.

6.1.4 Rapid voltage changes

Figure 6.3 illustrates the effect of cable size, cable length, and RDDS without PoW implementation on the peak half-cycle RMS L-L voltages.

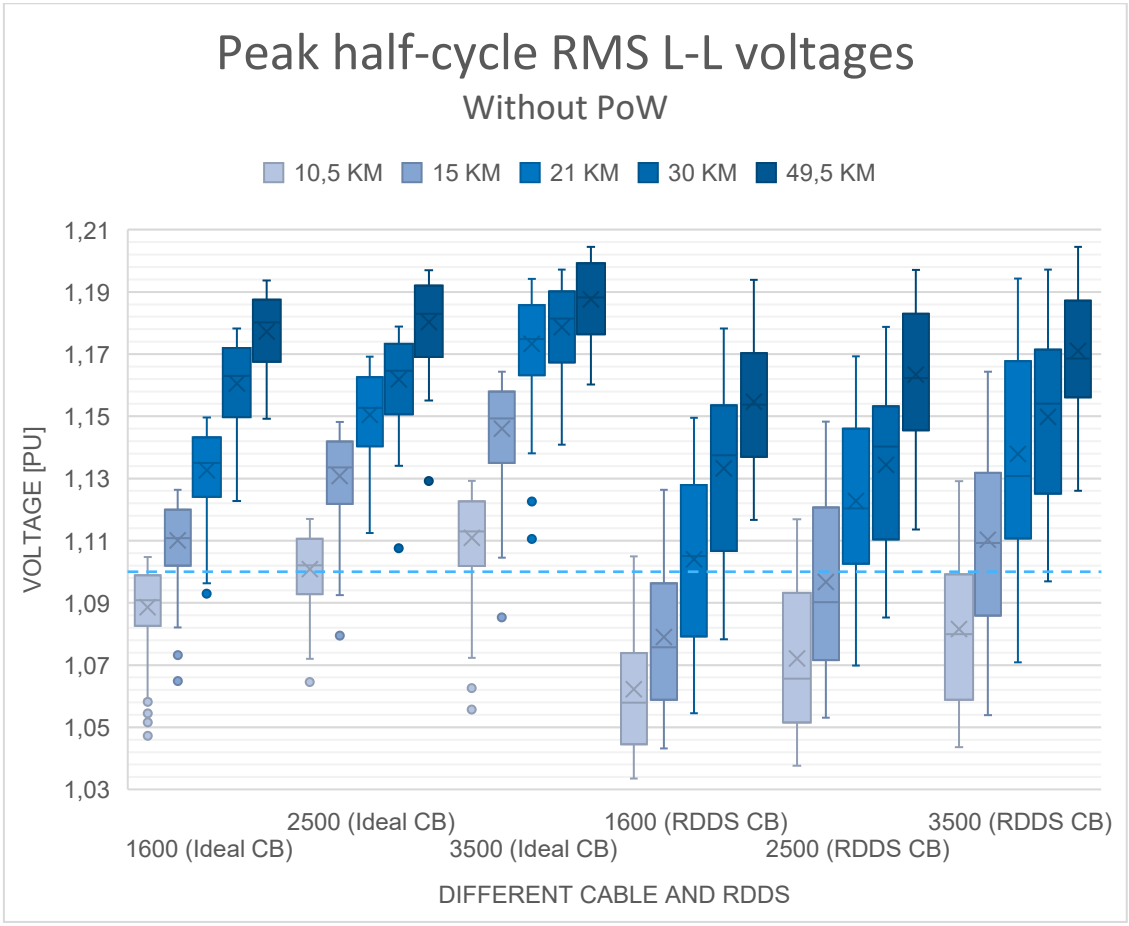

Figure 6.3: Effect of cable type, cable length, and RDDS on the RVCs without PoW implementation

Based on the simulation results, the following remarks can be made:

- As can be observed, an increase in cable size or cable length results in an increase in the peak RMS L-L voltages. However, the increase in peak RMS voltages becomes less noticeable as the length further increases, due to the increase in cable resistance.
- The performance of the CB with imperfect RDDS is, on average, better than the ideal CB, as the overvoltage values are, on average, lower for the CB with imperfect RDDS.
- According to TenneT's policy (see Chapter 3), PoW is only an acceptable solution if the peak RMS overvoltages are less than 1.10 p.u. As can be observed in Figure 6.3, most of the simulation results show higher overvoltage values than 1.10 p.u.

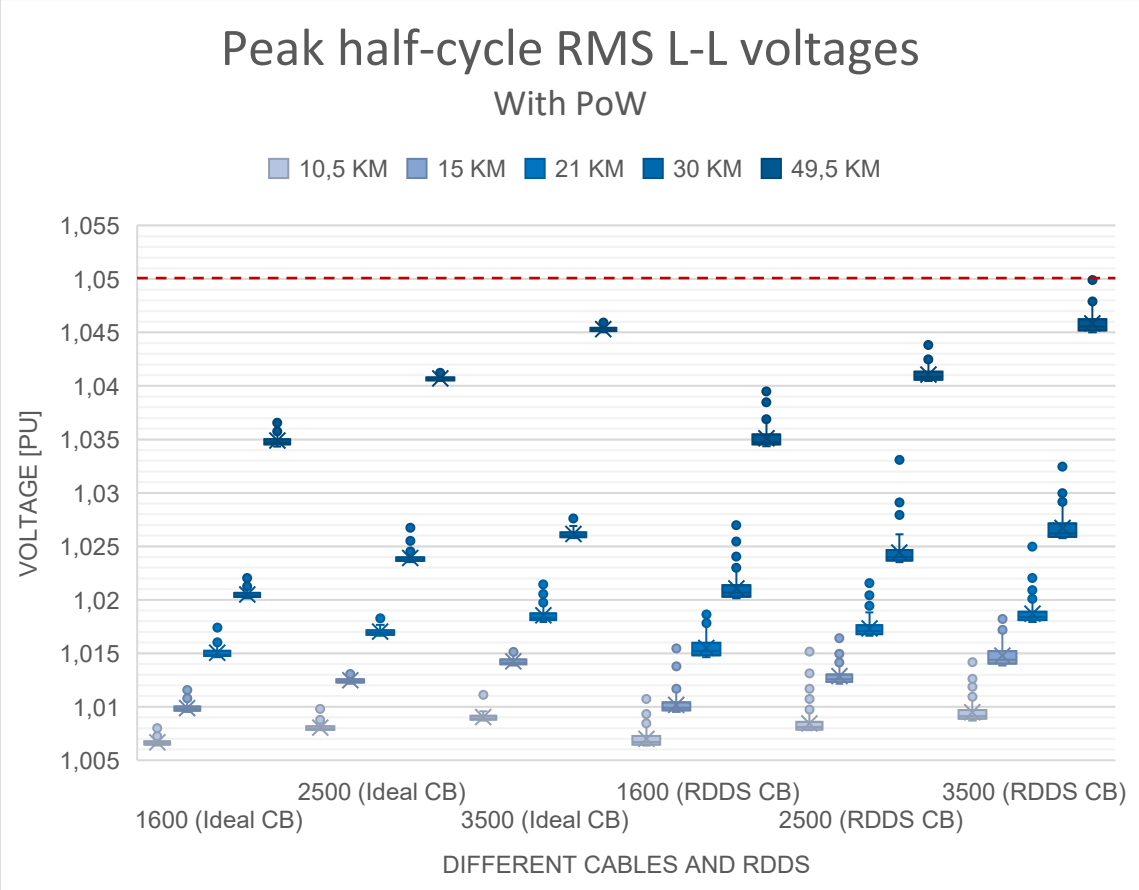

Figure 6.4: Effect of cable type, cable length, and RDDS on RVCs with PoW implementation

Figure 6.4 depicts the effect of cable size, cable length, and RDDS without PoW implementation on the peak half-cycle RMS L-L voltages. Based on the simulation results, the following remarks can be made:

- As expected, when PoW is applied, the trend is similar to the case where no PoW is applied. However, the maximum overvoltages are less because of the PoW implementation.
- As described in Chapter 3 and in the Grid Code, he maximum peak RMS L-L overvoltage is 1.05 p.u to comply with the Dutch "Grid code". As can be observed in Figure 6.4, none of the overvoltage values of the simulated cables exceed this 1.05 p.u. limit.

6.2 Comparison between cable circuit and capacitor bank

In this section, a comparison is made between the capacitor bank and various cable circuits of approximately equal capacitance. This comparison potentially provides useful information as it makes it possible to predict the effectiveness of PoW for energising a cable circuit if the effectiveness on the capacitor bank is known, and vice versa.

6.2.1 RVC's

Figure 6.5 depicts a comparison between capacitor banks and cable circuits of equal capacitance. This is done by performing simulations of feasible cable setups that closely (within 2%) match the standard capacitor bank sizes.

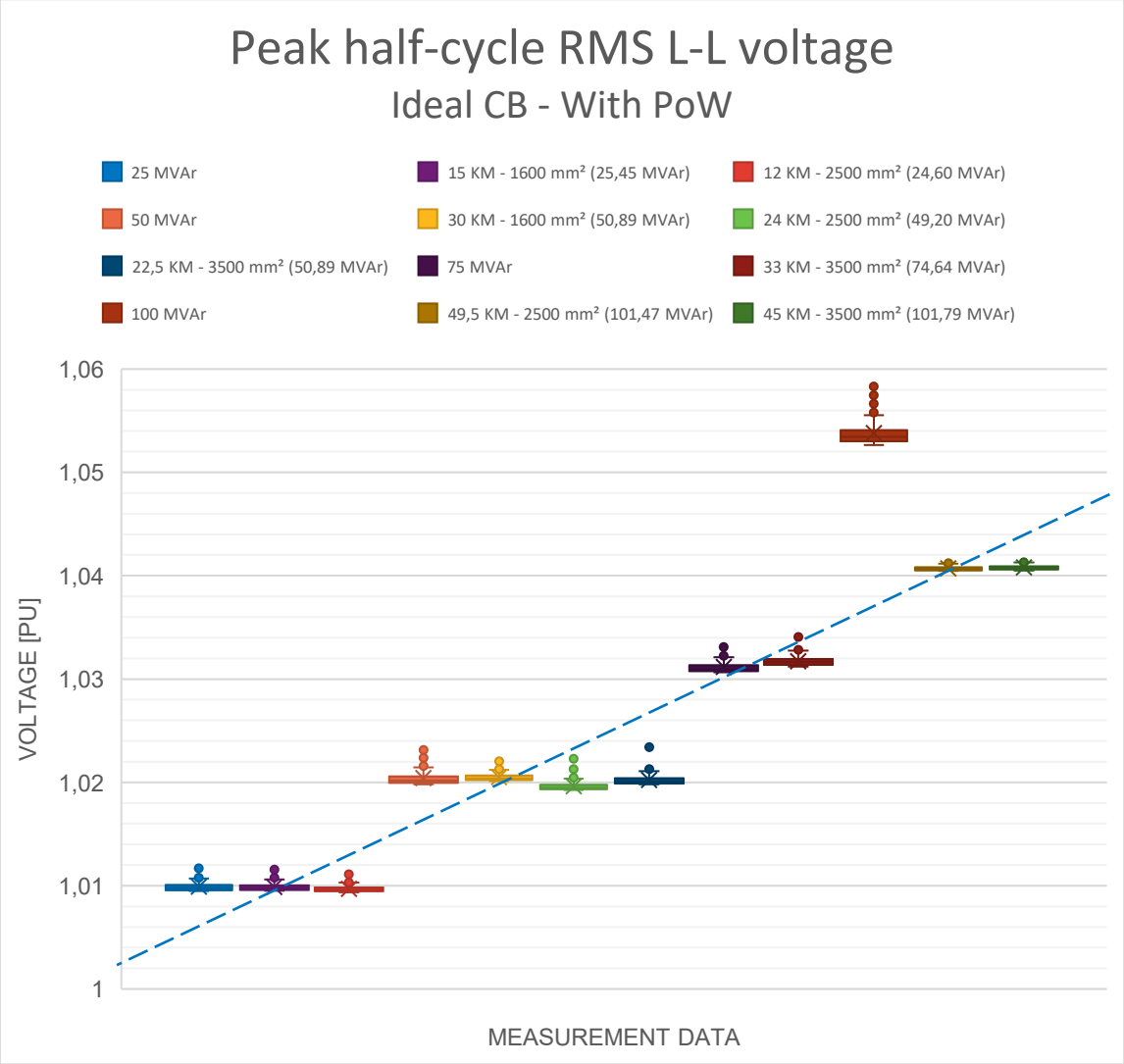

Figure 6.5: Comparison of RVCs between cable and capacitor with the same capacitance

Based on this data, the following remarks can be made:

- For the 25 MVAr, 50 MVAr, and 75 MVAr capacitor bank ratings, the corresponding cables perform comparably when considering the RVCs.
- The RVCs of the cable circuits follow a trend of a peak voltage increase of 0,01 p.u. per 25 MVAr increase in capacitance.
- The 100 MVAr capacitor bank performs significantly worse than the 100MVAr equivalent cables. It seems that the 100 MVAr capacitor bank is negatively affected by resonances, as the equivalent cable follows the trend line of approximately 0,01 p.u. per 25 MVAr.

6.2.2 Peak inrush current

Comparisons of the peak inrush currents between the capacitor banks and approximately equal capacitance cable circuits are depicted in Figure 6.6.

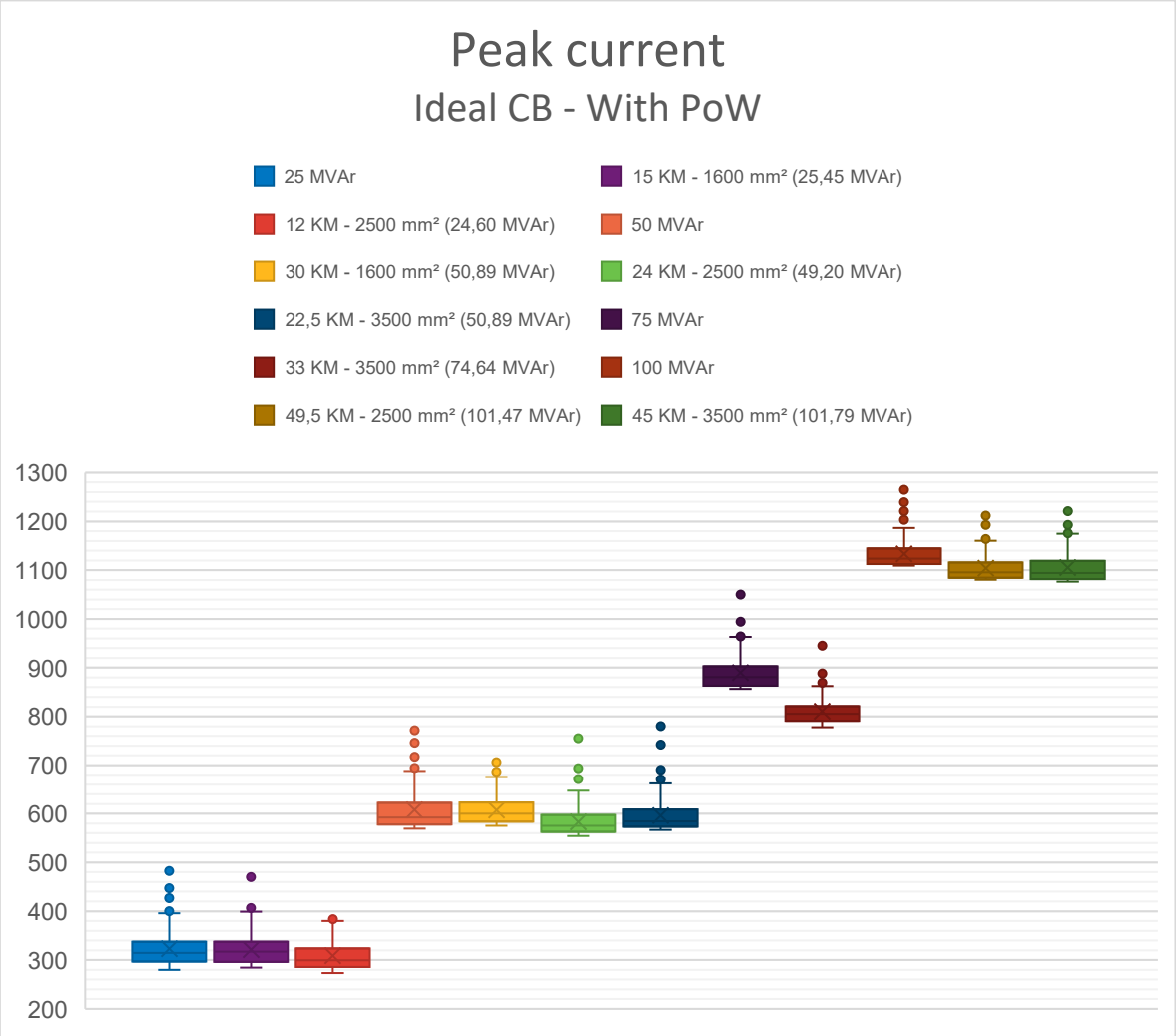

Figure 6.6: Comparison of RVCs between cable and capacitor with the same capacitance

Based on this data, the following remarks can be made:

- Overall, all the peak inrush currents of the capacitor banks and the corresponding cable circuits match closely.
- For the 75 MVAr capacitor bank and the corresponding cable circuits, the peak inrush current through the cable circuit is lower. This is expected to be due to different resonance behaviour because of the inductance of the cable, the suppressing effect of the inductance of the cable, and to the fact that the capacitor bank has a slightly lower capacitance of 74,64 MVAr.
- Overall, the cable circuit has a lower peak inrush current than the corresponding capacitor banks for longer cables due to the increase in cable inductance. This cable inductance suppresses the change in current.

7 Discussion

This chapter addresses discussion points that underpin the recommendations for future work.

7.1 PoW implementation at other TSOs

In this section, the implementation policies of PoW at other TSOs are briefly summarised. This information is the result of a questionnaire that was prepared by TenneT and shared with a few TSOs in 2021.

7.1.1 TSO 1

TSO 1 shared the following details regarding PoW implementation:

- PoW is used for shunt reactor de-energisation to limit possible circuit breaker re-ignitions.
- PoW is used for the limitation of inrush currents and, consequently, limitation of voltage transients in HVDC power transformers.

7.1.2 TSO 2

TSO 2 shared the following details regarding PoW implementation:

- PoW is standardly applied for shunt reactor and capacitor bank switching.

7.1.3 TSO 3

TSO 3 shared the following details regarding PoW implementation:

- PoW is standardly applied to power transformers with a power rating above 350 MVA, unless the circuit breaker is already equipped with pre-insertion resistors.
- PoW is standardly applied to shunt reactors and capacitor banks for energisation and de-energisation.

7.1.4 TSO 4

TSO 4 shared the following details regarding PoW implementation:

- PoW is applied to large power transformer units to mitigate voltage dips. As a rule of thumb, PoW is applied if the rating is above 500 MVA.
- PoW is applied to shunt reactors and capacitor banks
- PoW is applied to 220 kV and 400 kV cable circuits longer than a specific length.

7.1.5 TSO 5

TSO 5 shared the following details regarding PoW implementation:

- PoW is standardly applied to 380 kV shunt reactors and capacitor banks to mitigate voltage dips under energisation and circuit breaker re-ignitions under de-energisation.
- PoW is not applied to mixed line-cable connections where the cable sections are compensated by means of shunt reactors, as a study analysis indicated PoW is not able to mitigate all the risks. Therefore, pre-insertion resistors are being applied.

7.2 Critical view on the statistical simulation data application for deterministic requirements

A deterministic approach means that the output is solely determined by the input and the initial conditions. This means that the results are predictable and reproducible [27]. A statistical approach, however, means that the output is determined based on stochastic data varied by a specific probability distribution function. A deterministic approach is not chosen in this study, as it is hard to determine all the effects of the inputs and initial conditions perfectly, such as temperature, component wear, humidity, voltages, idle time, spring tension variability, and changes in lubrication. In a statistical study, on the other hand, probability distribution functions are applied to approximate the behaviour of these nearly impossible to determine effects.

The grid code and TenneT's power quality policy requirements are deterministic, while the performed study and circuit breaker switching in general are statistical. Based on the simulation analysis, PoW switching cannot be considered as an acceptable mitigation option, as in certain cases the absolute limits are exceeded. Consequently, other mitigation options need to be considered to comply with the power quality requirements. This could result in non-cost-effective solutions or a mix of solutions that do not facilitate the standardisation of designs. However, a statistical approach could allow the application of PoW switching in a wider range of cases. As an example, statistical approaches could be evaluated similarly to, e.g., insulation coordination (IEC 60071-1 and IEC 60071-2).

7.2.1 Capacitor bank

In Figure 7.1, the percentage of simulations in which the RVC exceeds the 5% limit for different capacitor bank sizes and standard deviations is depicted for the case with PoW utilisation. The simulation data for the 100 MVAr capacitor bank is not depicted, as all the simulations of the 100 MVAr capacitor bank case exceed the 5% limit. Based on these results, the following remarks can be made when, for instance, the 2% exceedance rate is applied:

- The deterministic requirement for the RVCs in the Grid Code is met for the 25 MVAr capacitor bank if the standard deviation is not higher than 0.60 ms.
- The deterministic requirement for the RVCs in the Grid Code is met for the 50 MVAr and 75 MVAr capacitor bank if the standard deviation is not higher than 0.30 ms.
- The deterministic requirement for the RVCs in the Grid Code is not met for the 100 MVAr capacitor bank, regardless of the standard deviation.

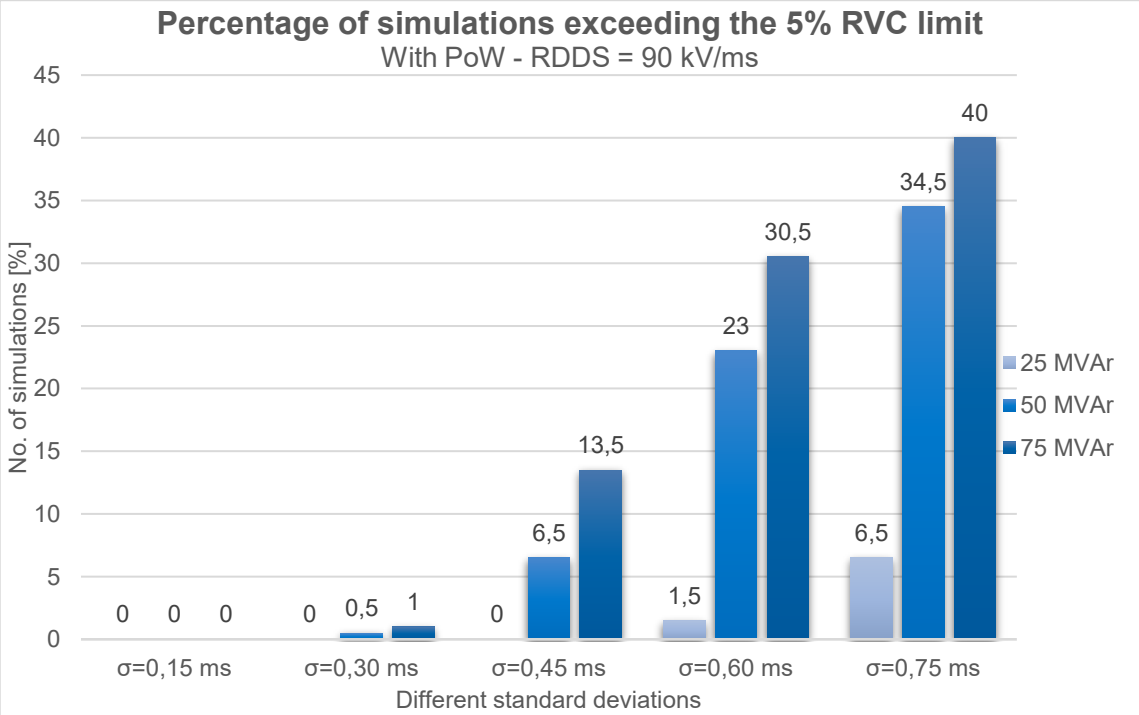

Figure 7.1: No. of simulations exceeding 5% for different capacitor bank sizes and standard deviations

Without PoW utilisation, however, all capacitor bank sizes exceed the 10% RVC limit in TenneT's power quality policy by more than 2%, as depicted in Figure 7.2.

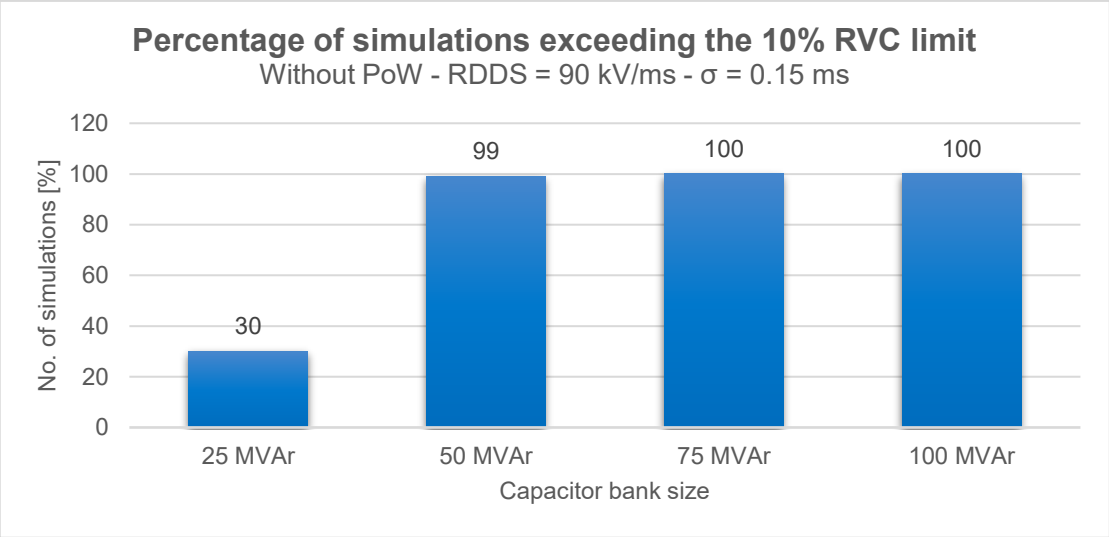

Figure 7.2: No. of simulations exceeding 10% for different capacitor bank sizes

7.2.2 Cable circuit

In Figure 7.3, the percentage of the simulations exceeding TenneT's 10% policy limit when no PoW is utilised is depicted. It can be observed that for all the simulated cables and lengths, more than 2% exceeds the 10% RVC limit.

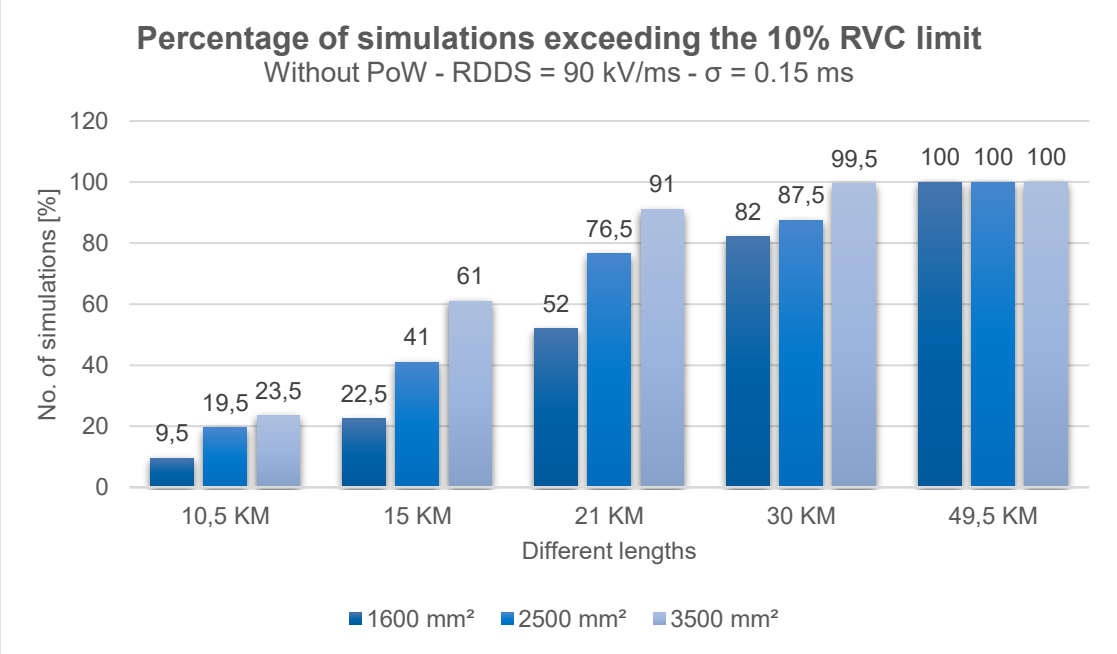

Figure 7.3: No. of simulations exceeding 10% for different cable lengths and sizes

When PoW is utilised, however, the highest RVC observed is 5%, so it can be concluded that all the simulated cables comply with the Grid Code if PoW is utilised, even if the 2% exceedance rate is not applied.

7.3 Critical view on the implemented pole scatter standard deviation

Based on switching tests performed with circuit breakers applied to TenneT's grid, a standard deviation of 0.15 ms has been assumed to be the most realistic. However, other performance tests suggest a standard deviation of 0.27 ms to be more realistic [28]. However, as it can be observed in Figure 7.1, a CB with a scatter of 0.30 ms would still comply with the grid code for 25 MVAr, 50 MVAr and 75 MVAr capacitor banks when an exceedance rate of 2% is tolerated. For higher standard deviations, PoW is possibly not effective enough anymore to comply with the "Grid code" for capacitor bank sizes above 25 MVAr. It is necessary to determine which standard deviation applies to the project-specific circuit breakers to have a better understanding of the exact PoW effectiveness.

7.4 Critical view on the need to compensate external variables

For the simulations, a Gaussian distribution is applied (See Figure 7.4) to approximate the scatter of the circuit breaker. For this Gaussian distribution, the most applicable standard deviation is chosen, and the mean value is assumed to be perfectly aligned. External variables, such as temperature and control voltage, however, can also affect the mean value of the Gaussian distribution.

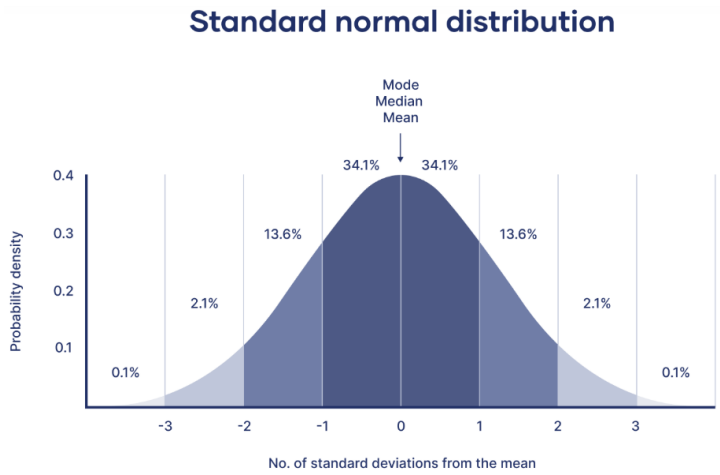

Figure 7.4: Gaussian distribution [22]

Correct mathematical compensation of these external variables in the PoW controller (as described in Section 2.1) is vital for the effective use of PoW, as a shift in the mean switching instant is detrimental to the PoW switching effectiveness. The "American Institute of Physics" has published a journal, called "AIP Advances", which contains an example that estimates the effects of various external variables, more specifically temperature, number of switching operations, and working hours, on the closure time of a CB. This example estimate is obtained with measurement data of an 800kV circuit breaker and a prediction model based on a Broyden–Fletcher–Goldfarb–Shanno (BFGS) neural network algorithm. [29]

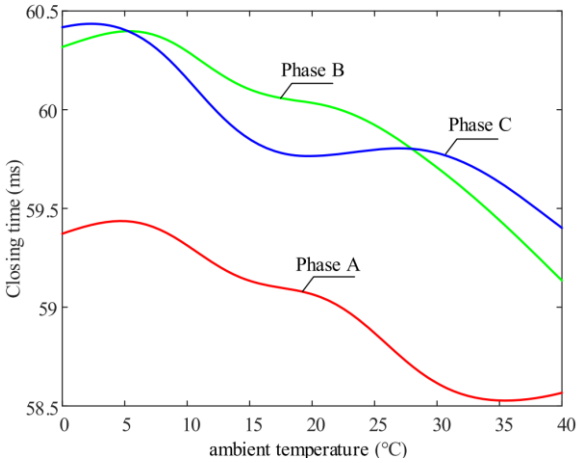

Figure 7.5: Example estimate of the relation between ambient temperature and closing time [29]

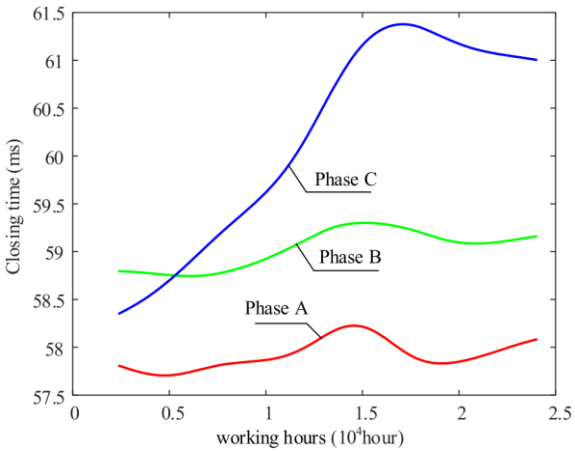

Figure 7.6: Example estimate of the relation between working hours and closing time [29]

Figure 7.6, Figure 7.5, and Figure 7.7 depicts an example estimate of the relation between No. of actions, temperature, and working hours on the closing time of a CB.

Based on these graphs, the following remarks can be made:

- The closing time is expected to vary by more than 1 ms over a temperature ranging from 7 – 40 C°.
- The closing time is expected to vary by more than 3 ms over a working time of 15000 hours.
- The closing time is expected to vary by more than 2 ms over the number of actions ranging from 100 – 200 actions.

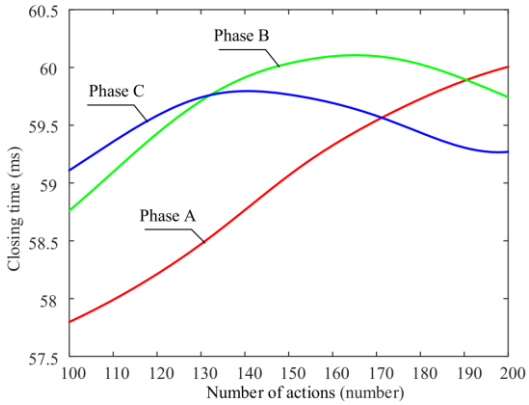

Figure 7.7: Example estimate of the relation between No. of actions and closing time [29]

It can be concluded that accurate compensation of temperature, operation time, and amount of switching actions is vital for effective PoW operation, as, e.g., a 50 MVAr capacitor bank that is energised with a scatter of 0,45 ms already fails to comply with the Grid Code, let alone a deviation of 3 ms. It is expected that an algebraic correction is optimal for the temperature, as all three poles have a similar closure time vs temperature trend. For compensation of the working hours and number of closing actions, however, adaptive compensation is expected to be optimal (see Section 2.1.9), as the relation between these aspects and the closure time is expected to be harder to describe algebraically.

7.5 Importance of monitoring the PoW effectiveness in practice

Continuous monitoring of the effectiveness of PoW in practice can be beneficial for the following reasons:

- To check whether errors are made during this study or whether aspects have been overlooked.
- To verify if external variables, such as temperature, number of switching operations, operation time and control voltage, are correctly compensated in the PoW controller. Furthermore, if not correctly compensated, the measurement data can provide help with optimising the compensation model.
- To have a better foundation for changing or setting up policies regarding PoW usage.

7.6 Other mitigation options

There are other mitigation options than PoW switching for suppressing inrush currents and voltage transients. This section provides a brief overview of other mitigation options. It needs to be noted that for reasons of completeness and for selecting proper and cost-effective mitigation options, further analyses are essential.

7.6.1 Pre-insertion resistor

A pre-insertion resistor (PIR) is temporarily connected in series with the circuit during switching to limit the inrush current and reduce the steepness of voltage transients [30]. After a brief period (typically a few milliseconds), the resistor is bypassed as the main contacts close completely. Pre-insertion resistors can be applied for the switching of power transformers, capacitor banks and line/cable circuits.

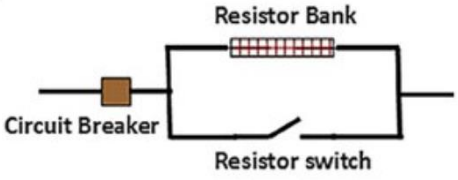

Figure 7.8: Schematic of a parallel pre-insertion resistor [38]

Within TenneT, pre-insertion resistors (PIR) were traditionally used to suppress inrush currents and transient overvoltages during the switching of capacitor banks (see Figure 7.8). Comparing the effectiveness of PIR and point-on-wave (PoW) switching is complex, as the optimal resistance value

and insertion duration depend heavily on the specific configuration. However, to provide an indicative comparison, a PIR resistance of 40 Ω with an insertion time of 8 ms is considered here, based on a 110 kV 66 MVAr capacitor bank application [24]. EMTP-ATP simulations have been carried out to compare the performance of PoW and the PIR based on this configuration. This comparison is purely illustrative, as further optimisation of the insertion time and resistance value could potentially enhance the performance of PIR.

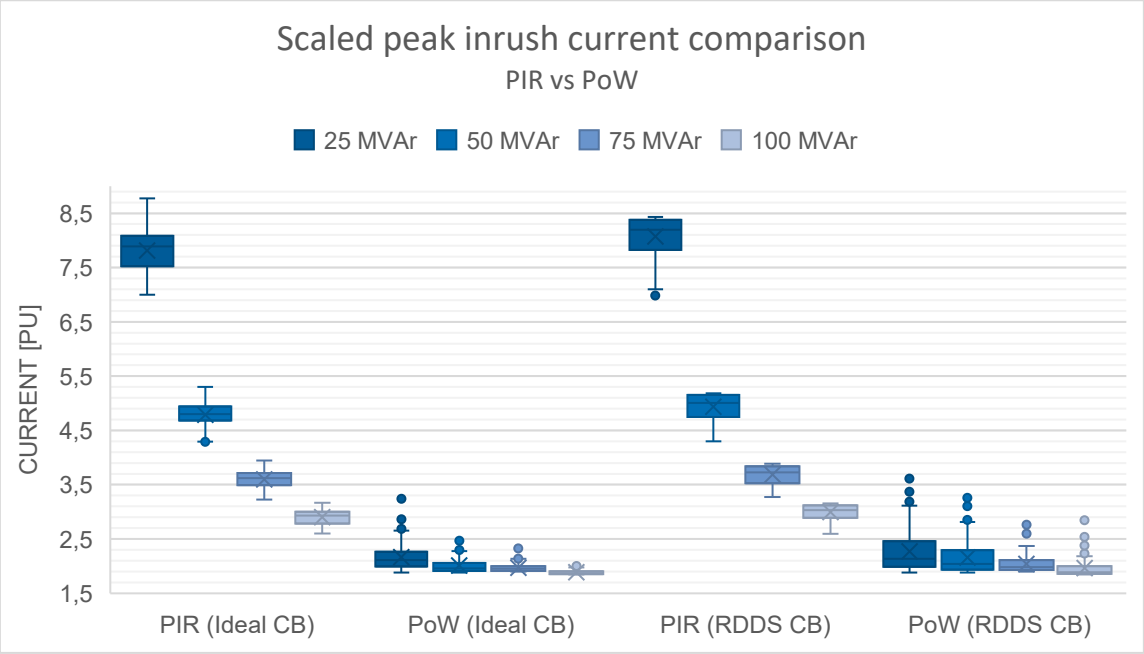

Figure 7.9: Effect of PIR vs PoW on the scaled peak inrush currents

Figure 7.9 shows a comparison of the scaled peak inrush currents for PIR, for a resistance value of 40 Ω and an insertion duration of 8 ms, and PoW, with a standard deviation of 0.15 ms. Furthermore, this comparison is shown for an infinitely high RDDS (Ideal CB) and an RDDS of 90 kV/ms (RDDS CB). Based on these results, the following remarks can be made:

- Overall, in this particular example, PoW outperforms PIR, as the scaled inrush currents are consistently lower for PoW than for PIR.
- For PIR, the inrush currents remain relatively constant across different capacitor bank sizes, leading to a decrease in scaled peak currents as the capacitor bank rating increases.
- When PIR is used, an RDDS of 90 kV/ms performs better than an infinitely high RDDS, whereas for PoW, the opposite is true.

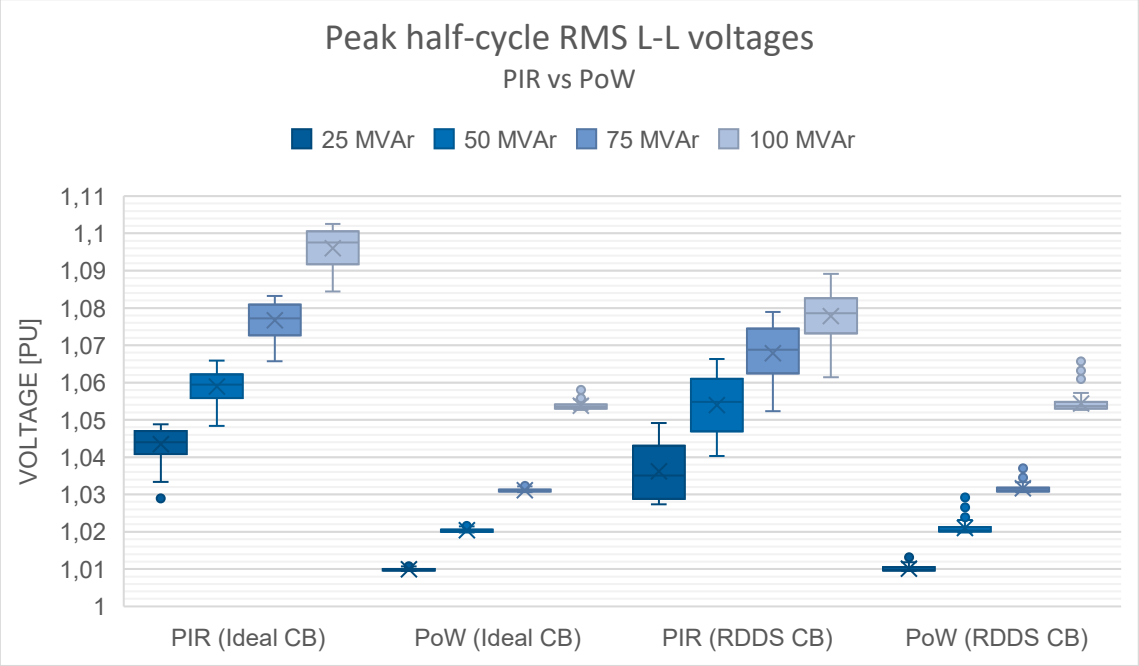

Figure 7.10: Effect of PIR vs PoW on the peak half-cycle RMS L-L voltages

Similarly, Figure 7.10 shows a comparison of the RVCs for PIR and PoW. Based on these results, the following remarks can be made:

- Overall, in this particular example, PoW outperforms PIR, as the RVCs are consistently lower for PoW than for PIR.
- For both PIR and PoW, the RVCs increase with an increasing capacitor bank rating.
- When a PIR is used, an RDDS of 90 kV/ms performs better than an infinitely high RDDS, whereas for PoW, the opposite is true.

7.6.2 Filter

In TenneT's high-voltage grid, capacitor bank designs typically include a filter section to suppress inrush currents and transient overvoltages during energisation. Such a filter, which is only applicable to capacitor banks and not to cable circuits, generally consists of an inductor, a resistor, and a capacitor. Since filter designs are project-specific, detailed modelling is complex. Therefore, an example configuration based on a 150 kV 75 MVAr capacitor bank used within TenneT is presented here. To assess the filter's effectiveness and to examine whether combining a filter with PoW switching offers additional benefits, EMTP-ATP simulations were performed comparing a 75 MVAr capacitor bank without a filter and the same bank equipped with a filter. The schematic of the capacitor bank with a filter is shown in Figure 7.11, where the 10.61 µF capacitor represents the 75 MVAr bank.

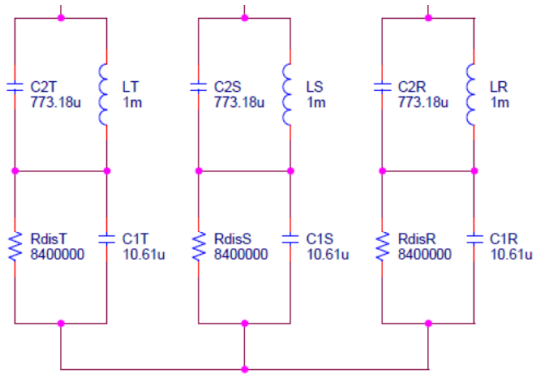

Figure 7.11: Schematics of 75 MVAr capacitor bank with filter [35]

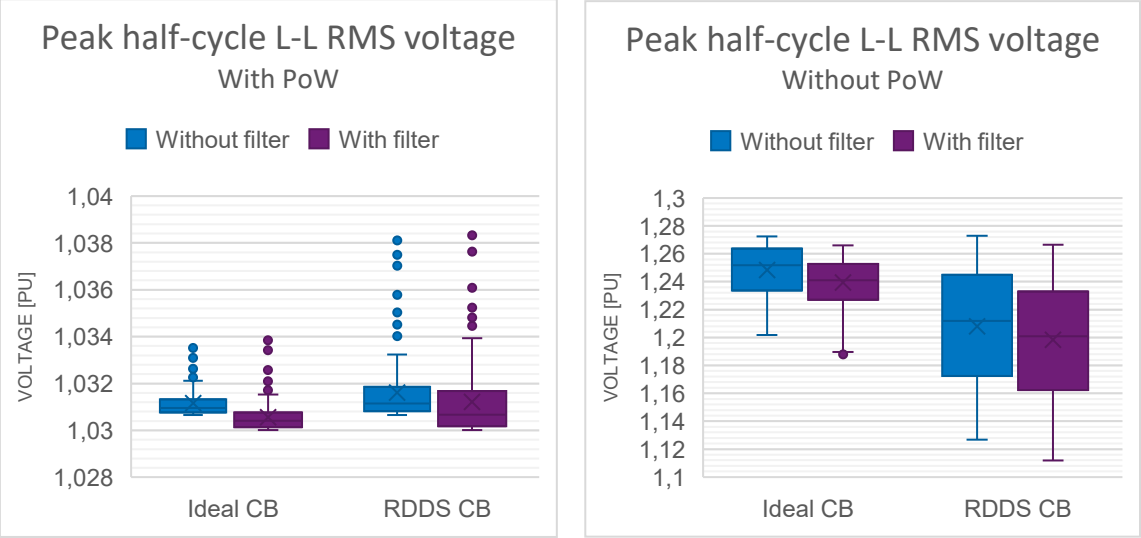

Figure 7.12: Comparison of with filter vs without filter on peak L-L half-cycle RMS voltages

In Figure 7.12, a peak L-L RMS voltage comparison between a 75 MVAr capacitor bank that consists of only a capacitor bank (without a filter) and a 75 MVAr capacitor bank with a filter is shown. Based on the simulation results, the following conclusions are drawn:

- The effect of the filter on the RVCs is limited and may, therefore, be considered negligible, as the average difference in peak half-cycle L-L RMS voltage between the "without filter" and "with filter" case is less than 0.02 p.u. without PoW utilisation and less than 0.002 p.u. with PoW utilisation.
- When PoW is used, the "with filter" case performs on average better than the "without filter" case. However, the highest observed overvoltage is the highest for the capacitor bank with a filter.

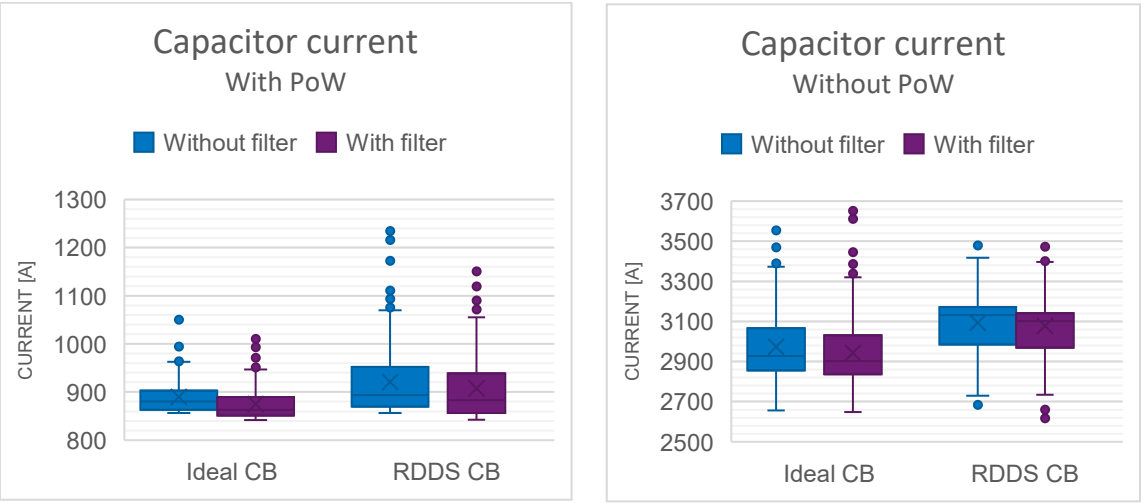

Figure 7.13: Comparison of with filter vs without filter on peak capacitor currents

In Figure 7.13, a peak L-L RMS voltage comparison between a 75 MVAr capacitor bank that consists of only a capacitor bank (without filter) and a 75 MVAr capacitor bank with a filter is depicted. Based on the simulation results, the following remarks can be made:

- The effect of the filter on the capacitor's peak current is limited and may, therefore, be considered negligible, as the average difference between the "without filter" and "with filter" case is less than 30 A without PoW utilisation and less than 15 A with PoW utilisation.
- Without PoW utilisation, the average performance of the "with filter" case is better than the "without filter" case, but also, for the ideal CB case, the higher outliers can be observed for the case without filter.

In general, the filter has little effect on the inrush current and RVCs, likely because the 1 mH filter inductance is small compared to the inductance of the source and transformers. The instantaneous L-G and L-L voltages were not considered in this simulation but are expected to remain largely

unchanged, especially the L-G voltages, as it is mathematically proved in Appendix E that they are unaffected by variations in capacitance and inductance.

7.6.3 Pre-insertion inductor

A pre-insertion inductor is similar to a filter but is only used during energisation. Its main advantages are that it has no continuous losses during normal operation and that the inductor does not need to handle continuous duty. However, it only provides protection during switching and does not suppress voltage fluctuations during steady-state operation.

7.6.4 Sequential phase energisation

Sequential phase energisation involves closing the three phases of a circuit breaker one by one with short and controlled delays, rather than energising all phases simultaneously. By spreading the energisation over a few milliseconds, the total inrush current and transients can be reduced, which is especially helpful for unbalanced or highly capacitive networks [31]. Unlike PoW switching, which controls the exact closing instant of each phase relative to the AC waveform to minimise transients, sequential phase energisation focuses on the order and timing between the phases. Although relatively simple to implement, it must be carefully coordinated to prevent unwanted zero-sequence currents or voltage imbalance. This is particularly important for star-connected capacitor banks with low ground impedance, where the benefits of sequential switching can be limited by zero-sequence current flow. Moreover, it is expected that sequential phase energisation alone does not provide sufficient suppression of transient overvoltages to comply with the Grid Code requirements, as even small deviations from the optimal switching instant can result in transients that exceed the permitted limits, as shown in the simulation results of this study.

7.6.5 Surge arresters

A surge arrester might be useful for transient voltage mitigation when energising a capacitor bank or cable circuit because it becomes (more) conductive when the system voltage rises above a certain threshold, providing a controlled current path to suppress the transient overvoltages [32]. A surge arrester does not mitigate the inrush currents and is most probably not effective for the mitigation of RVCs.

8 Conclusions & Recommendations

8.1 Conclusions

The conducted analysis in the thesis provides insight into the effectiveness of PoW for the switching of capacitor banks and underground cable circuits in the Dutch High Voltage transmission grid of TenneT. Furthermore, insight into the effect of breaker imperfections, such as pole scatter and imperfect RDDS, on the effectiveness of PoW is desired. The study is based on the following research question: “Is PoW switching an effective solution to meet the TenneT NL policy requirements when switching capacitor banks and cable circuits?”

To answer this research question, the state-of-the-art of PoW and TenneT’s power quality policies have been addressed. This research focused on the Rapid Voltage Change requirements and, more specifically, on the peak RMS L-L overvoltage limit of 1.10 p.u (10% above the nominal peak value) and that the peak RMS L-L overvoltages must be less than 1.05 p.u. (5% of the nominal peak value).

The study was based on a number of EMT simulation cases. Regarding the capacitor banks, simulations have been performed with 25 MVAr, 50 MVAr, 75 MVAr, and 100 MVAr ratings. Based on the obtained results of the simulation analysis, the following can be concluded regarding the energisation of capacitor banks:

- The use of PoW is an effective approach to mitigate transient overvoltages and inrush currents, as the peak values and the amount of dispersion are significantly lower with PoW implementation.
- With PoW implementation, energisation takes place at (or close to) zero voltage, resulting in a transient current with an amplitude equal to the nominal current, superimposed on the steady-state current, so that the minimum inrush current can only be reduced to approximately as low as twice the nominal peak current.
- Worsening of the pole scatter, represented by an increase in standard deviation, results in a) higher transient overvoltages and inrush currents, and b) a worsened PoW effectiveness.
- Without the PoW application, all the capacitor banks have simulation results exceeding the 10% RVC limit of TenneT’s policy.
- With PoW application, none of the RVCs for all simulated capacitor bank ratings, except the 100 MVAr capacitor bank, exceed the 5% limit of the Grid Code.

Regarding cable circuits, numerous simulations have been performed for cable circuits with a cross-section area of 1600 mm², 2500 mm² and 3500 mm², and lengths of 10,5 km, 15 km, 21 km, 30 km and 49,5 km. The following can be concluded regarding the energisation of cable circuits:

- Without PoW application, exceedances of the 10% RVC limit were observed for all the simulated cables.
- With PoW application, none of the simulations exceeded the 5% limit from the Grid Code.

8.2 Recommendations for future work

Based on the findings of this research, the following recommendations for future work are proposed:

1. **Investigate the appropriateness of TenneT's policy regarding PoW switching**
   According to this study, PoW cannot be considered a feasible mitigation option for energising capacitor banks and cable circuits, as most RVCs, without PoW, exceed the 10% power quality policy limit. Therefore, it is recommended to investigate the actual validity of this policy on the application of PoW switching.

2. **Investigate and evaluate possible statistical approaches for the power quality policy requirements**
   The grid code and TenneT's power quality policy requirements are deterministic in their requirements, while the performed study and circuit breaker switching in general are statistical. Based on the simulation analysis, PoW switching cannot be considered as an acceptable mitigation option, as in certain cases the absolute limits are exceeded. Consequently, other mitigation options need to be considered to comply with the power quality requirements. This could result in non-cost-effective solutions or a mix of solutions that do not facilitate the standardisation of designs. However, a statistical approach could allow the application of PoW switching in a wider range of cases. As an example, statistical approaches could be evaluated similarly to, e.g., insulation coordination (IEC 60071-1 and IEC 60071-2).

3. **Investigate the potential performance benefit of applying a shift in the target switching instant when RDDS is present**
   It is recommended to investigate whether applying a small shift in the target switching instant can help mitigate the increased occurrence of inrush current outliers, rapid voltage changes (RVCs), and L-L and L-G peak voltages observed when an RDDS of 90 kV/ms is present. Since lower RDDS values can cause earlier conduction due to pre-strikes, adjusting the target instant may reduce these undesired effects and improve overall switching performance.

4. **Further research on the effect of external variables on the effectiveness of PoW**
   In this study, the effect of external variables on the effectiveness of PoW is briefly considered. However, this research was only enough to prove the importance of external variable compensation in general. For obtaining accurate insights into the specific CBs used by TenneT, it is recommended to perform more in-depth research on CB-specific deviations that can occur for different external variables, such as temperature, idle time, and switching frequency.

5. **Continuously monitor the effectiveness of PoW in practice**
   It is recommended to continuously monitor PoW performance to identify possible errors, verify correct compensation of external factors, and strengthen the basis for future improvements and policy decisions. See Section 7.5 for more information.

6. **Investigate the correctness of the applied 0.15 ms standard deviation**
   It is recommended to carry out more detailed research into the actual scatter of TenneT's circuit breakers, as the currently applied standard deviation of 0,15 ms may be too optimistic for some CBs (see Section 7.3). This will help confirm realistic values and ensure that PoW remains effective and compliant with the Grid Code for different capacitor bank sizes.

7. **Further research on other mitigation options**
   It is recommended to perform further research and analysis on other mitigation options (e.g., pre-insertion resistors, capacitor banks with a filter) before selecting a standard solution. See Section 7.6 for more information on other mitigation options.

9 List of References

[1] TenneT TSO B.V., “About TenneT,” [Online]. Available: https://www.tennet.eu/about-tennet. [Accessed 19 12 2024].

[2] TenneT, “TenneT Link,” [Online]. Available: https://link.tennet.eu/nl/. [Accessed 19 12 2024].

[3] TenneT TSO B.V., "Grid expansion," [Online]. Available: https://www.tennet.eu/grid-expansion. [Accessed 25 06 2025].

[4] TenneT TSO B.V., "Target Grid," [Online]. Available: https://www.tennet.eu/target-grid-0. [Accessed 25 06 2025].

[5] TenneT TSO B.V., "Modulair bouwen," [Online]. Available: https://www.tennet.eu/nl/modulair-bouwen. [Accessed 25 06 2025].

[6] TenneT TSO B.V., "Bay replacement program," [Online]. Available: https://www.tennet.eu/nl/projecten/provincies/heel-nederland/bay-replacement-program. [Accessed 25 06 2025].

[7] TenneT TSO B.V., "Pocketvorming," [Online]. Available: https://www.tennet.eu/nl/pocketvorming. [Accessed 25 06 2025].

[8] European EMTP-ATP Users Group e.V., "EEUG," [Online]. Available: https://www.atp-emtp.org/. [Accessed 12 1 2025].

[9] Y. Chai, "Capacitive current interruption with high voltage air-break," Eindhoven University of Technology, Eindhoven, 2012.

[10] ABB, "Controlled Switching Buyer’s Guide, Application Guide," 2010.

[11] G. VERNOVA, "CSD100 Point-on-Wave Controller," GE VERNOVA, 2024.

[12] Cigre, "Guidelines and best practices for the commissioning and operation of controlled switching projects," Cigre, 2019.

[13] ENTSO-E, “Controlled switching device: Application, use and maintenance problems,” 2022.

[14] G. Granada, "Controlled Switching with Switchsync PWC600 Point-on-Wave Controller," ABB, 2017.

[15] "Netcode elektriciteit," Wettenbank, 2025.

[16] A. Dabin, S. Uytterhoeven and R. Bosch, "Onderzoek Spanningskwaliteit Elektriciteitsnetwerken," Autoriteit Consument & Markt (ACM), 2023.

[17] F. van Erp and J. van Waes, "[Internal] TenneT beleidsdocument spanningskwaliteit voor TenneT TSO B.V. AMN," TenneT, Arnhem, 2019.

[18] Prysmian Group, "Datasheet: EYAKrvlwd 87/150kV 1x1600 mm² aluminium," Prysmian Group, 2019.

[19] Prysmian Group, "Datasheet: EYAKrvlwd 87/150kV 1x2500 Alu," Prysmian Group, 2017.

[20] Prysmian Group, "Datasheet: EYAKrvlwd 87/150kV 1x3500mm² aluminium," Prysmian Group, 2019.

[21] Ludvinka, "[INTERNAL] SATS Certification 06-A05," SINTEF Energy Research, Trondheim, 2006.

[22] P. Bhandari, "Normal Distribution | Examples, Formulas, & Uses," Scribbr, 21 06 2023. [Online]. Available: https://www.scribbr.com/statistics/normal-distribution/. [Accessed 14 06 2025].

[23] Ludvinka, "[INTERNAL] SATS Certification 06-A23," SINTEF Energy Research, Trondheim, 2006.

[24] K. Velitsikakis, "[Internal] Bay Replacement Program - Capacitor bank switching at HGLW110, TERW150 and NEDW150," TenneT, Arnhem, 2022.

[25] M. Galarnyk, "Understanding Boxplots," KDnuggets.

[26] J. W. Nilson and S. A. Riedel, ELECTRIC CIRCUITS.

[27] Dictionary, 01 07 2025. [Online]. Available: https://www.dictionary.com/browse/deterministic.

[28] KEMA Nederland B.V., "Report of performance," KEMA Nederland B.V., Arnhem, 2011.

[29] L. Dai, J. Yu, Z. Huang, H. Ni, Y. Zhang and J. Dou, "Research into prediction and influential factors of circuit breaker closing time using BFGS-NN," American Institute of Physics, 2025.

[30] M. Beanland, T. Speas and J. Rostron, "Pre-insertion Resistors in High Voltage Capacitor Bank Switching," Western Protective Relay Conference, Spokane, 2004.

[31] S. Abdulsalam and W. Xu, "Sequential phase energisation technique for capacitor switching transient reduction," Wiley, 2007.

[32] K. D. Sharma and M. Harpreet, Study and Analysis of Substation Mitigation Techniques Using MATLAB, International Journal of Scientific Research & Engineering Trends, 2024.

[33] ENTSO-E, “(Variable) Shunt Reactor,” [Online]. Available: https://www.entsoe.eu/Technopedia/techsheets/variable-shunt-reactor#:~:text=Shunt%20reactors%20(SRs)%20are%20used,to%20provide%20reactive%20power%20compensation.. [Accessed 11 12 2024].

[34] Cigre, “Controlled Switching of HVAC Circuit Breakers - Planning, Specification and Testing of Controlled Switching Systems,” Cigre, 2004.

[35] NEN, "NEN-EN 50160 Voltage characteristics of electricity supplied by," NEN, 2022.

[36] Southern States, “Synchronous Close (Zero Voltage Close/Point on Wave) Circuit Breakers vs Southern States CapSwitcher® Capacitor Switch with Closing Resistors”.

[37] H. Andersson, "[Internal] Inrush current study for TenneT TERW150," ABB, 2019.

[38] K. Munji, J. Horne and J. Ribecca, "Design and Validation of Pre-Insertion Resistor," International Conference on Power Systems, Seoul, 2017.

Appendix A

This appendix provides the mathematical derivation for the formula that determines the new required target switching instant to prevent prestrikes based on the RDDS.

The voltage across the breaker when open:

$$U(t) = U_m \cdot \sin(2\pi f t) \tag{A.1}$$

The rate of change of the breaker voltage in open condition:

$$U'(t) = 2\pi f U_m \cdot \cos(2\pi f t) \tag{A.2}$$

To calculate the target switching instant, it is important to know at what time instant the rate of change in breaker voltage equals the RDDS.

$$2\pi f U_m \cdot \cos(2\pi f t_{int}) = -RDDS \rightarrow \cos(2\pi f t_{int}) = \frac{-RDDS}{2\pi f U_m} \rightarrow t_{int} = \frac{1}{2\pi f} \cdot \cos^{-1}\left(\frac{-RDDS}{2\pi f U_m}\right) \tag{A.3}$$

The new target switching instant is the sum of the instant calculated in equation A.3 and the time it takes for the breaker to move from this instant to zero dielectric strength:

$$t_{target} > t_{int} + t_{RDDS} = t_{int} + \frac{U(t_{int})}{RDDS} = t_{int} + \frac{U_m \cdot \sin(2\pi f t_{int})}{RDDS}$$

Substitution leads to:

$$t_{target} > \frac{1}{2\pi f} \cdot \cos^{-1}\left(\frac{-RDDS}{2\pi f U_m}\right) + \frac{U_m \cdot \sin\left(\cancel{2\pi f}\frac{\cancel{1}}{\cancel{2\pi f}} \cdot \cos^{-1}\left(\frac{-RDDS}{2\pi f U_m}\right)\right)}{RDDS}$$

Rewriting trigonometric functions:

$$\sin\left(\cos^{-1}\left(\frac{-RDDS}{2\pi f U_m}\right)\right) = \sqrt{1 - \left(\frac{RDDS}{2\pi f U_m}\right)^2}$$

The target instant such that no prestrike occurs:

$$t_{target} > \frac{1}{2\pi f} \cdot \cos^{-1}\left(\frac{-RDDS}{2\pi f U_m}\right) + \frac{U_m \sqrt{1 - \left(\frac{RDDS}{2\pi f U_m}\right)^2}}{RDDS} \pm \frac{k}{2f} \; for \; k \epsilon \mathbb{Z} \; if \; RDDS < 2\pi f U_m \tag{A.4}$$

Where:

$$U_m: Peak\ voltage\ across\ CB\ [V], f: Frequency\ [Hz]$$
$$RDDS: Rate\ of\ Decrease\ of\ Dielectric\ Strength\ [V/s]$$

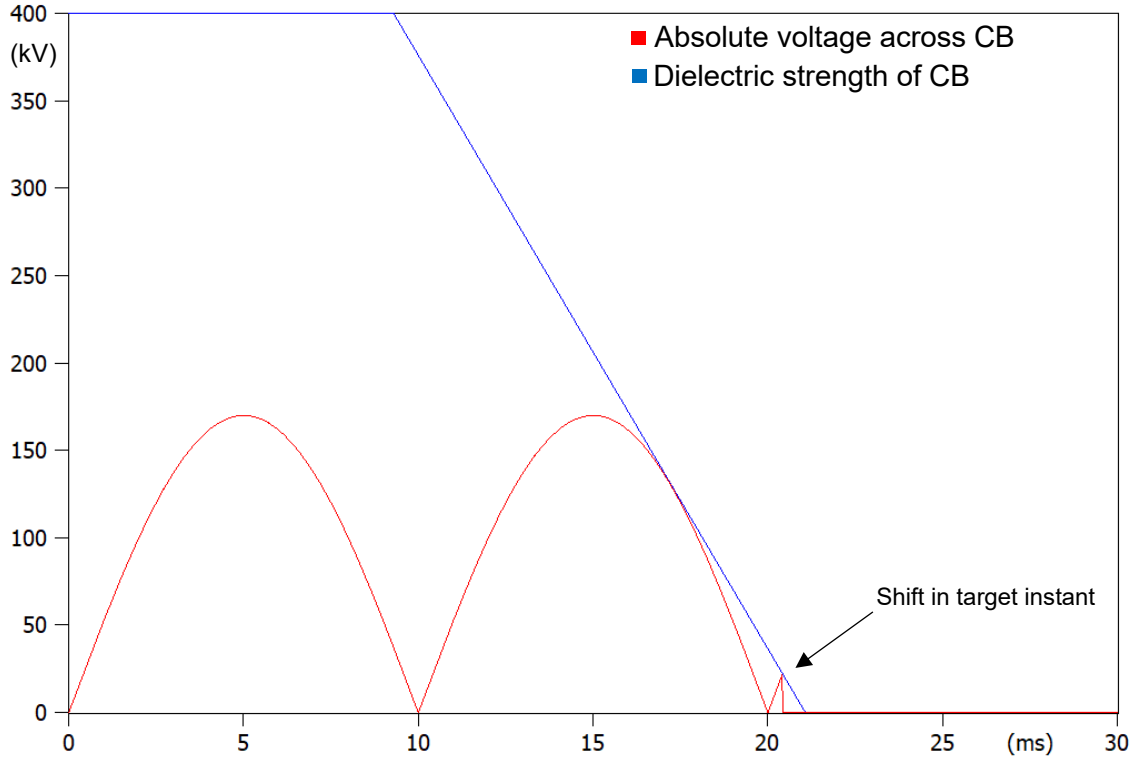

Figure A.1: Result when formula is applied

Figure A.1 illustrates the end result when the target instant is set according to the formula. One can observe that no pre-strike occurs.

Appendix B

This appendix elaborates on the applications of PoW that are not considered in this study.

Point-on-Wave switching for preventing transients when de-energising shunt reactors

Shunt reactors are used for reactive power compensation. However, the load applied to the grid vary from time to time and thus does the reactive power that has to be compensated. For this reason, the shunt reactors have to be switched from time to time [33].

Issues related to shunt reactor switching [12]:

1. Circuit breaker re-ignition during shunt reactor de-energisation;
2. Current asymmetry during energisation;
3. Voltage transient during energisation.

Circuit breaker re-ignition during shunt reactor de-energisation

Since a shunt reactor behaves as an inductive load, high peak voltages will be induced by the shunt reactor during a current interruption. This can cause circuit breaker restrikes, which hurt the lifespan of the circuit breaker. Furthermore, current chopping can cause overvoltages that are not only harmful to the circuit breaker but also to the shunt reactor [12].

Current asymmetry during energisation

Random energisation of shunt reactors yields current asymmetry, also referred to as DC-offsetted currents. This may result in saturation of the current transformers' iron cores and may lead to protective relay maloperation. When the goal is to reduce current asymmetry, ideally, energisation takes place at each phase's respective voltage peak. [13]

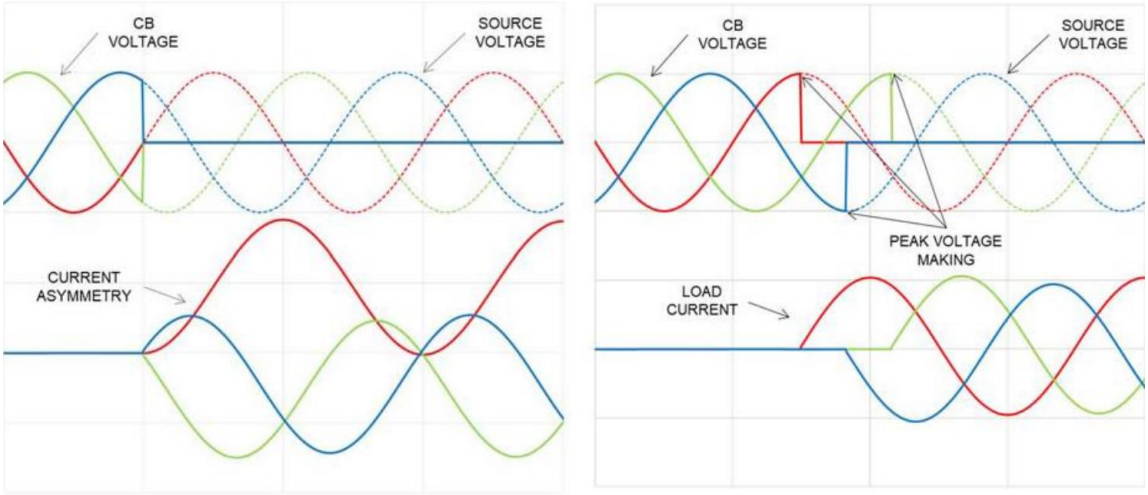

Figure B.1: A) Uncontrolled switching, B) Controlled switching [13]

Figure B.1 displays a shunt reactor's current for random and controlled energisation. One can directly observe that random energisation yields a DC offset in the currents. This asymmetry is due to the inductive behaviour of the shunt reactor. For the perfect inductor, the inductor current as a function of time is described by equation B.1.

$$I(t) = I(t_0) + \frac{1}{L}\int_{t_0}^{t} V(t)dt = I(t_0) + \frac{1}{L}\int_{t_0}^{t_{v_p}} V(t)dt + \frac{1}{L}\int_{t_{v_p}}^{t} V(t)dt \qquad (B.1)$$

Furthermore, if not energised at the peak value, and if $V(t)$ is perfectly sinusoidal,

$$\lim_{t\to\infty}\frac{1}{t}\int_0^t\left(\frac{1}{L}\int_{t_{v_p}}^{t}V(t)dt\right)dt\ =0 \qquad (B.2)$$

$$\lim_{t\to\infty}\frac{1}{t}\int_0^t\left(\frac{1}{L}\int_{t_{t_0}}^{t_{v_p}}V(t)dt\right)dt\ \neq 0 \qquad (B.3)$$

Where,

$$t_0\text{: Energisation instant } (s), \qquad t_{v_p}\text{: Instant of voltage peak } (s), \qquad t\text{ : time } (s)$$

The integral between the energisation instant t_0 and the voltage peak instant t_{v_p}, as shown in equation B.3, forms the DC-offset component.

Fast transient voltage during energisation

Due to stray capacitances of the shunt reactor, transient overvoltages can occur when energising near peak voltage [12]. For the suppression of these transients, ideally, the energisation occurs at zero voltage. However, this is detrimental to the current symmetry [34].

Point-on-Wave switching for preventing voltage peaks on overhead lines due to voltage reflections

When a voltage is applied to a line, the voltage will travel through the line as a wave. When the impedance of the medium through which the wave travels suddenly increases, a part of the wave gets reflected and is added to the original voltage. When the line is open-ended, the new impedance can be considered infinite, thus yielding a full reflection of this voltage (see Figure B.2). As this full reflection is added to the original voltage, theoretically, a voltage peak of 2 p.u. can occur.

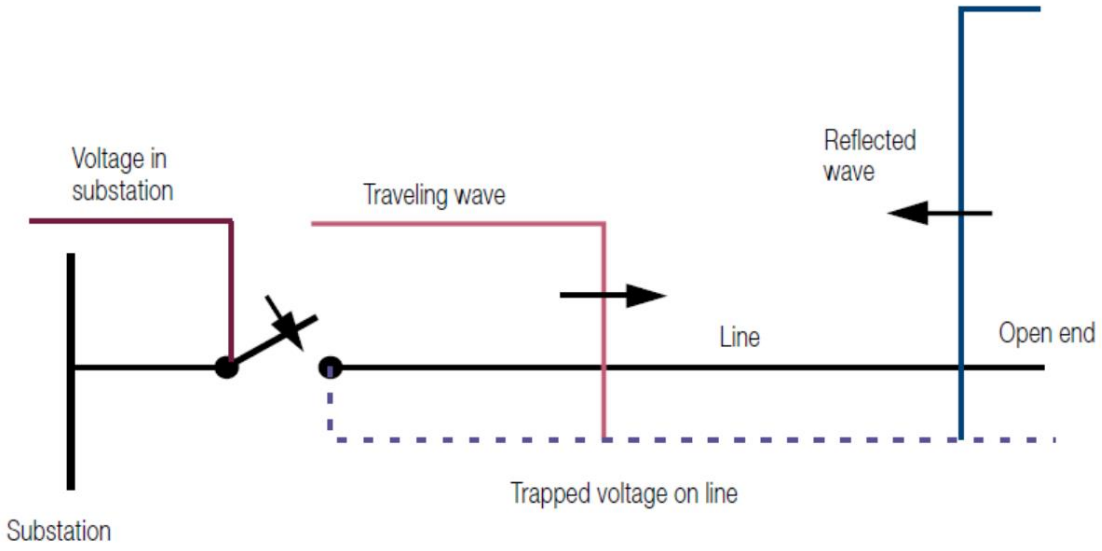

Figure B.2: Travelling wave phenomenon [10]

When considering mitigation techniques, the transmission line arrangement must be taken into consideration [12]:

- Lines without compensation elements;
- Lines with shunt reactors;

Lines with shunt reactors (Shunt compensated line)

When there is a shunt reactor present, the voltage on the line will be a gradually damped sinusoidal oscillation. The dampened frequency will be dependent on the line capacitance and the inductance of the shunt reactor. Generally, this frequency will be lower than the frequency of the supply voltage. The combination of these voltages will yield an amplitude-modulated voltage on the circuit breaker (see Figure B.3). Ideally, re-closure occurs at a zero-crossing of the CB voltage [13].

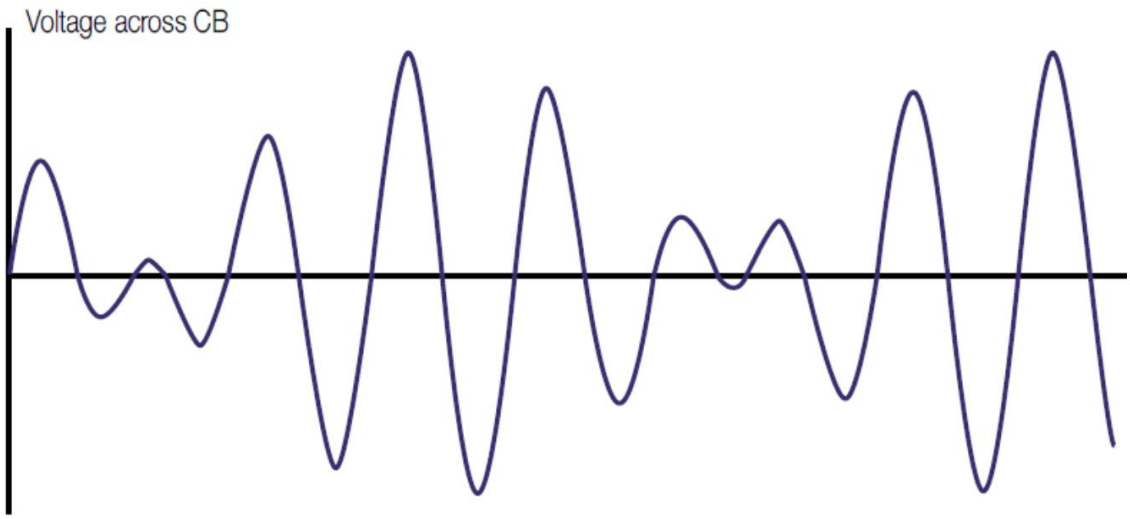

Figure B.3: Example of amplitude-modulated voltage across the circuit breaker before reclosing [10]

When energising a shunt-compensated line, two undesirable scenarios can occur [12]:

- If energised near voltage zero, high DC offset can occur in the currents;
- If energised near a voltage peak, overvoltages can occur due to reflections.

A DC offset in the current can result in saturation of the measurement or power transformers. Saturation of a measurement transformer can result in maloperation of the protective system. Furthermore, Saturation of the power transformers results in high inrush currents, which can also trip the protective system. Transients may harm devices or cause re-ignition of the circuit breaker. The optimal switching instant is dependent on the allowed inrush current and voltage transient. However, most often, current asymmetry is more detrimental than the voltage transients.

Uncompensated lines

There is no shunt reactor present to compensate for the capacitive component in an uncompensated transmission line. Therefore, energising near voltage zero is optimal, as a DC offset in current will not occur. Energising near voltage zero will result in the lowest overvoltage transients.

Point-on-Wave switching for transformer energisation

Point-on-Wave switching for preventing asymmetrical magnetic flux in unloaded power transformers

When energising an unloaded power transformer, a magnetic flux asymmetry can occur. This asymmetry is undesirable, as it can cause saturation of the transformer core, which results in high inrush currents. This phenomenon is comparable to the current asymmetry that can occur when energising a shunt reactor. However, in transformers, residual flux can be present. The presence of this residual flux changes the optimal energisation moment if suppression of flux asymmetry is desired.

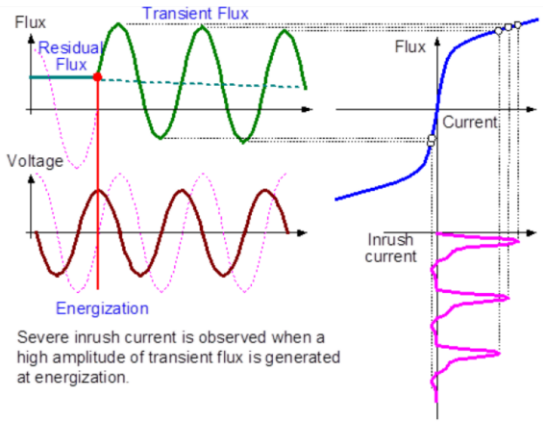

Figure B.4: Energisation at peak voltage with residual flux [13]

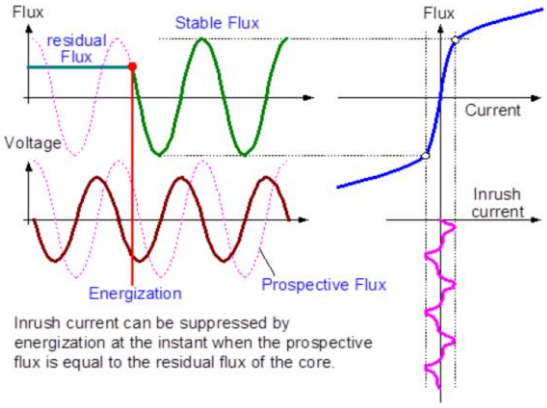

Figure B.5: Optimal energisation moment with residual flux [13]

Figure B.4 illustrates that energising at the respective phase voltage peak can still result in high inrush currents due to the residual flux. To overcome this problem, energisation takes place at a different instant (see Figure B.5).

Point-on-Wave switching to prevent a steep voltage front

When switching near the peak value, transient overvoltages may occur. Potentially, transient overvoltages can be reduced by optimising the switching instants. However, this optimisation can increase the inrush currents due to asymmetric flux. Therefore, it is important to find an optimal balance.

Point-on-Wave switching for preventing overvoltages when de-energising power cables

Sometimes overhead lines are not suitable due to environmental issues. Therefore, power utilities are more likely to use underground cables for network upgrading. In contrast to overhead lines, underground and submarine cables have less conductor spacing, and thus higher capacitance to the earth. This capacity forms challenges for the circuit breaker, as it involves the interruption of highly capacitive current.

Often, the capacitive current is compensated with a shunt reactor to reduce the losses and improve the power transfer capability of the cable. Due to the presence of the shunt reactor, DC offset in current may occur if energised near zero voltage (see Figure B.6). This issue is similar to the asymmetric current issue and the asymmetric magnetic flux issue, as described in this appendix. Due to this initial DC offset, it takes time before the first zero-current-crossing occurs. If a fault occurs during this time, it is hard for the circuit breaker to interrupt the current, as there is no zero-current crossing. This problem can be overcome by switching near the voltage peak (see Figure B.7). Therefore, the implementation of Point-on-Wave switching can be useful.

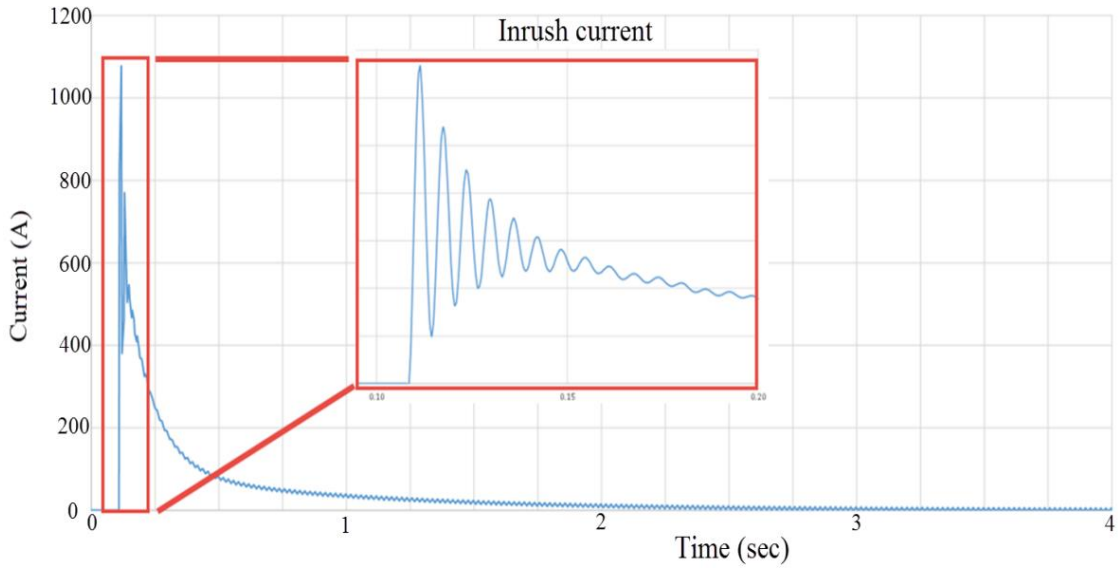

Figure B.6: Energisation at zero voltage [12]

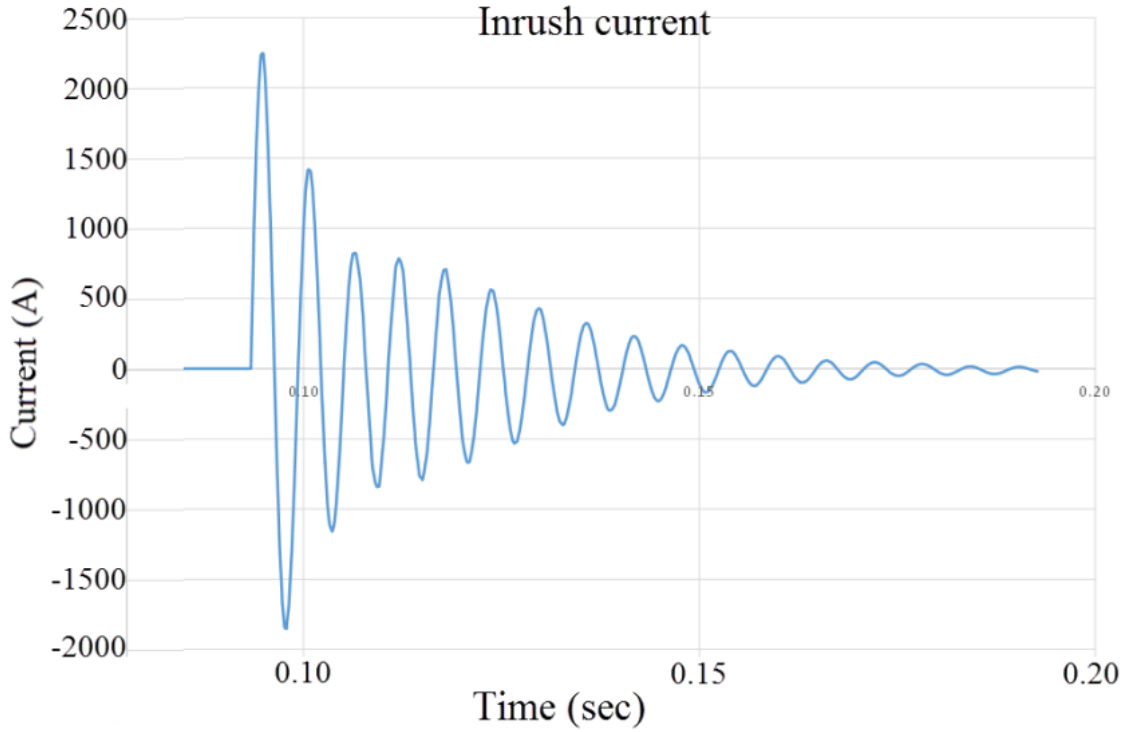

Figure B.7: Energisation at peak voltage [12]

Appendix C

This appendix elaborates on Power Quality related distortions. The aspects covered in this appendix, however, are only marginally influenced by the PoW implementation and are therefore not considered in the PoW switching effectiveness assessment.

Harmonic distortion

The total harmonic distortion can be calculated with equation C.1.

$$THD = \sqrt{\sum_{n=2}^{\infty} \frac{U_n}{U_1}^2} \qquad (C.1)$$

Table C.1 shows the allowed harmonic distortion in TenneT's grid.

Table C.1: Allowed harmonic distortion [16]

Time	Limit
95%	$THD \leq 8\%\ (LV, MV)$
95%	$THD \leq 6\%\ (HV)$
95%	$THD \leq 5\%\ (EHV)$
95%	$All\ indivudial\ harmonics \leq 8\%\ (LV, MV)$
99,9%	$THD \leq 12\%\ (LV, MV)$
99,9%	$THD \leq 7\%\ (HV)$
99,9%	$THD \leq 6\%\ (EHV)$
99,9%	$All\ indivudial\ harmonics \leq 12\%\ (LV, MV)$

Flicker

The flicker intensity is evaluated by two quantities, which are "short-term flicker severity" (P_{st}) and "long-term flicker severity" (P_{lt}).

The "short-term flicker severity" is defined as the intensity of the flicker irritation for humans over a 10-minute period.

The "long-term flicker severity" is calculated from a sequence of twelve "short-term flicker severity" (P_{st}) values over a two-hour interval (See equation C.2) [35].

$$P_{lt} = \sqrt[3]{\sum_{i=1}^{12} \frac{P_{sti}^3}{12}} \qquad (C.2)$$

Table C.2: Allowed flicker limits [16]

Time	Limit
95%	$P_{lt} \leq 1\ (\mathrm{LV, MV, HV, EHV})$
100%	$P_{lt} \leq 5\ (\mathrm{LV, MV, HV, EHV})$

Table C.2 describes the allowed flicker limits in TenneT's grid.

Slow voltage variations

TenneT's maximum permitted slow voltage variations are shown in Table C.3. The maximum deviation is expressed as a percentage of the nominal voltage U_n.

Table C.3: Allowed slow voltage variations

Time	Limit
95%	$\pm 10\%\ of\ U_n\ (LV)$
95%	$\pm 10\%\ of\ U_n\ (MV)$
99,9%	$\pm 10\%\ of\ U_n\ (HV, EHV)$
100%	$+10\%\ /\ -15\%\ of\ U_n\ (MV)$
100%	$+10\%\ /\ -15\%\ of\ U_n\ (LV)$

Voltage asymmetry

The voltage asymmetry describes the imbalance in voltage between the phases. In a perfectly balanced system, the positive sequence component equals the negative sequence component. The difference in positive and negative sequence components is described by V_{un}. The maximum allowed differences for TenneT's grid are shown in Table C.4.

Table C.4: Maximum allowed voltage asymmetry [16]

Time	Limit
100%	$V_{un} \leq 3\%\ (LV, MV)$
99,9%	$V_{un} \leq 1\%\ (HV, EHV)$
95%	$V_{un} \leq 2\%\ (LV, MV)$

Appendix D

In this appendix, the Excel Typescript code that is used for the extraction of the simulation data from ATP-EMTP that is obtained with the “EXTREMA OUTPUT FOR EXCEL” command in the user-specified -> additional block is described. The Typescript (See Figure D.1 and Figure D.2) extracts the data, organises it, and places it in new Excel columns.

```
function main(workbook: ExcelScript.Workbook) {
  // Get the active cell and worksheet.
  let selectedCell = workbook.getActiveCell();
  let selectedSheet = workbook.getActiveWorksheet();
  let nrOfDataRows = 6;

  ExtractData(workbook, "A2", 1, 0, 1);
  let finished = false;

  let dataRowIndex = 0;
  while (!finished) {
    dataRowIndex++;
    finished = ExtractData(
      workbook,
      incrementCellAddress("A2", 2 * dataRowIndex),
      1,
      dataRowIndex,
      1,
    );
  }
}

function ExtractData(
  workbook: ExcelScript.Workbook,
  address: string,
  rowOffset: number,
  colOffset: number,
  delFirst: number,
) {
  let sheet = workbook.getActiveWorksheet();

  // Define the input cell containing the tab-delimited text
  let inputCell = sheet.getRange(address); // Change this to any desired cell
  let rawText = inputCell.getText(); // Get the text from the cell
  if (!rawText) {
    return true;
  }

  // Split data into rows (based on new lines)
  let rows = rawText.split("\n");

  for (let rowIndex = 0; rowIndex < rows.length; rowIndex++) {
    // Split each row into columns (using tab as the delimiter)
    let newRows = rows[rowIndex].split(/\s+/);

    for (let rowIndex = delFirst; rowIndex < newRows.length; rowIndex++) {
      // Insert data into Excel, starting at cell B2
      sheet
        .getCell(rowIndex - 2 + rowOffset, colOffset + 1)
        .setValue(newRows[rowIndex].trim());
    }
  }
}
```

Figure D.1: Excel Typescript code for extrema extraction (part 1)

```
function incrementCellAddress(address: string, increment: number): string {
  const match = address.match(/^([A-Z]+)(\d+)$/);

  if (!match) {
    throw new Error("Invalid cell address format");
  }

  const column = match[1]; // "A"
  const row = parseInt(match[2], 10) + increment; // 262 + 5

  return `${column}${row}`;
}
```

Figure D.2: Excel Typescript code for extrema extraction (part 2)

Figure D.3, D.4, and D.5 depicts the code used for extracting the exact switching instants used by the statistical switches from the .lis file, which was useful to investigate the instantaneous voltage graphs of outliers in the statistical data and to determine the standard deviation accuracy of ATP-EMTP. The code extracts the switching instants, organises them, and places them in new rows. This makes it possible to determine the exact switching instant of every pole that corresponds to the statistical data.

```
function main(workbook: ExcelScript.Workbook) {
    let addressOfIndex = SearchIndex(workbook, "Step      Time");
    let amountOfData = SearchIndex(workbook, "Random switching times for simulation number
").length;
    let addressOfData = SearchIndex(workbook, "Random switching times for simulation number
");

    for (let dataNr = 0; dataNr < amountOfData; dataNr++) {
        ExtractData(workbook, incrementCellAddress(addressOfData[dataNr], 1), 1, 1 +
dataNr, 1);
        ExtractData(workbook, incrementCellAddress(addressOfData[dataNr], 2), +11, 1 +
dataNr, 1);
        ExtractData(workbook, incrementCellAddress(addressOfData[dataNr], 3), +21, 1 +
dataNr, 1);
    }

    console.log(addressOfData);

}
```

Figure D.3: Extraction of switching instants (part 1)

```
function SearchIndex(workbook: ExcelScript.Workbook, searchValue: string): string[] {
    let sheet = workbook.getActiveWorksheet();
    if (!searchValue) {
        console.log("Internal error");
        return;
    }

    let foundCells: string[] = [];
    let usedRange = sheet.getUsedRange();

    if (usedRange) {
        let values = usedRange.getValues();
        let rowCount = values.length;
        let colCount = values[0].length;

        // Loop through all cells in the used range
        for (let row = 0; row < rowCount; row++) {
            for (let col = 0; col < colCount; col++) {
                if (values[row][col] && values[row][col].toString().includes(searchValue)) {
                    let cellAddress = sheet.getCell(row, col).getAddress().split("!").pop();
                    foundCells.push(cellAddress);
                }
            }
        }
    }
    return foundCells;
}

function ExtractIndex(workbook: ExcelScript.Workbook, address: string, rowOffset: number,
colOffset: number, delFirst: number) {
    let sheet = workbook.getActiveWorksheet();

    // Define the input cell containing the tab-delimited text
    let inputCell = sheet.getRange(address); // Change this to any desired cell
    let rawText = inputCell.getText(); // Get the text from the cell
    if (!rawText) {
        console.log("Error: No data found");
        return;
    }

    // Split data into rows (based on new lines)
    let rows = rawText.split("\n");

    for (let rowIndex = 0; rowIndex < rows.length; rowIndex++) {
        // Split each row into columns (using tab as the delimiter)
        let newRows = rows[rowIndex].split("     ");

        for (let rowIndex = delFirst; rowIndex < newRows.length; rowIndex++) {
            // Insert data into Excel, starting at cell B2
            sheet.getCell(rowIndex - 2 + rowOffset, colOffset +
1).setValue(newRows[rowIndex].trim());
        }
    }
}
```

Figure D.4: Extraction of switching instants (part 2)

```
function ExtractData(workbook: ExcelScript.Workbook, address: string, rowOffset: number,
colOffset: number, delFirst: number) {
    let sheet = workbook.getActiveWorksheet();

    // Define the input cell containing the tab-delimited text
    let inputCell = sheet.getRange(address); // Change this to any desired cell
    let rawText = inputCell.getText(); // Get the text from the cell
    if (!rawText) {
        console.log("Error: No input data found");
        return;
    }

    // Split data into rows (based on new lines)
    let rows = rawText.split("\n");

    for (let rowIndex = 0; rowIndex < rows.length; rowIndex++) {
        // Split each row into columns (using tab as the delimiter)
        let newRows = rows[rowIndex].split(/\s+/);

        for (let rowIndex = delFirst; rowIndex < newRows.length; rowIndex++) {
            // Insert data into Excel, starting at cell B2
            sheet.getCell(rowIndex - 2 + rowOffset, colOffset +
1).setValue(newRows[rowIndex].trim());
        }
    }

}

function incrementCellAddress(address: string, increment: number): string {
    const match = address.match(/^([A-Z]+)(\d+)$/);

    if (!match) {
        throw new Error("Invalid cell address format");
    }

    const column = match[1]; // "A"
    const row = parseInt(match[2], 10) + increment; // 262 + 5

    return `${column}${row}`;
}
```

Figure D.5: Extraction of switching instants (part 3)

Appendix E

This appendix presents the simulation results of the line-to-ground voltages and line-to-line voltages regarding the energisation of capacitor banks.

Effectiveness of PoW on the line-to-ground voltages

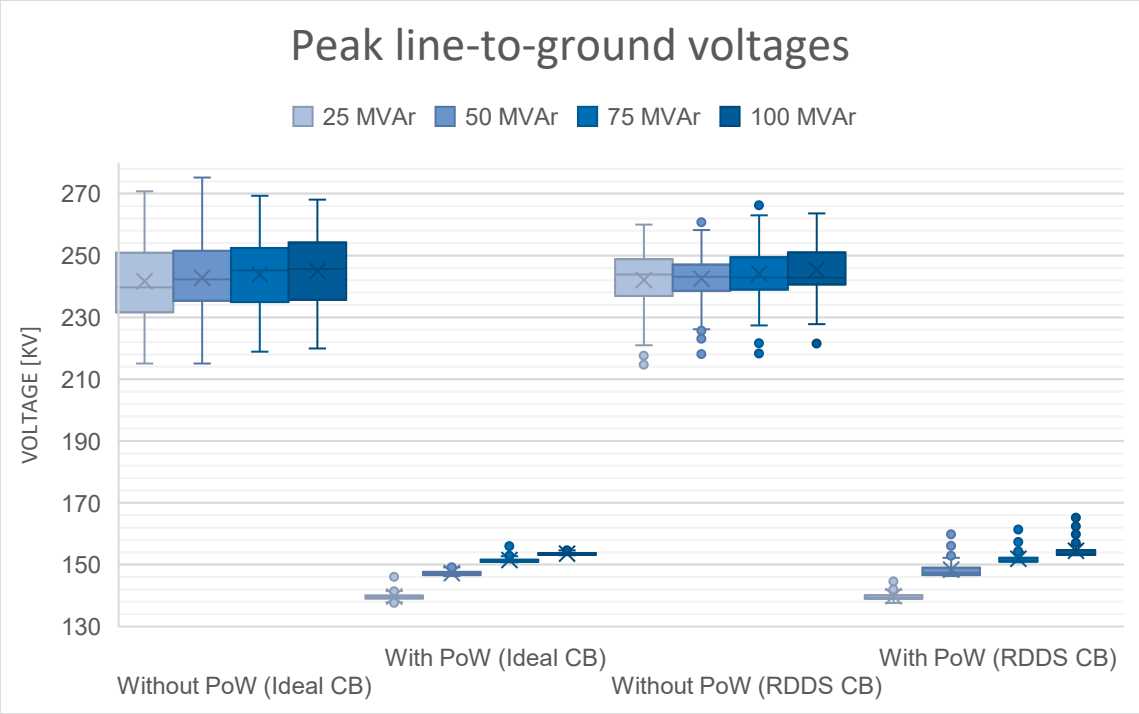

Figure E.1: Effect of PoW on line-to-ground voltages

The effectiveness of PoW implementation on the peak L-G voltages for multiple capacitor banks is depicted in Figure E.1. Based on the simulation results, the following remarks can be made:

- If no PoW is applied, the size of the capacitor bank does not have a significant effect on the peak values of the L-G voltage.
- When no PoW is applied, the CB case with imperfect RDDS has lower peak values than the ideal CB case.
- When PoW is applied, one can observe a significant drop in the peak voltages. In contrast to when PoW is not applied, when PoW is applied, the size of the capacitor bank affects the peak overvoltage values, as an increase in the capacitor bank size results in an increase in the peak overvoltage values.
- When PoW is implemented, a CB with imperfect RDDS has bigger outliers. Due to the RDDS, the effect of deviations in switching instant can be increased due to the addition of pre-strike.

The L-G voltages and capacitor currents are strongly correlated. With the help of the equations below, a mathematical proof for this consistency in L-G peak voltage values is provided.

The measured line-to-ground voltages are the same as the voltages across the capacitor bank when the CB is closed. Therefore, if the resistances in the grid are neglected, the following is true:

$$V_{capacitor} = V_{source} - V_{inductor} = V_{source} - L\frac{di}{dt} \qquad (F.1)$$

Furthermore,

$$I = C\frac{dV_{capacitor}}{dt} \qquad (F.2)$$

Substituting Equation F.2 in F.1:

$$V_{capacitor} = V_{source} - L\frac{dC\frac{dV_{capacitor}}{dt}}{dt} = V_{source} - LC\frac{d^2V_{capacitor}}{dt^2} \qquad (F.3)$$

The change in capacitor bank size affects the resonance frequency, and thus affects dt:

$$\omega_0 = \frac{1}{\sqrt{LC}} \rightarrow dt \propto \sqrt{LC} \rightarrow dt^2 \propto LC \qquad (F.4)$$

Based on Equations F.3 and F.4, it can be proved that the peak L-G voltages ($V_{capacitor}$) remain constant even if the inductance L or capacitance C change, because the second derivative $\frac{d^2V_{capacitor}}{dt^2}$ scales inversely if LC. This compensates the product LC in the equation, resulting in a constant peak voltage, assuming the source voltage V_{source} remain unchanged.

Figure E.2 presents the instantaneous voltages for the 25 MVAr, 50 MVAr, and 100 MVAr capacitor banks. It can be observed that the amplitudes stay rather constant among all simulated capacitor bank sizes and that the rise time of the transient increases with approximately the square root of two when the capacitor bank size doubles, which is as described by Equations F.3 and F.4.

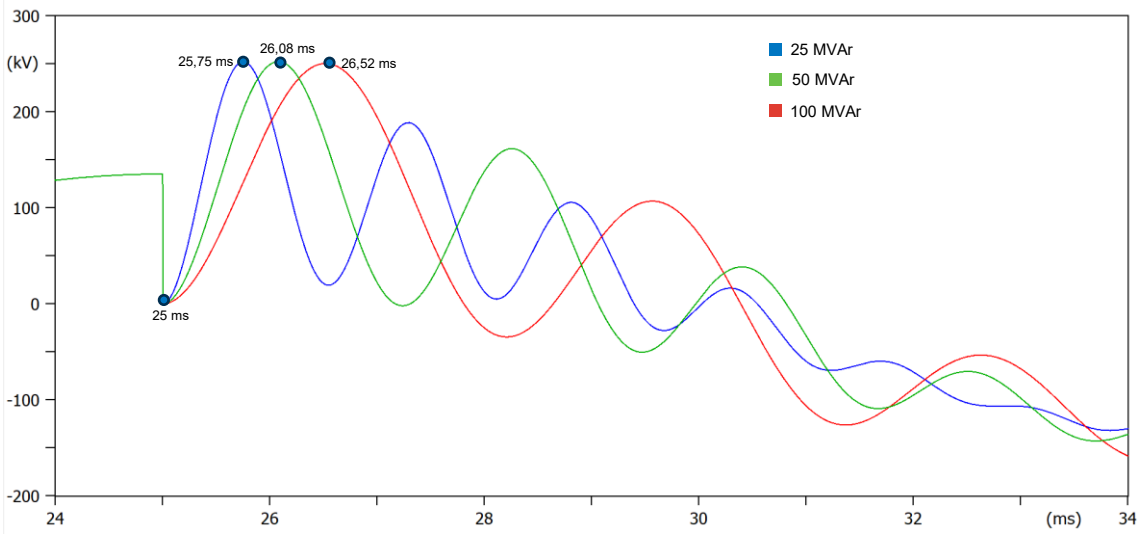

Figure E.2: Instantaneous peak voltages

Counterintuitively, when no PoW is utilised, a CB with imperfect RDDS perform better than the ideal CB, as the highest peaks are observed for the Ideal CB case (see Figure E.1). The highest peak in voltage will occur when a pole is switched near a peak of a phase. This voltage, however, can be pushed even higher by the currents in the other phases. When imperfect RDDS is present, this effect is less, as the other phases are switched later due to the RDDS (see Figure E.3), and thus there is no current flowing in the other conductors yet.

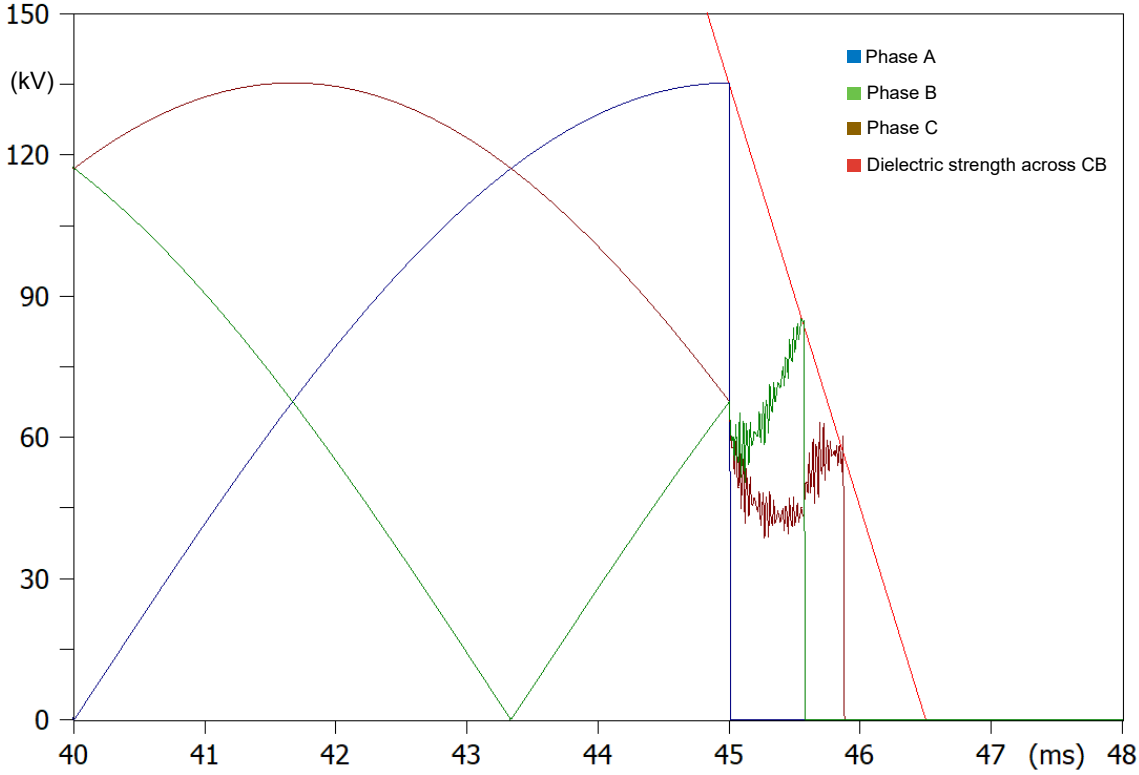

Figure E.3: Voltages across breaker

Effect of pole scatter on the effectiveness of PoW

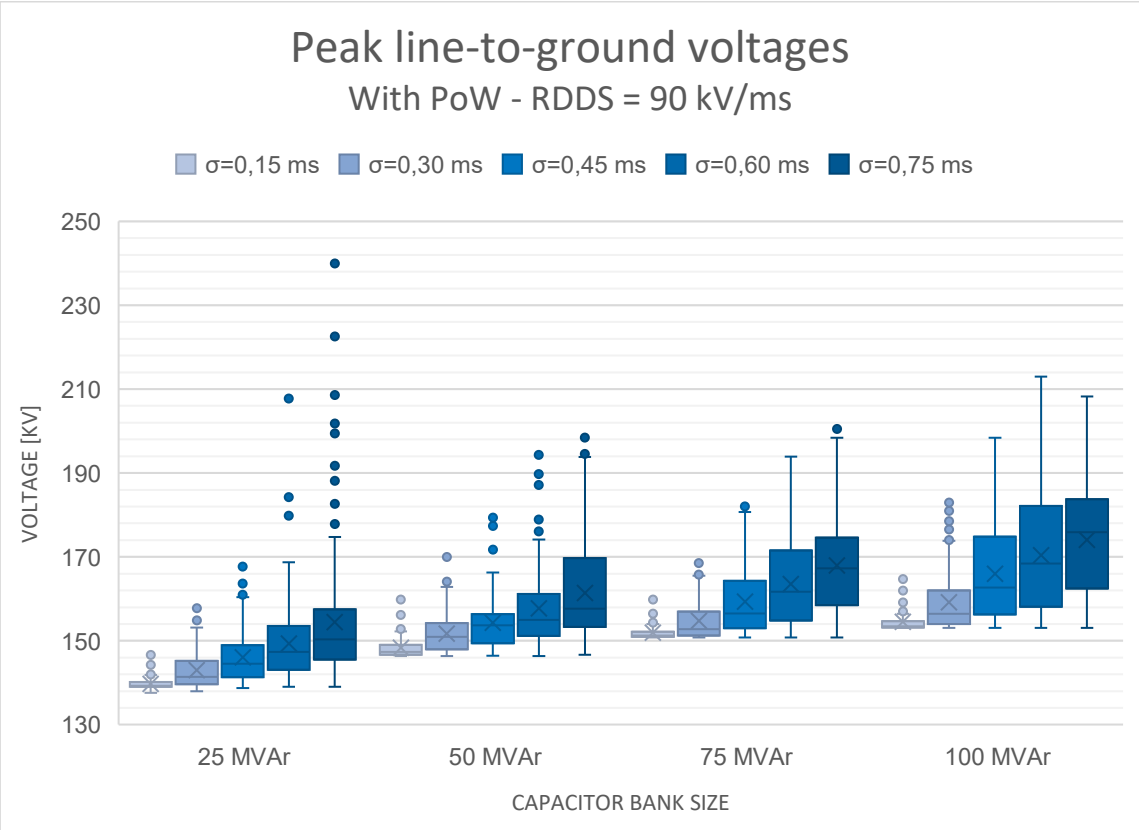

Figure E.4: Effect of scatter on line-to-ground voltages

Figure E.4 depicts the effect of CB scatter on the L-G voltages by showing box plots with the peak voltages for different standard deviations. Based on the simulation results, the following remarks can be made:

- Overall, an increase in standard deviation results in a bigger spread in L-G voltages.
- For high standard deviations, above 0.60 ms, the 25 MVAr capacitor bank becomes prone to outliers higher than the maxima of the other capacitor bank sizes. For a standard deviation of 0.75 ms, three out of the 200 overvoltage values of the 25 MVAr capacitor banks exceed the maximum value of the 100 MVAr.
- At higher standard deviations, the transient behaviour gets more similar to the case where no PoW is applied.

For a standard deviation of 0.75 ms, the 25 MVAr capacitor bank has much higher outliers for the following reasons:

- The study is fully statistical, meaning that the switching instants of each capacitor bank are different, which can result in different outliers.
- The instantaneous voltage during energisation is the sum of the base voltage and the oscillations. For a standard deviation of 0.75 ms, in combination with a limited RDDS, the energisation of the pole may happen right after the peak value. Such an example is shown in Figure E.5. As the resonance frequency is higher for lower capacitor banks (see equation F.5), the peak value is reached earlier, and the sum of the base voltage and resonance value reaches a higher peak. For this reason, the 25 MVAr capacitor bank has a higher observed peak value than the other capacitor banks when the standard deviation is 0.75 ms.

$$f_0 = \frac{1}{2\pi\sqrt{LC}} \qquad (F.5)$$

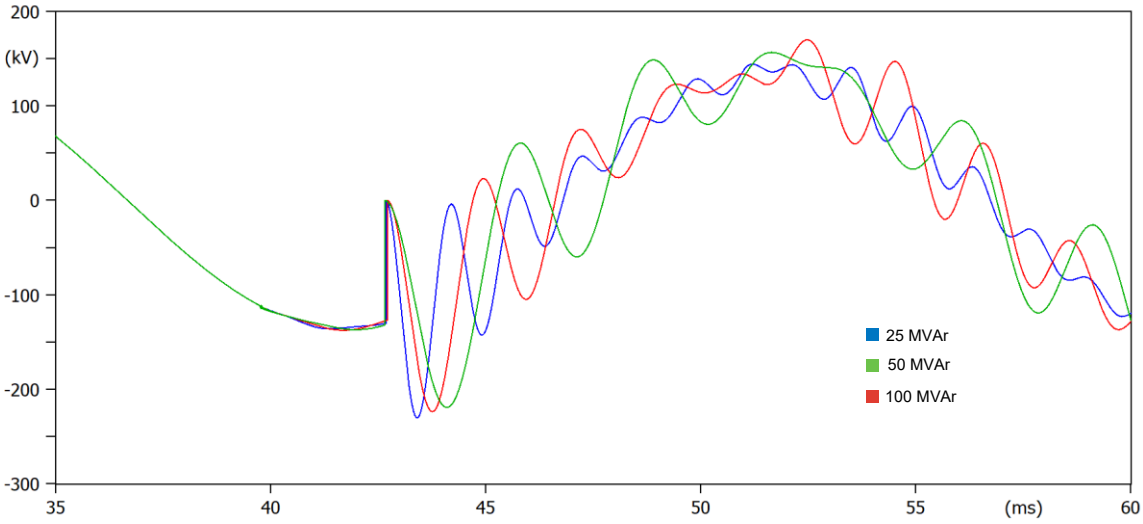

Figure E.5: Example L-G voltage of pole energisation right after peak

Effectiveness of PoW on the line-to-line voltages

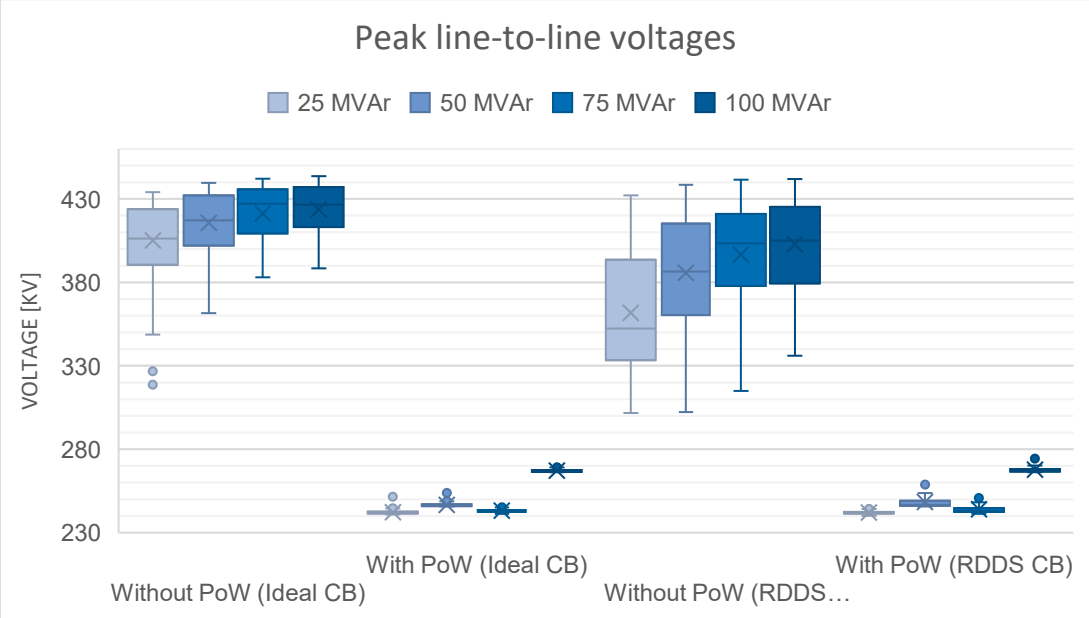

Figure E.6: Effectiveness of PoW on L-L peak voltages

The effectiveness of PoW implementation on the peak L-L voltages for multiple capacitor banks is depicted in Figure E.6. Based on the simulation results, the following remarks can be made:

- In general, an increase in capacitor bank size results in an increase in peak L-L voltages, which is as expected.
- The peak overvoltage values of the 75 MVAr capacitor bank with PoW case would be expected to lie between the 50 MVAr and 100 MVAr capacitor banks, based on its size. However, the 75 MVAr capacitor bank falls outside this range, as its peak overvoltage values are even lower than the peak overvoltage values of the 50 MVAr capacitor bank.

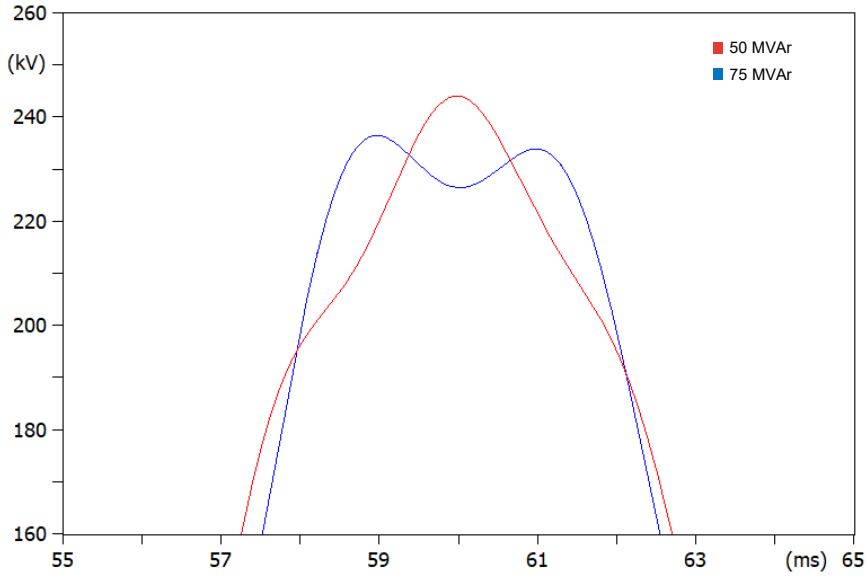

Figure E.7: L-L voltage at peak

Figure E.7 depicts the rare phenomenon that results in the 75MVAr capacitor having a lower than expected L-L overvoltage value. As can be seen in Figure E.7, the energisation of a 75 MVAr capacitor bank results in harmonic distortion of the voltage due to a resonance at 500 Hz. Due to this distortion, the voltage around the peak is suppressed compared to the energisation of a 50 MVAr capacitor bank. This alignment in frequencies results in almost equal suppression of all voltage peaks. This phenomenon only applies when switching occurs close to the zero crossing, thus, when PoW is utilised accurately, as a significant phase shift in this higher order frequency can result in the peak voltage being added to the peak ground voltage. For this reason, this phenomenon cannot be observed for the case without PoW implementation (See Figure E.6).

The resonance frequency can be calculated with the following formula:

$$f_r = \frac{1}{2\pi\sqrt{LC}} \qquad (F.6)$$

Of which:

$$f_r\text{: } resonance\ freqency\ [Hz]$$
$$C\text{: } capacitance\ of\ the\ capacitor\ bank\ [F]$$
$$L\text{: } inductance\ of\ the\ transformers\ [H]$$

The following data is known:

$$X_L = 6.2\ \Omega \rightarrow L = \frac{\frac{X_L}{2}}{2\pi f} = \frac{\frac{6}{2}}{2\pi * 50} = 0.00955\ H$$
$$C = 10.6\ \mu F$$

The reactance X_L is divided by two as there are two transformers utilised in parallel, yielding a total inductance L.

The resonance frequency is:

$$f_r = \frac{1}{2\pi\sqrt{LC}} = \frac{1}{2\pi\sqrt{0.00955 * 10.6 * 10^{-6}}} = 500\ Hz$$

This frequency is exactly ten times the base frequency, yielding equal peak suppression of all L-L voltage peaks.

The parallel resistance at the source impedance (see Figure E.8) plays a crucial role in this peak voltage suppression phenomenon, as this resistor creates a path for these resonances. Without the resistor, this specific harmonic would not exist.

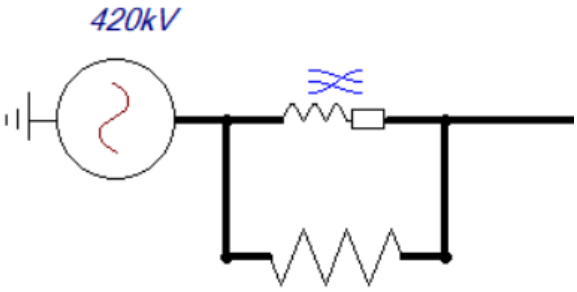

Figure E.8: Source impedance

Appendix F

This appendix shows the simulation results of the line-to-ground voltages and line-to-line voltages regarding the energisation of cable circuits.

Effectiveness of PoW on the line-to-ground voltages

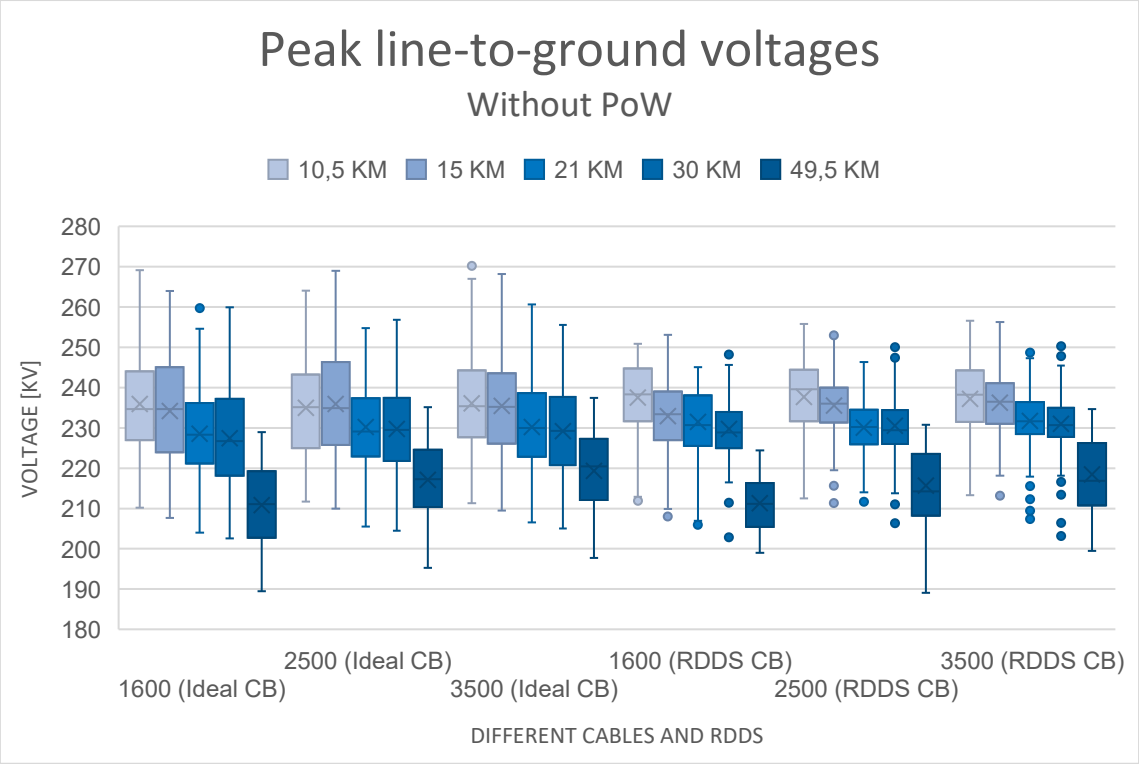

Figure F.1: Effect of cable size, cable length, and RDDS on L-G overvoltages without PoW utilisation

In Figure F.1, the peak L-G voltages for different cable circuit setups without the utilisation of PoW are depicted. Based on the simulation results, the following remarks can be made:

- It can be observed that an increase in cable length yields, overall, a decrease in peak overvoltages, due to the suppression of the reflections by the cable's resistance.
- Overall, the CB with imperfect RDDS performs better than the ideal CB, as the maximum outliers tend to be lower. The reason for this is described in Appendix E.

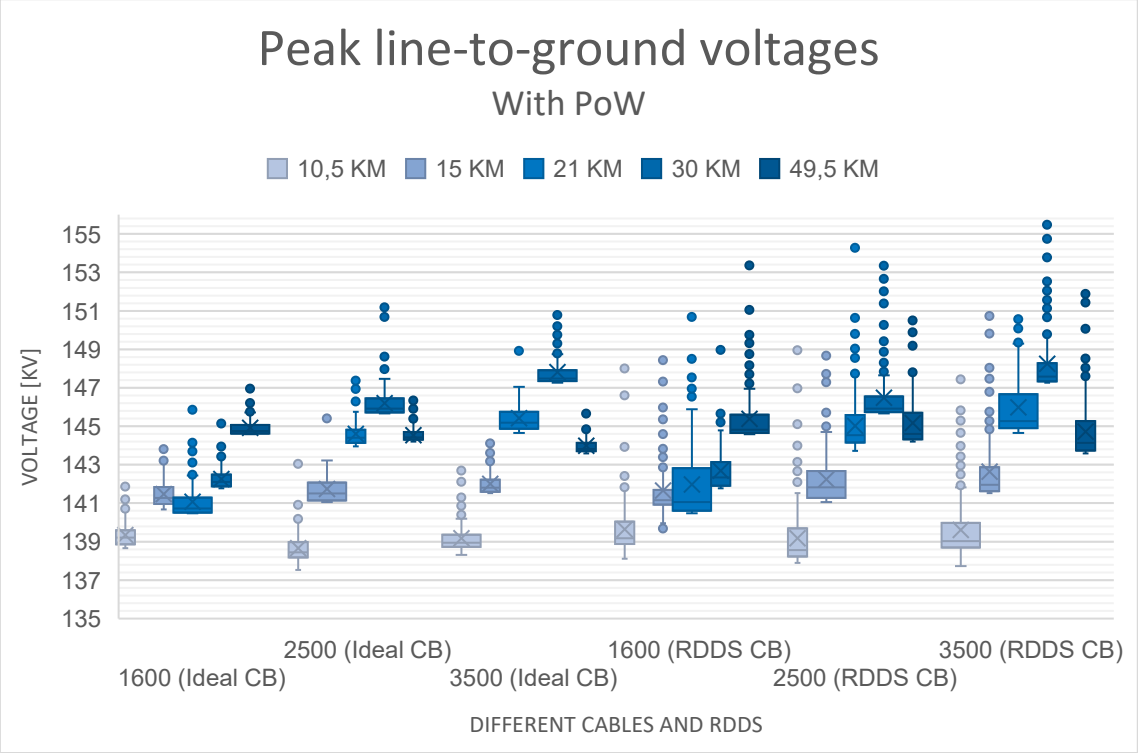

Figure F.2: Effect of cable size, cable length, and RDDS on the L-L voltages with PoW implementation

The effect of different cable circuit setups on the peak L-G voltages with the implementation of PoW is depicted in Figure F.2. Based on the simulation results, the following remarks can be made:

- Counterintuitively, for the 2500 mm² and the 3500 mm² cables, the highest peak overvoltages occur when using the 30 km cable.
- Imperfect RDDS results in higher outliers compared to the ideal CB. The reason for this is described in Appendix E.

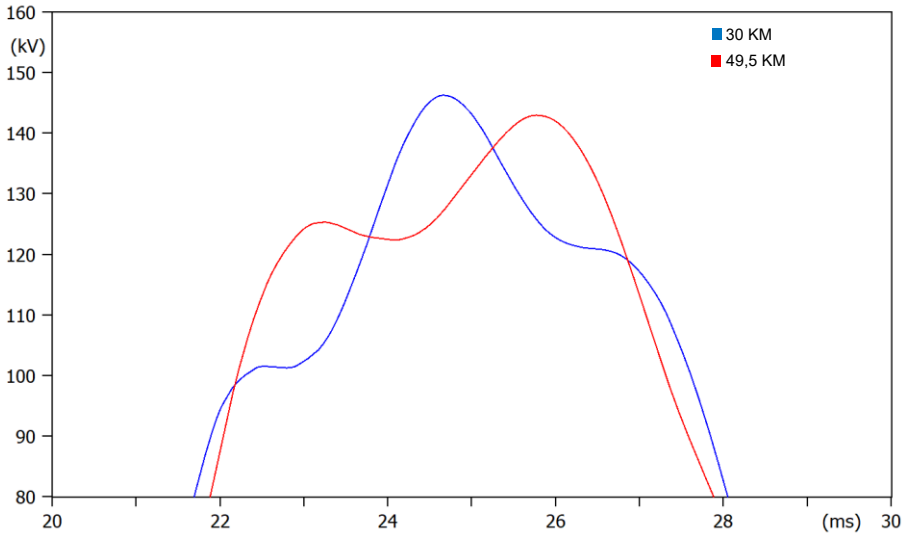

Figure F.3: Comparison of L-L voltage of 30 km and 49,5 km at the highest peak

Figure F.3 depicts why the 30 km cable has lower peak L-L overvoltage values than the 49,5 km cable. One can observe that the higher-order oscillation of the 49,5 km cable is better aligned, yielding better suppression of the peak value.

Effectiveness of PoW on the line-to-line voltages

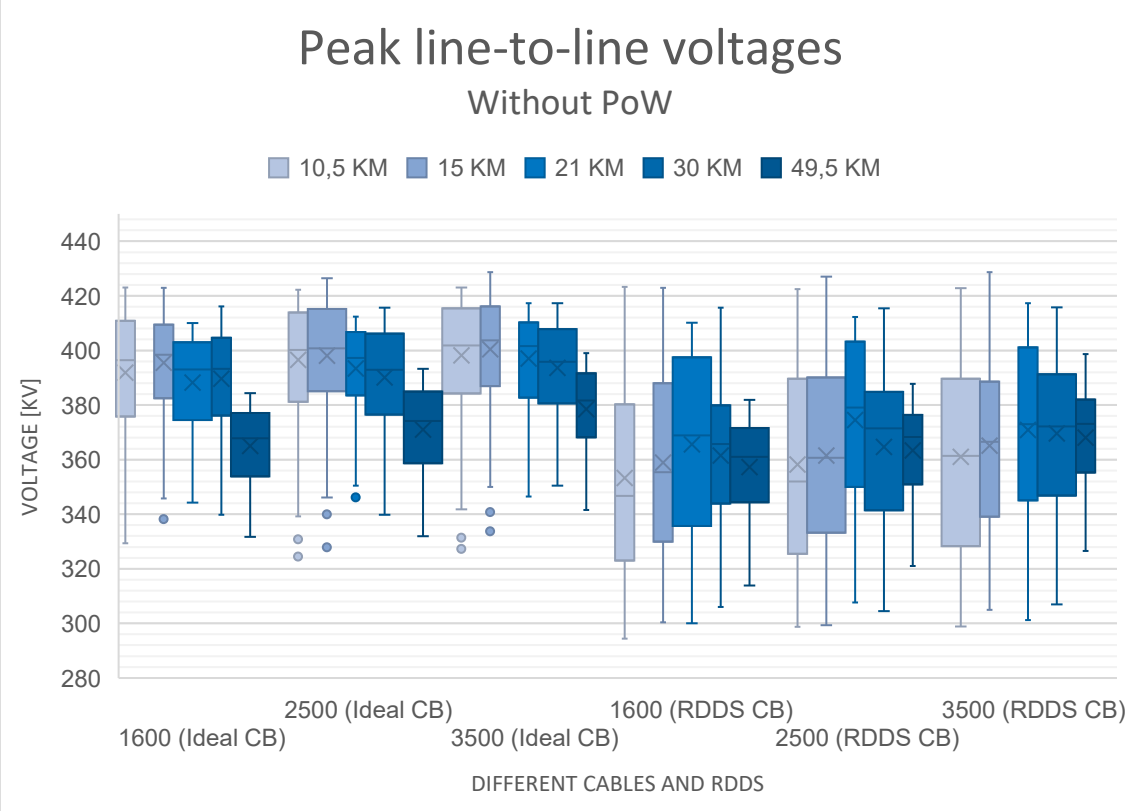

Figure F.4: Effect of cable size, cable length, and RDDS on L-L overvoltages without PoW utilisation

Figure F.4 depicts the effect of variations in cable size, cable length, and RDDS on the peak L-L voltages. Based on the simulation results, the following remarks can be made:

- It can be observed that, in general, an increase in length results in a decrease in L-L overvoltages.
- Overall, the CB with imperfect RDDS performs better compared to the ideal CB, as the average overvoltages tend to be lower.

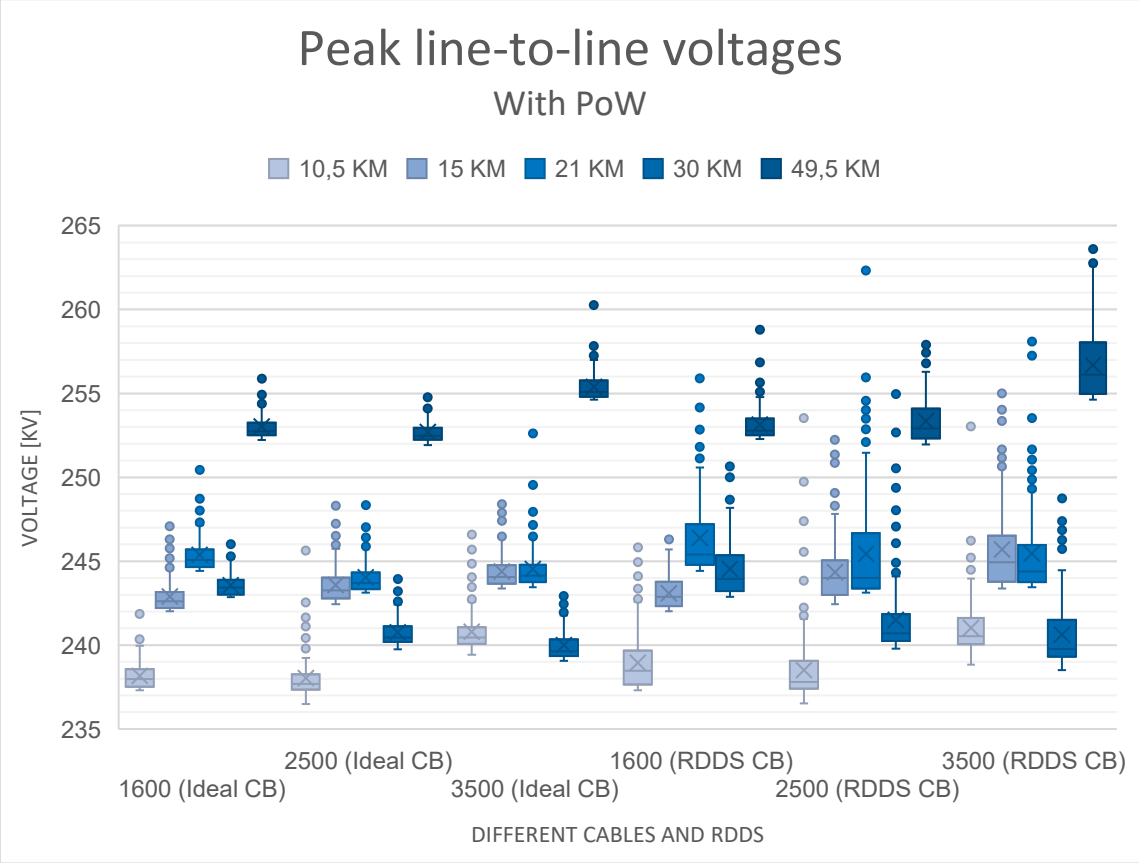

Figure F.5: Effect of cable size, cable length, and RDDS on L-L overvoltages with PoW implementation

Figure F.5 depicts the effect of cable size, cable length and RDDS on the L-L overvoltages when PoW is implemented. Based on the simulation results, the following remarks can be made:

- Counterintuitively, a cable of 30 km shows significantly lower overvoltages than the 21 km cable, due to the right alignment of the higher order oscillations of the 30 km cable.

The CBs with an imperfect RDDS perform, on average, deteriorated than de ideal CB, due to the average higher overvoltages.